



**UNIVERSITY OF
BIRMINGHAM**

**Population and evolutionary dynamics of *Pseudomonas
aeruginosa* during anti-adhesion therapy**

And

**The purification and crystallisation of five *Bdellovibrio*
proteins used during attack phase**

By David Hardy

963241

A thesis submitted to the University of Birmingham for the degree of: Molecular and Cellular Biology - Master by Research (MRes)

Biosciences
University of Birmingham
January 2015

UNIVERSITY OF
BIRMINGHAM

University of Birmingham Research Archive

e-theses repository

This unpublished thesis/dissertation is copyright of the author and/or third parties. The intellectual property rights of the author or third parties in respect of this work are as defined by The Copyright Designs and Patents Act 1988 or as modified by any successor legislation.

Any use made of information contained in this thesis/dissertation must be in accordance with that legislation and must be properly acknowledged. Further distribution or reproduction in any format is prohibited without the permission of the copyright holder.

Summary

This Masters by Research thesis comprises of two different projects each conducted at the University of Birmingham between 2013 and 2014. The first project was about using an anti-adhesion FimH antagonist on *P. aeruginosa* to evaluate their population and evolutionary dynamics. This data was then used to help mathematical models on the effects of anti-adhesion molecules during and bacterial infection. Six clinical isolates were for their antibiotic resistance to meropenem and imipenem. Once a resistant and susceptible isolate was found their growth rates, killing rates, attachment amounts and phagocyte killing capacity was measured. The second project involved protein purification and crystallisation of five *Bdellovibrio* proteins during attack phase. During attack phase *Bdellovibrio* up regulates certain proteins and finding the structure of these proteins will help understand how the function. This could be used as way to control *Bdellovibrio* and use it as at living antibiotic. *Bdellovibrio* is a predatory bacterium capable of invading and replicating within Gram negative bacteria. The overall goal of this project was to purify five *Bdellovibrio* proteins to a high enough purity and concentration to create protein crystals. The crystals would then be diffracted through x-ray crystallography to deduce the molecular structure.

Acknowledgments

I would like to take the time and thank certain people who helped me throughout this masters project. For the first project I would like to thank my supervisor Dr. Anne-Marie Krachler for her expertise and guidance. I would also like to thank all the people in the May lab at the University of Birmingham who made it a fun and enjoyable experience. For the second project I would like to thank my supervisor Dr. Andy Lovering for all his help and for making it an amazing project. I would like to thank Dr. Ian Cadby for his management and assistance throughout the project. I would also like to thank all the friends I have made over this project for making it an absolutely wonderful experience.

Table of Contents

MRes Project 1- Population and evolutionary dynamics of *Pseudomonas aeruginosa* during anti-adhesion therapy

Abstract.....	1
Introduction	2- 15
Materials and Methods.....	16 - 20
Results.....	21 - 44
Discussion.....	45 - 52
Conclusion.....	53 - 54
References.....	55 - 61

MRes Project 2- The purification and crystallization of five *Bdellovibrio* proteins used during attack phase

Abstract.....	63
Introduction	64 - 76
Materials and Methods.....	77 - 85
Results.....	86 - 116
Discussion.....	117 - 131
Conclusion.....	132 - 135
References.....	136 - 139

Molecular and Cellular Biology MRes Project 1

Population and evolutionary dynamics of *Pseudomonas aeruginosa*
during anti-adhesion therapy

Abstract

Pseudomonas aeruginosa is an opportunistic nosocomial Gram negative pathogen mainly causing infections in immunocompromised patients. Through a variety of mechanisms *P. aeruginosa* can become resistant to many antibiotics including carbapenems. Anti-adhesion therapy is one method of reducing the emergence of antibiotic resistant as it puts minimal selective pressure on the bacteria. To understand how the dynamics of a bacterial infection works mathematical models have been developed. Six clinical isolates of *P. aeruginosa* were used to gain data on some parameters that these mathematical models were based on. All six *P. aeruginosa* isolates were resistance to imipenem ($>8 \mu\text{g/mL}$), one was also resistant to meropenem ($>8 \mu\text{g/mL}$) and the other five were sensitive to meropenem with an MIC of $2 \mu\text{g/mL}$. The growth rates between meropenem sensitive and resistant isolates showed no difference. Only the meropenem resistant strain was able to maintain almost stable levels of growth over 20 hours in levels up to $20 \mu\text{g/mL}$ of meropenem. All susceptible strains showed a decrease growth at $\geq 2 \mu\text{g/mL}$ of meropenem. Twice the amount of the meropenem resistant isolate was able to attach to J774 macrophages compared to any of the sensitive strains. LDH release assays were used to measure the percent of macrophage lysis which showed no difference between meropenem sensitive and resistant isolates. Interestingly the meropenem resistant isolate had a small, round morphology compare to the large, flat colonies of the sensitive isolates. Due to the natural fluorescence properties of *P. aeruginosa* the levels of a FimH anti-adhesion molecule could not be examined.

Introduction

Aims and Objectives

With antibiotic resistance increasing it calls for a new method of treatment to overcome this growing problem. This increase in antibiotic resistance is true for many bacterial species including *Pseudomonas aeruginosa*. Imipenem and meropenem are classed as last resort treatment options when confronted with a *P. aeruginosa* infection and yet this bacterial species has evolved to be able to survive in the presence of these two antibiotics even at high concentrations. One such method to deal with the problem of antibiotic resistance is anti-adhesion therapy as it puts little to no selective pressure on the bacteria. Anti-adhesion works by inhibiting the initial interactions between the host and pathogen. This would make the pathogen more susceptible to the host's immune system and antibiotics.

In order to test this theory mathematical models have been produced to simulate the population and evolutionary dynamics of bacteria during anti-adhesion therapy. To produce a better working mathematical model experimental data must be obtained. Certain parameters such as growth and killing rates, phagocyte interactions and the effect that antibiotics and anti-adhesion molecules have on bacteria were investigated. This was to gain experimental data to not only improve the mathematical models but to assess the dynamics of bacterial during anti-adhesion therapy. Six *P. aeruginosa* isolates were obtained from the Queen Elizabeth hospital and used to carry out this study. They were chosen because they should have a variety of resistance to imipenem and meropenem. This allows a better understanding

into the workings of resistant and susceptible populations of when treated with either antibiotics or anti-adhesion molecules or a combination of both.

Pseudomonas aeruginosa

Pseudomonas aeruginosa is a Gram negative, coccobacillus bacterium that has unipolar motility. This opportunistic pathogen is mostly associated with the nosocomial environment and causes infections in open wounds and burn injuries, especially in those who are immunocompromised. It also causes infections in the urinary tract and pulmonary tract through invasive instruments such as catheters and respiratory tubes (Morita, 2014). But the amount of data of health-care associated infections by *P. aeruginosa* is limited with the best indicator of severe infection being bacteraemia. In the UK *P. aeruginosa* only accounts for ~4% of bacteraemia cases with an incidence of 7.3 per 100,000 population making it the seventh most common cause of bacteraemia (Loveday et al., 2014). As there are more outbreaks in intensive care units (ICU), patients with chronic obstructive pulmonary disease (COPD) and cystic fibrosis (CF) are more susceptible to *P. aeruginosa* infections because they are in a nosocomial environment with invasive instruments being used on them and are immunocompromised (Lovewell, 2014). As there is a growing elderly population due to longer life expectancy leading to more immunocompromised patients, the risk of *Pseudomonas* infections is increasing. This coupled with *P. aeruginosa* ability to thrive in a wide variety of environments armed with its arsenal

of virulence factors (shown below) makes it an efficient pathogen that needs more effective treatment (Schurek, 2012).

<u>Virulence Factor</u>	<u>Example</u>
Toxins	Exotoxin A, exoenzymes, lipopolysaccharide
Drug resistance	Efflux pumps, beta-lactamases
Biofilm formation	Survival in harsh environments and highly adaptable
Quorum Sensing	Cell communication and gene regulation

Antibiotic Resistance of *P. aeruginosa*

Antibiotic resistance is a particular problem with *P. aeruginosa* as there have been links between antibiotic resistance and an increase in the length of hospital stays and morbidity/mortality rates (Morita, 2014). *P. aeruginosa*'s outer membrane barrier along with its multidrug efflux transporters and endogenous antimicrobial inactivation has led to its intrinsic antibiotic resistance (Poole, 2007). This intrinsic antibiotic resistance is mostly through mutations in chromosomal genes (efflux mutations) but can also be through horizontal gene transfer of exogenous resistance genes (acquired resistance). This antibiotic resistance is against a wide variety of β -lactams and aminoglycosides but more worryingly the level of resistance to these antibiotics is increasing (Jones, 2009; Zilberberg, 2010). β -lactams are the most commonly used antibiotic to treat *P. aeruginosa* infections and there have been reports that all four molecular classes (A-D) of β -lactamases have been reported in *P. aeruginosa* (Zhao and Hu, 2010).

The endogenous β -lactamases found in *P. aeruginosa* are normally encoded by two β -lactamase genes; one class C cephalosporinase (AmpC) and one class D oxacillinase (PoxB). This common gene AmpC is found in many Gram negative bacteria but in *P. aeruginosa* it has been link to the natural antibiotic resistant to β -lactam in clinical isolates (Poole, K). In *P. aeruginosa* the most common mechanism of resistance to β -lactams, including expanded-spectrum cephalosporins and penicillin's, are ones that contain a mutation of AmpC (Poole, 2011). Acquired resistance in *P. aeruginosa* usually come through the acquisition of extended-spectrum β -lactamase (ESBL classes A and D) and carbapenemases (classes A, B and D) which are able to hydrolyse most β -lactams including carbapenems. The genes that encoded these enzymes are usually plasmid- or transposon-borne genes which are often on integrons that can capture and mobilize resistant genes (Cambray et al., 2010).

Carbapenems (imipenem and meropenem) are used to treat *P. aeruginosa* infections as they are highly stably compared to other β -lactams and have been useful in the treatment of ESBL enzymes and AmpC producers (El Gamal and Oh, 2010). Although carbapenems are more stable against β -lactamases compared to other β -lactams *P. aeruginosa* is finding ways to combat these antibiotic leading to antibiotic resistant and multi-drug resistant *P. aeruginosa* strains. Carbapenems will induce AmpC but is also effective against AmpC due to its bactericidal activity and stability. In *P. aeruginosa* AmpC along with other mechanisms of resistance contribute to the resistance of carbapenems (Jones, 1998). The enzymes responsible for the carbapenem resistance are β -lactamases which are capable of hydrolyzing carbapenems. In *P. aeruginosa* these are class A and D carbapenemases and a class B

metallo- β -lactamases (MBL) (Queenan and Bush 2007; Walsh, 2010). There are five class A β -lactamases that have activity against carbapenems but only two of these (Guiana extended-spectrum (GES) and *Klebsiella pneumoniae* carbapenemase (KPC) enzymes) have been reported in *P. aeruginosa* (Zhao and Hu, 2010). The number of reports that found KPC enzymes in *P. aeruginosa* is increasing and so far two types of KPC enzyme (KPC-2 and KPC-5) have been found in *P. aeruginosa* (Villegas et al., 2007; Wolter et al., 2009). What's more worrying is that isolates that have the KPC enzyme and are resistant to carbapenem are also found to be lacking the OprD outer membrane porin (Villegas et al., 2007; Wolter et al., 2009) which is used as one of the primary entry routes of β -lactams (Trias and Nikaido, 1990). This allows these bacteria to not only be able to break down β -lactamases but can also stop their entry into the cell. The two GES enzymes (GES 2 and 5) that have been reported in *P. aeruginosa* and shown to have activity against carbapenems are ESBLs (Poole, 2011). The class B metallo beta-lactamases (MBLs) are the main reason for β -lactamase mediated resistance to carbapenems with Verona integron-encoded metallo- β -lactamase (VIM) and imipenem (IMP) enzymes being the most common MBLs found in carbapenem-resistant bacteria (Walsh et al., 2005). VIM and IMP have been found in carbapenem-resistant *P. aeruginosa* (Gupta, 2008) with VIM predominating in Europe and IMP predominating in Asia. VIM-2 can now be found in five continents (Gupta, 2008; Walsh, 2010; Zhao and Hu, 2010) and SPM-1 which was found only previously in Brazil is now being reported in Europe (Salabi et al., 2010). These enzymes that are contributing to antibiotic resistance have now been found all over the world are not

the only way in which *P. aeruginosa* can become resistance to highly effective compounds such as carbapenems.

Other mechanisms of resistance include efflux pumps, outer cell membranes, quorum sensing genes and biofilm formation. The outer cell membrane is one of the largest contributors to antibiotic resistance in *P. aeruginosa*. In particular the alteration or loss of the outer membrane porin protein OrpD which is the major entry route of carbapenems leads to carbapenem resistance (Trias and Nikaido, 1990). This mechanism only provides high levels of resistance in non-MBL-produces and requires the presences of AmpC (Livermore, 1992; Poole, 2011). As mentioned before the loss or alteration of OrpD is usually accompanied by the KPC enzyme which increases their resistance to beta-lactams including carbapenems especially when KPC-2 is present.

Efflux pumps are able to expel antimicrobials for the bacteria and are a common mechanism of resistance in many bacterial species including *P. aeruginosa*. The members of the Resistance Nodulation Division (RND) of which there are 12 provide significant contributions to antimicrobial resistance in *P. aeruginosa* (Poole, 2004, 2007). Three of these 12 RND (MexAB-OprM, MexCD-OprJ, and MexXY-OprM) have been shown to supply resistance to β -lactams with MexAB-OprM having the most frequent and broadest range of resistance to β -lactams in clinical isolates (Drissi et al., 2008; Tomas et al., 2010). All three of these efflux systems have been shown to accommodate carbapenems, but not imipenem (Okamoto et al., 2002) resistance with MexAB-OprM having the greatest increase in resistance in clinical isolates (Pai et al., 2001). MexXY-OprM has also been found in clinical isolates of *P. aeruginosa* that

are resistant to β -lactams but as with all of these efflux pumps are usually found in conjunction with other mechanisms to provide high levels of resistance (Vettoretti et al., 2009)

Carbapenems

Carbapenems which include meropenem and imipenem are a class of broad spectrum beta-lactam antibiotics. Thienamycin is a naturally occurring antibiotic which is a product of *Streptomyces cattleya* and was the first carbapenem which led to the invention of all subsequent carbapenems (Birnbaum, 1985; Papp-Wallace et al., 2011). Imipenem and meropenem were the first two FDA approved carbapenems gaining approval in 1985 and 1996 respectively. Carbapenems were used in response to beta-lactamases which first emerged in the 1960's. What makes carbapenems different from conventional penicillins is the hydroxyethyl side chain along with them having a 4:5 fused lactam ring. Carbapenems also have a double bond between C-2 and C-3 and a substitution at the C-1 position swapping carbon for sulphur (Papp-Wallace et al., 2011).

Imipenem works by inhibiting cell wall synthesis but has to be co-administered with cilastatin which provides prolonged blockade of imipenem metabolism (Birnbaum, 1985). Dehydropeptidase-1 (DHP-1) is the enzyme that degrades imipenem reducing its effects so the DHP-1 inhibitor cilastatin is administered with imipenem. Meropenem mode of action is also against bacterial cell wall synthesis and is a bactericidal antibiotic when used against *P. aeruginosa* but

has to be administered intravenously. Meropenem has increased stability to DHP-1 so a DHP-1 inhibitor is not needed when administering meropenem. By inhibiting cell wall synthesis the bacterium is unable to repair any damages in the cell wall and cannot divide as cell wall synthesis is need for complete division and replication. Carbapenems work by binding to the penicillin-binding-protein (PBP) which is a group of enzymes that are essential for cell wall synthesis. By binding to PBP carbapenem prevents the linkage of peptidoglycan strands which will prevent cell wall synthesis. The bactericidal activity of carbapenem is at its highest when binding to PBPs 1a, 1b and 2 with meropenem having the highest affinity to PBP2. Meropenem also has an affinity for PBP3 which is species specific for *P. aeruginosa*.

Anti-Adhesion Therapy

There is an increasing amount of antibiotic resistance not only in *P. aeruginosa* but in many species of bacteria. This is a worrying prospect globally as the transmission of these drug resistance and multi-drug resistance bacteria or superbugs can be from one country to another in a matter of hours. For bacteria like *P. aeruginosa* which can survive in a variety of environments this transmission is more likely to occur as the bacteria is more likely to survive over longer periods of time in harsh environments. Antibiotic resistance is driven through the improper use of antibiotics when the incorrect antibiotic is used, the wrong dose is administered or patients do not follow administrative instructions properly. One way of combating

the problem of antibiotic resistance is to produce new antibiotics that are more powerful and would prevent pathogenic bacteria becoming resistance.

A different method to reduce antibiotic resistance but still cure infections is through the use of anti-adhesion therapy. The idea behind anti-adhesion therapy is stopping pathogenic bacteria adhering to host cells, which is the first step of infections. If bacteria are able to adhere to host cells they are more likely to avoid the host immune system and can start to release their arsenal of virulence factors. If bacteria are stopped adhering to host cells they should be more likely to be cleared by the host's immune system and not produce their virulence factors. Bactericidal antibiotics like carbapenems kill the bacteria but by not killing the bacteria using anti-adhesion therapy it puts less selective pressure on the bacteria causing less resistance. This is because the anti-adhesion therapy is only stopping the interaction between host and bacteria and is not disrupting the integrity of the bacteria. The host immune system should be able to more effectively clear the infection as the bacteria cannot adhere to the host cell, start to colonise and release virulence factors. Selective pressure is what produces drug resistance in bacteria as only the portion of the bacterial population that are able to survive the antibiotic or drug will be viable after treatment. Mutations in certain proteins and enzymes allow bacteria to become resistant to antibiotics under selective pressure, without this selective pressure the mutations may not occur especially if they have a negative cost on fitness. It is more than possible for bacteria to produce mutations in the cell surface proteins that would counteract anti-adhesion molecules but these would affect the binding of the bacterial pathogen to host cells. This means that it would be more detrimental to the

bacteria to become resistant to anti-adhesion molecules as it would then also not be able to bind to host cells.

The initial step in the adhesion process of bacteria to host cells is a weak non-specific binding using charge and hydrophobicity between the host and bacteria cell surface (Yuehuei, 2000). Specific interactions follow allowing the bacteria to sample the host cell environment in a gliding or rolling motion (Anderson, 2007) before making high-affinity strong specific interactions with either sugars, proteins or lipids. Each part of this binding process can be targeted through anti-adhesion therapy by interfering with either the host or bacterial cell surfaces. There are several ways in which this can be achieved: inhibiting the biogenesis of cell surface receptors in the host or bacterium, attaching anti-adhesion molecules to specific sugars, proteins or lipids to prevent host-pathogen interactions or by actively or passively immunising the host using antibodies that can recognise bacterial surface epitopes.

By inhibiting the biogenesis of cell surface receptors of bacteria, the bacteria are unable to produce the correct cell surface receptors such as fimbrial adhesions, pili and outer membrane proteins that are used in the host-pathogen interaction. This inhibition can be achieved by either prematurely halting the biogenesis of proteins which produces incomplete or incorrectly folded proteins or by stopping the translocation of these proteins to the cell surface. The former has been shown to be accomplished by sub-inhibitory concentration of fluoroquinolone ciprofloxacin and the aminoglycoside amikacin (Krachler, 2013). Chaperone-usher (C/U) pili can translocate pilin subunits via the Sec pathway to the outer membrane usher complex

which can secrete them and also act as assembly platforms. Pilus assembly can be therefore be interrupted by disrupting this chaperon-pilin complex with small molecules known as pilicides which subsequently inhibit bacterial adhesion (Svensson, 2001; Pinkner, 2006). These C/U pili are found in *P. aeruginosa* and are conserved among many species of bacteria making pilicides an effective molecule against many species of bacteria (Krachler, 2013). Host cells can also be manipulated to decrease bacterial adhesion by interfering with host glycosphingolipids (GSLs) (Svensson, 2003). This inhibition works by blocking the ceramide-specific glycosyltransferase which is able to catalyze the formation the precursor of GSLs. By inhibiting the GSLs pathway it has been proven that this will reduce bacterial colonisation of the urinary tract of murine models (Svensson, 2001).

Another strategy to inhibit the host-pathogen interaction is by competitively binding molecules to either the bacteria or host cells. Carbohydrates cover the surface of bacteria and host cells; lipopolysaccharides and glycoproteins for bacteria and glycoproteins and glycosphingolipids for host cells. These carbohydrates offer potential for anti-adhesion therapies like glycomimetics and synthetic glycosides which can competitively bind to the cell surface of bacteria and host cells stopping the attachment of bacteria to host cells. Two lectins produced by *P. aeruginosa*, LecA and LecB, could be potential target for anti-adhesion therapy as they are known to contribute to the adhesion process of *P. aeruginosa* (Chemani, 2009). One good example of this is the use of FimH antagonists which target the FimH adhesive subunit on type 1 pili. This subunit is used in the host-pathogen interaction between fimbriated uropathogenic *E. coli* (UPEC) and bladder cells during a urinary tract

infection (UTI). The first experiments based on mannoside-based host receptor analogs, of which a FimH antagonist is, were in murine models of UTI infections in the 1970s. Since then many alterations and advances have been made to this compound using structural studies. Multivalent scaffolds were added to make this FimH inhibitor a multivalent inhibitor that works by using a synthetic polymer, sugar core or peptide backbone to cross link bacteria (Almant, 2011). An aglucan moiety was also added which can improve the affinity, solubility and metabolic stability and now the most recent FimH antagonists are biphenyl mannoside. Compared to D-mannose based antagonists these most recent FimH are approximately 200,000-fold more potent and orally available (Han, 2012). These FimH antagonists have low cytotoxicity, are not cross reactive with human mannose receptors (Scharenberg, 2012; Hartmann, 2012) and have been able to decrease bacterial colonisation in murine models as much as when ciprofloxacin was administered (Klein, 2010; Jiang, 2012)

Host-pathogen interactions

The immune system in humans and animals is what defends the host against pathogenic organisms such as *P. aeruginosa*. Phagocytic immune cells such as neutrophils and macrophages are some of the first immune cells to respond to an infection. These cells are capable of phagocytosing and destroying pathogenic bacteria very quickly in a non-specific manner. As macrophages and neutrophils are the first to respond to a bacterial infection they help to reduce the colonisation of the

bacteria and are therefore reduce the rate at which the infection can spread.

Phagocytes are part of the innate immune system and without them the host is prone to infections from organisms like *P. aeruginosa* which are opportunistic pathogens. It has been shown that people suffering from immune compromising diseases such as chronic obstructive pulmonary disease (COPD) and cystic fibrosis (CF) have recurrent or chronic lung infections. In fact >80% of adults suffering from CF have either an acute or chronic *P. aeruginosa* infection and others with genetically compromised immune systems such as leukocyte adhesion deficiency (LAD) have a pre-disposition to *P. aeruginosa* infections. The evidence to support the role of phagocytes in the clearance of *P. aeruginosa* is from animal models which have impaired immune systems are more susceptible to *P. aeruginosa* infections.

A controversial topic is the difference between bacterial invasion and cellular uptake or phagocytises. This is particularly controversial in the cases of phagocytic cells such as macrophages as these cells are capable of phagocytosing bacteria as well as being invaded by certain species of bacteria. *P. aeruginosa* has been found to be able to invade corneal, epithelial, embryonic kidney (HEK) and HeLa cells but is engulfed by phagocytic cells. This claim is supported by the fact that clearance of *P. aeruginosa* is mediated by immune cells such as macrophages and has been shown that people lacking completely function immune systems succumb to *P. aeruginosa* infections more easily. Another idea to support the claim of macrophages engulfing *P. aeruginosa* through phagocytosis rather than *P. aeruginosa* invading the macrophage is that *P. aeruginosa* is not generally considered an intracellular pathogen and it has no specific adaptations built for intracellular survival. There is no really benefit for *P.*

aeruginosa to invade macrophages as it is able to survive and thrive extracellularly through its array of virulence factors. The one advantage *P. aeruginosa* may gain from invading macrophages is to evade the immune system and replicate but this can be achieved through the invasion of non-phagocytic cells and are therefore less likely to be destroyed by phagosomes.

Studies have shown that whether it be invasion or the phagocytosis of *P. aeruginosa* relies on phosphoinositide 3-kinase (PI3K). PI3K is able to convert phosphatidylinositol (4, 5) bisphosphate (PIP₂) into phosphatidylinositol (3, 4, 5) triphosphate (PIP₃) located at the host cell membrane. PI3K is responsible for the recruitment of Akt in the host cytoplasm and this phosphorylation is needed for both phagocytic engulfment and invasion of *P. aeruginosa*. Mice that have suffered the loss of the phosphatase that regulates the conversion of PIP₃ to PIP₂, murine PTEN (phosphatase and tensin homolog), have increased *in vivo* clearance of *P. aeruginosa* from the lung through phagocytosis (Hubbard LL). Toxins produced from *P. aeruginosa* are able to block the activity of Rac1 and CDC42 which are GTPases necessary for macrophage phagocytosis but not engulfment by epithelial cells. But *P. aeruginosa* is able to activate other upstream GTPase in epithelial cells which promote engulfment and vascular permeability allowing *P. aeruginosa* to block phagocytosis by macrophages and also promote invasion into epithelial cells (Lovewell, 2014).

Materials and Methods

***P. aeruginosa* Isolates taken from Queen Elizabeth Hospital, Birmingham**

Location	Isolate	Date	Imipenem	Meropenem
Patient	985	17/12/2012	S	S
Water sample	992	18/12/2012	S	S
Water sample	1004	19/12/2012	N/A	N/A
Patient	1007	21/12/2012	R	I
Patient	1008	31/12/2012	S	S
Patient	1009	31/12/2012	S	S

R = Resistant I = Insensitive S = Susceptible

The six *P. aeruginosa* isolates used in this study were either taken from a patient at the Queen Elizabeth (QE) hospital (patient) or from a water sample QE hospital. The patient samples were taken through throughout a course of antibiotic treatment to treat for a *P. aeruginosa* infection. The isolate were tested for their resistance against two antibiotics Imipenem and Meropenem at the QE hospital.

Minimum Inhibitory Concentrations (MIC)

According to the British Society of Antimicrobial Chemotherapy the MIC of *Pseudomonas* species was 4-8 µg/mL for Imipenem and 2-8 µg/mL for Meropenem. Based on these MIC the 6 clinical isolates of *P. aeruginosa* were tested for their

susceptibility to Imipenem and Meropenem. 5 mL of LB was inoculate with each *Pseudomonas* strain and grown overnight at 37°C whilst shaking. These were diluted down in LB to an OD of 0.2 at 600nm. 50 µL of each sample was then plated on a 96 well plate 50 µL of either Imipenem or Meropenem was added to a final concentration of 0-16 µg/mL at OD of 0.08-0.13 or 0.5 McFarland units. After 24 hours at 37°C the plate was visually inspected and the concentration at which no visible growth was taken as the MIC.

Growth Curves

5mL of Lysogeny Broth (LB) was inoculated with each *P. aeruginosa* strain and grown overnight at 37°C whilst shaking at 200 rpm. Optical density (OD) readings of the overnight culture were taken at 600 nm on an Eppendorf BioPhotometer plus spectrophotometer. When OD readings where over 1, the overnight culture was diluted down to an OD of <1. To gain the same amount of bacteria cells in each sample, the sample with the highest OD was taken and then divided by the other samples. All samples were then diluted 1:100 with LB and to a total volume of 1mL. 250µL was plated into a 96 well plate in and placed in a BMG Labtech FLUstar Omega microplate reader, shaking at 37°C for 24 hours. OD measurements at 600nm were taken every 10 minutes.

Killing Curves

Optical density (OD) readings of the overnight culture were taken at 600 nm on an Eppendorf BioPhotometer plus spectrophotometer. When OD readings were over 1, the overnight culture was diluted down to an OD of <1. To gain the same amount of bacteria cells in each sample, the sample with the highest OD was taken and then divided by the other samples. 100µL was plated into a 96 well plate and a 100µL of LB with a concentration of 0.5, 1, 2.5, 5, 10x MIC of Meropenem or Imipenem was added to each well. The 96 well plate was placed in a BMG Labtech FLUstar Omega microplate reader, shaking at 37°C for 24 hours. OD measurements at 600nm were taken every 10 minutes.

Optical Density (OD) to Colony Forming Units (CFU) conversion

5mL of LB was inoculated with each *P. aeruginosa* strain and grown overnight at 37°C whilst shaking. 10mL of LB was inoculated with 100µL of overnight culture and allowed to grow at 37°C whilst shaking. OD (600nm) readings were taken every 30 minutes and serially diluted down to 10⁻⁸ to original concentrations. 100 µL of 10⁻⁴-10⁻⁸ dilutions were plated out on LB agar plates at each time point. After 24 hours at 37°C the amount of CFU were counted.

LDH assays

1mL of J774 macrophages were seeded at a concentration of 100,000 cells/mL into a 24 well plate 24 hours prior to infection with *P. aeruginosa*. 5mL of LB was inoculated with each *P. aeruginosa* strain and grown overnight at 37°C whilst shaking. Overnight cultures of *P. aeruginosa* were diluted 1:1 with LB and OD (600nm) measurements were taken. These were diluted with colourless DMEM to give an multiplicity of infection (MOI) of 10 by using the equation $3/OD$ to give the amount of μL of *P. aeruginosa* per mL of colourless DMEM ($3/OD=\mu\text{L}/\text{mL}$). Old DMEM was removed and J774 macrophages were washed with 1 mL PBS. 1 mL of *P. aeruginosa* diluted in colourless DMEM was added to each well of J774 macrophages. Plate was spun at 1000 rpm at room temperature for 5 minutes. At 0, 1, 2, 3 hours after infection with *P. aeruginosa* 200 μL was taken from each well and transferred to a 96-well plate which was spun at 100rpm for 5 minutes at room temperature. 100 μL from each well was transferred to a fresh 96-well plate and stored at 4°C until measuring LDH release. LDH release assay was carried out using a Takara LDH cytotoxicity detection kit from Clontech. 11.25 mL of reagent A was mixed with 250 μL of reagent B by inversion. 100 μL of the mixture was place in each well. Absorbance was read at 600nm on a BMG Labtech FLUstar Omega microplate reader at 10, 20 and 30 minutes.

Attachment assays

1mL of J774 macrophages were seeded at a concentration of 100,000 cells/mL into a 24 well plate 24 hours prior to infection with *P. aeruginosa*. 5mL of LB was inoculated with each *P. aeruginosa* strain and grown overnight at 37°C whilst shaking. Overnight cultures of *P. aeruginosa* were diluted 1:1 with LB and OD (600nm) measurements were taken. These were diluted with DMEM to give an multiplicity of infection (MOI) of 10 by using the equation $3/OD$ to give the amount of μL of *P. aeruginosa* per mL of DMEM ($3/OD=\mu\text{L}/\text{mL}$). Old DMEM was removed and J774 macrophages were washed with 1 mL PBS. 1 mL of *P. aeruginosa* diluted in DMEM was added to each well of J774 macrophages. Plate was spun at 1000 rpm at room temperature for 5 minutes. Host J774 macrophages were left for one hour after *P. aeruginosa* was added then washed three time with PBS and lysed with 1mL of PBS+0.5% TX100. Each well was then plated out at a dilution factor of 10^4 and incubated overnight at 37°C and the colonies counted the next day.

Results

Minimum Inhibitory Concentration (MIC)

Table 1: MIC value according to BSAC

MIC	Imipenem ($\mu\text{g/ml}$)	Meropenem ($\mu\text{g/ml}$)
Resistant (R)	8	8
Insensitive (I)	8	4 to 8
Sensitive (S)	4	2

Table 2: MIC of Imipenem for the six *P. aeruginosa* isolates

	1 $\mu\text{g/mL}$	2 $\mu\text{g/mL}$	4 $\mu\text{g/mL}$	8 $\mu\text{g/mL}$	16 $\mu\text{g/mL}$
985					
992					
1004					
1007					
1008					
1009					

Grey indicates visible growth

Table 3: MIC of Meropenem for the six *P. aeruginosa* isolates

	1 $\mu\text{g/mL}$	2 $\mu\text{g/mL}$	4 $\mu\text{g/mL}$	8 $\mu\text{g/mL}$	16 $\mu\text{g/mL}$
985					
992					
1004					
1007					
1008					
1009					

Grey indicates visible growth

Minimum Inhibitory Concentrations (MIC) show at what concentration of antibiotic, in this case Meropenem and Imipenem, which inhibits the growth of bacteria. To determine the MIC of the six clinical isolates of *P. aeruginosa* were grown overnight in five different concentrations of each antibiotic. The five different concentrations of antibiotic ranged for resistance (R) to susceptible (S) levels. The MIC for *P. aeruginosa* according to the British Society of Antimicrobial Chemotherapy (BSAC) for Imipenem and Meropenem are stated in table 1. For *P. aeruginosa* to be resistant to either of these antibiotics they have to be able to show visible growth at 8 µg/mL. According to the testing done at the QE hospital all isolates except 1007 were sensitive to both imipenem and meropenem and no MIC for isolate 1004 was determined.

Table 2 and 3 show the MIC of all six *P. aeruginosa* isolates that were determined at the beginning of this study. Table 2 shows that all six isolates, not only 1007, were in fact resistant to imipenem as they all showed visible growth at both 8 and 16 µg/mL. The MIC of meropenem is shown in table 3 and shows that all isolates except 1004 were sensitive, not able to grow at 2 µg/mL. According to previous testing at the QE hospital isolate 1007 should have been insensitive to Meropenem but it was actually sensitive. Isolate 1004 illustrated high levels of resistance being able to grown in 16 µg/mL of Meropenem. From this the MIC for all isolates except 1004 was 2 µg/mL of meropenem and for imipenem the MIC for all isolate was >16 µg/mL.

Growth Curves

OD 600nm

OD 600nm

Figure 2: Graphs showing the growth of the six *P. aeruginosa* isolates over a 24 period. All six isolates were grown in the same Lysis Broth (LB) and Dulbecco's Modified Eagle's Medium (DMEM). Optical Density (OD) readings were taken at 600nm on a BMG Labtech FLUstar Omega microplate reader at 37°C. n=3 and the error bars are standard deviations.

The six *P. aeruginosa* isolates were grown in LB broth for 24 hours with optical density (600nm) reading taken every 10 minutes. All *P. aeruginosa* isolates had an initial lag phase of 2 hours where the OD did not increase. After 2 hours the OD was around 0.2 but then increased dramatically to its highest reading after 12 hours. At 12 hours the OD was 0.7 which was an increase of 0.5 OD units from the end of the lag phase at 2 hours. After 12 hours there is no significant increase in the OD with the readings staying between 0.55 and 0.7. The growth pattern for all six *P. aeruginosa* isolates were alike with the lag phase from 0-2 hours followed by an exponential growth phase for the next 10 hours and then reaching stationary phase after 12 hours.

Over the 24 hours that *P. aeruginosa* was grown in DMEM, which is the media used in cell culture, the highest OD reading was 0.5 at around 18 hours. There was a decrease with in the first two hours when the bacteria where in lag phase before they started to proliferate. The largest increase is OD was within in the first 12 hours with an increase from 0.2 OD to 0.45. After 12 hours the there was no significant increase in OD readings showing that *P. aeruginosa* had reached stationary phase. Although it appears there is a difference in growth between some isolates in DMEM this is only a minimal difference of 0.1 OD units. Compared to the growth in LB the six isolates did not proliferate as much in DMEM as the highest OD reached in DMEM was 0.45 compared to 0.7 in LB.

Sodium Benzoate Growth Curves

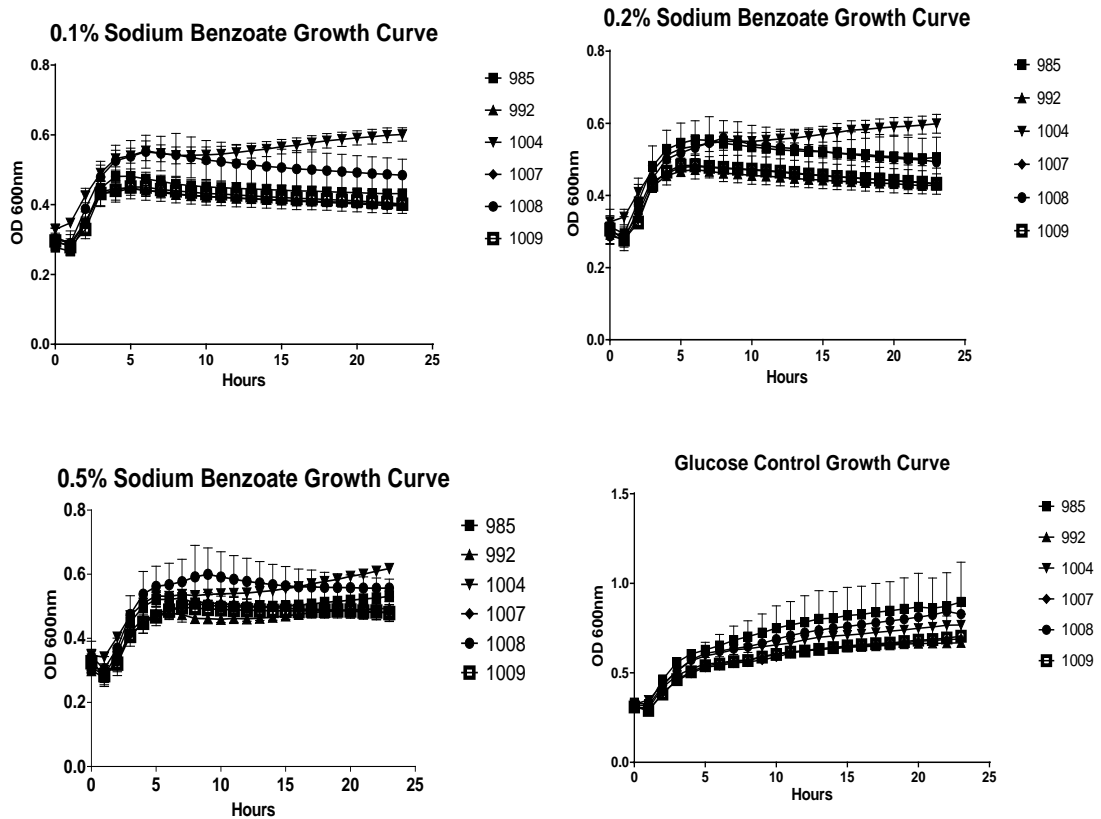


Figure 3: Sodium Benzoate Growth Curves. All six *P. aeruginosa* isolates were grown for 23 hours in M9 Minimal Media with 0.1, 0.2 and 0.5% Sodium Benzoate as the only carbon source. M9 Minimal Media with Glucose was used as a control, all OD reading were taken at 600nm on a BMG Labtech FLUstar Omega microplate reader at 37°C. n=3 and the error bars are standard deviations.

The six *P. aeruginosa* isolates were grown in sodium benzoate as it is a common ingredient in wound dressing that is applied to burns. All six *P. aeruginosa* isolates were able to grow but not maintain that growth at 0.1, 0.2 and 0.5% sodium benzoate when compared to the glucose control. At all different concentrations of

sodium benzoate all six *P. aeruginosa* isolates had an initial lag phase of around an hour before the exponential growth phase between 1 and 3-4 hours. After around 3-4 hours there was a general decrease averaging a drop of 0.5 OD units at 0.1 and 0.2% sodium benzoate in all samples except in 1004. The isolate 1004 was able to increase its OD units by 0.5 from the exponential growth phase to 23 hours. Interestingly at 0.5% sodium benzoate after the growth phase all six samples managed to maintain their OD reading at a steady level up to 23 hours. Once again the exception was the 1004 isolate which increased its OD by 0.1.

Imipenem Killing Curves

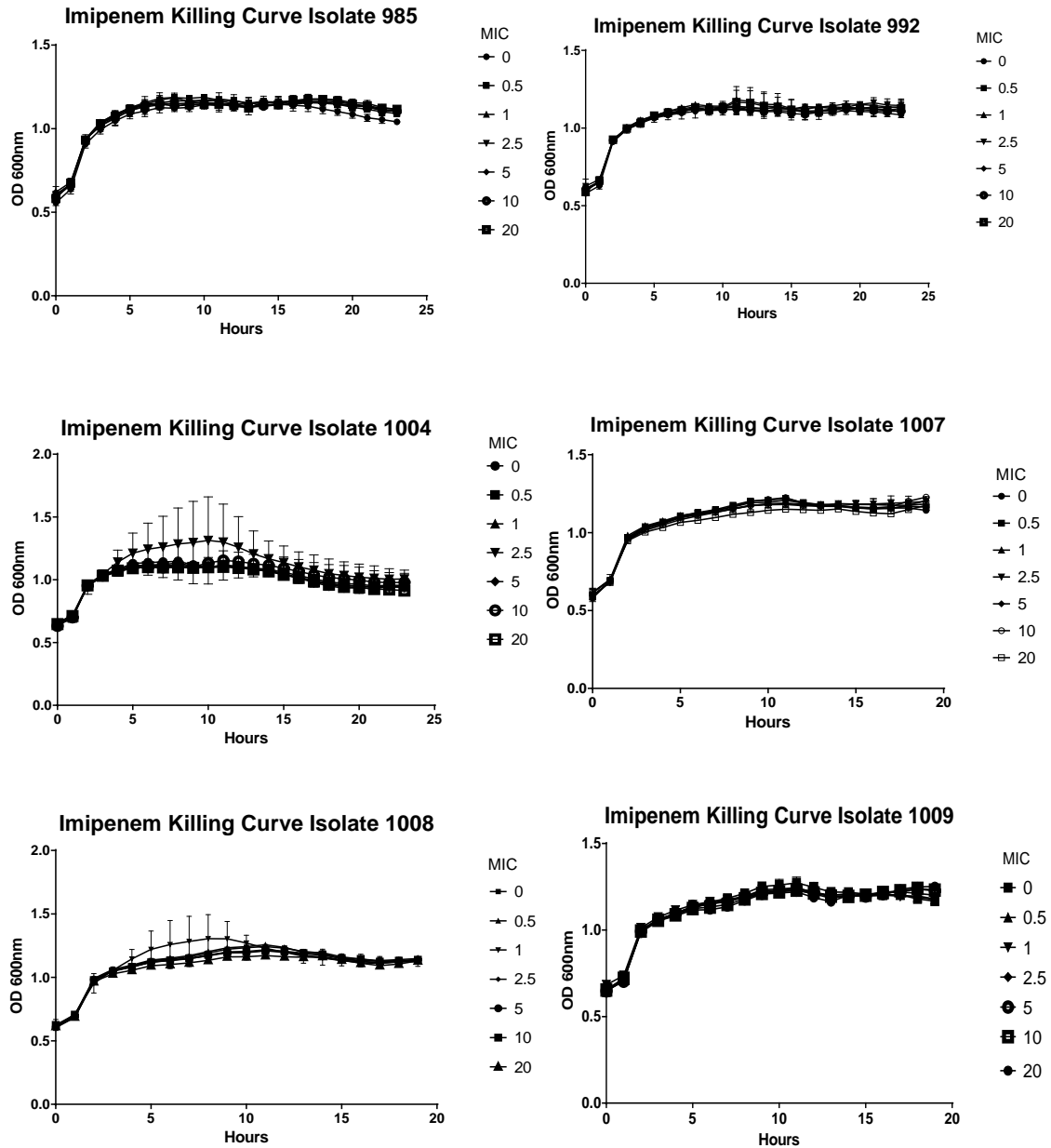


Figure 4: Imipenem killing curves. All six *P. aeruginosa* isolates were incubated with Imipenem at 0-20 times the MIC of meropenem (2 µg/mL). The isolates were incubated at 37°C for at least 19 hours and OD readings were taken at 600nm. n=3 and the error bars are standard deviations.

The six *P. aeruginosa* isolates were grown in LB containing 1, 2, 5, 10, 20, 40 µg/mL of imipenem which is an antibiotic used to treat *P. aeruginosa* infections. All six isolates with the exception of 1004 were able to proliferate and maintain that proliferation for at least 19 hours at all concentration of imipenem. The growth pattern for all six isolates was virtually identical with the exception of 1004. Within the first two hours there was a dramatic increase in OD readings increasing from around 0.6 to between 0.9 and 0.95. Isolates 985 and 992 then took 6 more hours to reach their peak where as 1007, 1008 and 1009 all took 8 more hours to reach their highest reading. After the 8 or 10 hour period for 985 and 992 or 1007, 1008 and 1009 respectively they had stable OD reading for the remaining time with no significant increase or decrease except for 1008. Isolate 1008 had stable OD reading between 10 and 13 hours but after 13 hours there was a slight decrease in OD reading from 1.2 to 1.1. *P. aeruginosa* isolate 1004 had the same initial dramatic increase in growth in the first two hours but then reached its peak after 6 hours. It was able to grow between 6 and 11 hours then there was a decrease in OD indicating a reduction in cell count. In all of the isolates at every concentration of imipenem with the exception of 1004 and 1008 grew at the same rate regardless of the concentration of imipenem. Isolate 1004 at 5µg/mL continued to increase its OD reading until 9 hours reaching an OD of 1.3. Isolate 1008 at 10µg/mL showed a similar pattern reaching its peak of 1.3 also after 9 hours. After around 9 hours there was a steady decrease in OD back down to the same level as all the other concentration in the respective isolate.

Meropenem Killing Curves

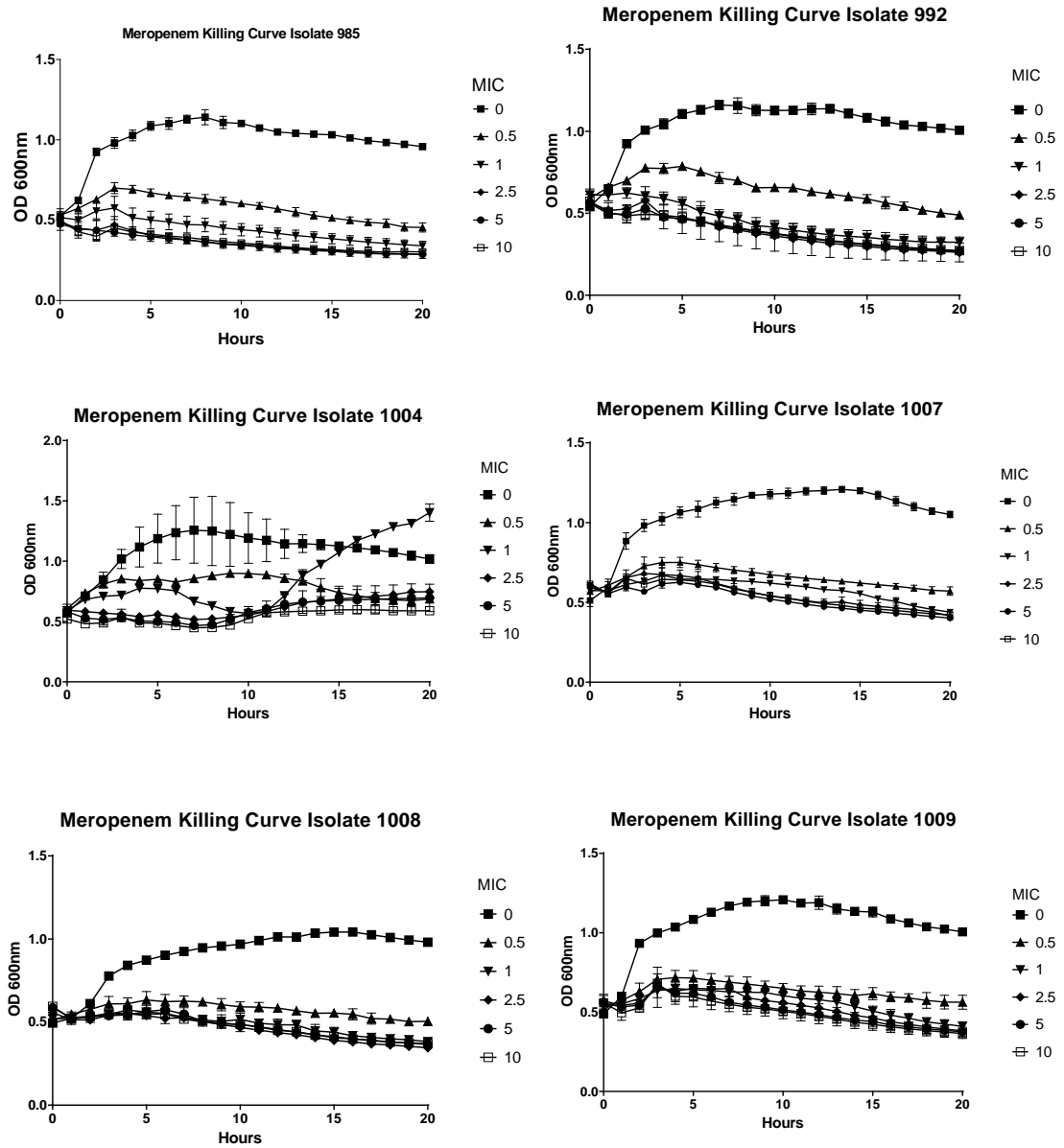


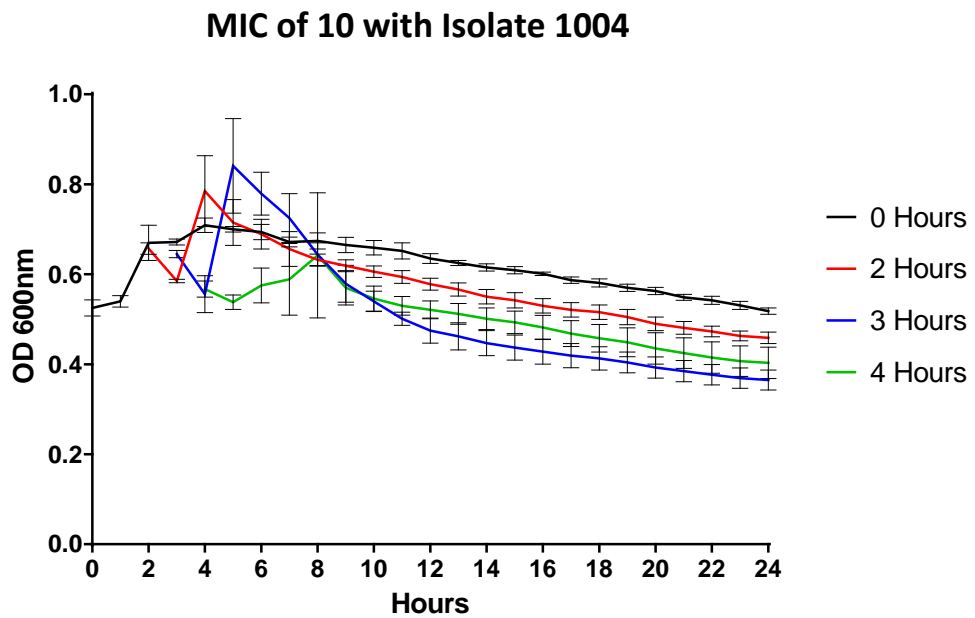
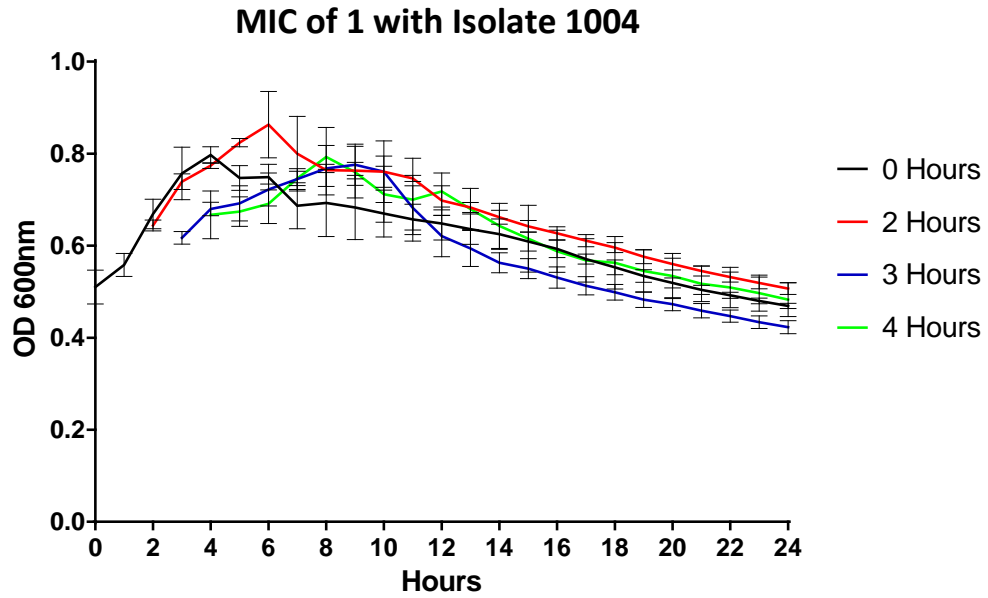
Figure 5: Meropenem killing curves. All six *P. aeruginosa* isolates were incubated with meropenem at 0-10 times the MIC of Meropenem (2 $\mu\text{g}/\text{mL}$). The isolates were incubated at 37°C for 20 hours and OD readings were taken at 600nm. n=3 and the error bars are standard deviations.

All six *P. aeruginosa* isolates were grown in LB containing 0, 1, 2, 5, 10, 20 µg/mL of meropenem for 20 hours. The 5 isolates that were classed as susceptible to meropenem (985, 992, 1007, 1008 and 1009) showed very similar killing curve profiles. All of these 5 isolates started out between OD of 0.5 and 0.6 and after 3-4 hours there was a slight increase in OD at 1 µg/mL. At all other concentrations of meropenem there was no increase within the first 3-4 hours for 985, 992 and 1008 with the two other susceptible isolate 1007, 1009 only showing a minimal increase of around 0.1 OD units. After 4 hours there was a slow and steady decrease in OD units for all susceptible isolates at all concentrations of meropenem. At 1 µg/mL all isolates managed to maintain a higher OD measurement throughout the time course ending on average 0.13 OD units higher than the 2 µg/mL. At the MIC of the susceptible isolates (2µg/mL) there was no increase in OD units over the time course except for 1008 where it was able to maintain OD readings slightly higher than 5-20 µg/mL but significantly lower than at 1µg/mL. Between 5 and 20 µg/mL only 1007 and 1009 showed a minimal increase in OD readings within the first 4 hours but after that there was a slow but steady decrease in OD units. The average loss between the start and finish of all the susceptible isolates at 5, 10 and 20 µg/mL meropenem was 0.22 OD units with 992 having the greatest loss of 0.29 OD units.

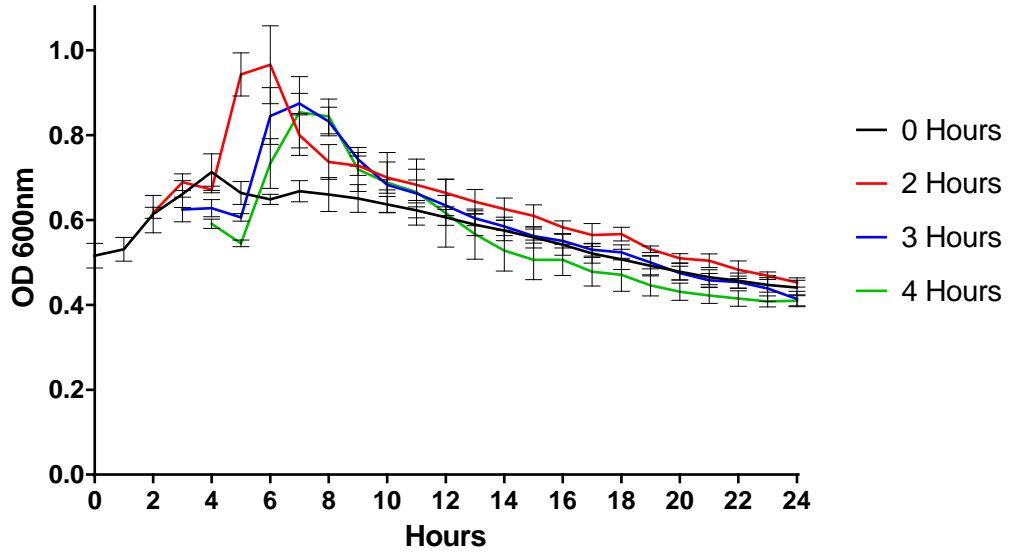
The resistant isolate 1004 showed a much different killing curve profile to the susceptible isolates. At 1 µg/mL there was an increase in OD at the rate of 0 µg/mL for the first 90 minutes. After that at 0 µg/mL 1004 continued increasing whereas at 1 µg/mL it plateaued off before starting to decrease at 10 hours ending up at the same level as 10 µg/mL. At 2 µg/mL 1004 began to increase for the first 5 hours followed by

a slight decline over the next 5 hours to the initial level but then dramatic increase to 1.4 at 20 hours. Between 5 and 20 $\mu\text{g}/\text{mL}$ of Meropenem showed the same pattern with a steady level up to 8 hours after which there was a small increase in OD units over the next three hour. At 11 hours 1004 with 20 $\mu\text{g}/\text{mL}$ meropenem starts to level off whereas at 5 and 10 $\mu\text{g}/\text{mL}$ there was a steady increase until the end of the time course.

Killing Curve at Different Time Points with Meropenem



MIC of 1 with Isolate 1008



MIC of 10 with Isolate 1008

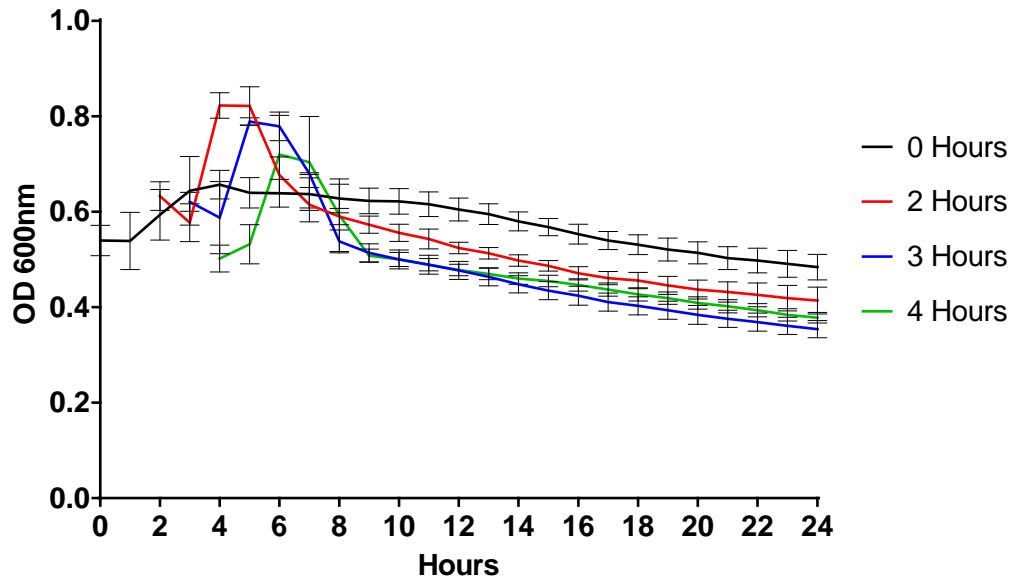


Figure 6: Meropenem killing curves at different time points. *P. aeruginosa* isolates 1004 (resistant) and 1008 (sensitive) were incubated with imipenem at 1 and 10 times the MIC of meropenem (2 µg/mL). After 0, 2, 3, and hours of growing the isolate in LB at 37°C they were then continued to be incubated at 1 and 10 times the MIC of meropenem. The isolates were incubated at 37°C for 20 hours and OD readings were taken at 600nm. n=3 and the error bars are standard deviations.

A susceptible (1008) and resistant (1004) isolate were grown at 2 and 20 µg/mL of meropenem at 0, 2, 3 and 4 hours after inoculation. 1008 showed similar profiles at both 2 and 20 µg/mL the only difference being the amount they were able to grow in after being treated with meropenem. At two hours after inoculation at 2µg/mL, 1008 managed to grow rapidly reaching around 1 OD after 3 more hours. There was also an increase with the 3 and 4 hour time point to a lesser extent but both taking 3 hours after treatment with 2 µg/mL meropenem to reach their highest OD. After they had all reached their peaks there was a decrease with all the different time points ending up at the same level of around 0.4 OD. The 2 hour time point of 1008 at 20µg/mL for was only able to reach a maximum of 0.86 after 2 hours. The 3 and 4 hour time points also took 2 more hours after 20 µg/mL of meropenem was given to reach their respective peaks but as with 2 µg/mL they were lower than the 2 hour time point. After reaching their peaks there was a sharp decline over the next 2 hours then a slow decrease to around 0.35-0.4 OD. The 0 hour time point had the same killing profile in both 2 and 20 µg/mL both with a slight increase with in the first

4 hours followed by a slow decrease at the same rate as all other time points at their respective meropenem concentrations.

1004 showed a similar pattern to 1008 with most of the different time points having an initial increase followed by a slow decrease at both 2 and 20 $\mu\text{g}/\text{mL}$. At 2 $\mu\text{g}/\text{mL}$ the 0, 2, 3 and 4 hour time point all reached their peak 4 hours after their respective starting points. They all reached a similar level of between 0.8 and 0.85 OD units before slowly declining to between 0.4 and 0.5. At 20 $\mu\text{g}/\text{mL}$ the 0, 2 and 3 hour time point all had an initial increase once incubation had begun. It took the 2 and 3 hour time points 2 hours to reach their peak but it took the 0 hour time point 4 hours. After 0, 2 and 4 hour time points had reached their peak there was a slight decline over the next two hours followed by steady loss in OD unit until the end of the time course. The 4 hour time point showed an initial drop in OD units in the first 2 hours then a small increase followed by the slow decline just like the other time points. All time points at both concentrations 1004 ended up between 0.34 and 0.47 OD units.

FimH and *P. aeruginosa* Fluorescence

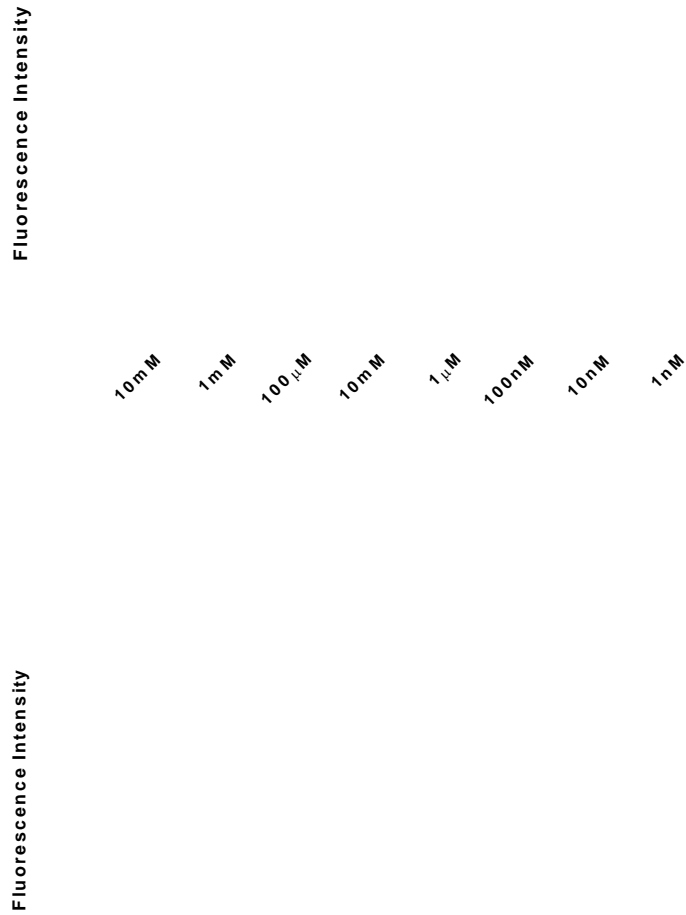


Figure 7: Fluorescence intensity of *P. aeruginosa* and the anti-adhesion molecule

FimH. All fluorescence readings were taken with an excitation wavelength of 355nm and an emissions wavelength of 460nm. FimH was diluted from 10mM down to 1nM in a 10 fold dilution. *P. aeruginosa* at 100% was an OD of 0.32 and was diluted down to 0% with an OD of 0.23. n=3 and the error bars are standard deviations

The fluorescence intensity of the FimH anti adhesion molecule was tested on a BMG FLOstar microplate reader. FimH was diluted to a concentration range of 10mM to 1nM in PBS and the fluorescence intensity read by exciting at 355nm and emitting at 460nm. Natural fluorescence produced by *P. aeruginosa* was also read at these wave lengths as well to determine the level of back ground noise. Starting at an OD of 0.31 where *P. aeruginosa* was at 100% it was diluted down to 0% with an OD of 0.23. The general trend of the FimH molecule is stable emission of 6000-7000 fluorescent units (FU) from 1nM to 1mM. After 1mM there was a sharp increase up to 10^5 fluorescent units. *P. aeruginosa* shows a slow incline in FU from 4.8×10^3 to 6.2×10^3 between 0% (OD 0.23) and 80% (OD 0.29) where it then had a steep increase to 9.7×10^3 .

Attachment Assay

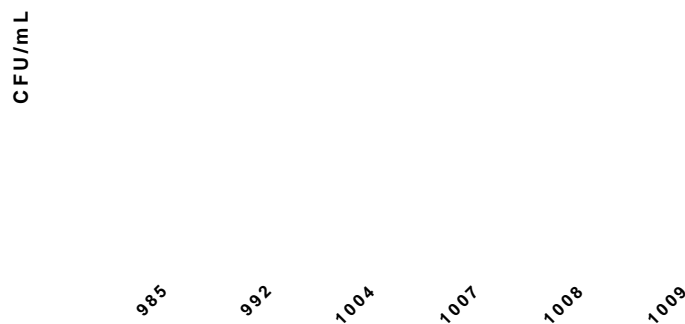


Figure 8: Attachment assay of all six *P. aeruginosa* isolates. All isolates were incubated with J774 macrophages at an MOI of 10 for 1 hour at 37°C. After washing with PBS the amount that remained were plated out on LB agar and counted after incubating for 24 hours at 37°C. n=3 and the error bars are standard deviations.

The six *P. aeruginosa* isolates were incubated with J774 macrophages for 1 hour. The average amount that remained after washing were measured and shown in figure 8. The meropenem resistant isolate 1004 was able to attach significantly more ($p=0.00012$), with almost double than any other isolate with 2.3×10^5 CFU/mL. There was no difference between any of the 5 susceptible isolates with 992 and 1009 having the second highest CFU count with 1.2×10^5 CFU/mL. The next was 1008 with 1×10^5 CFU/mL followed by 1007 at 0.8×10^5 CFU/mL and 985 having 0.4×10^5 CFU/mL.

LDH Release Assay

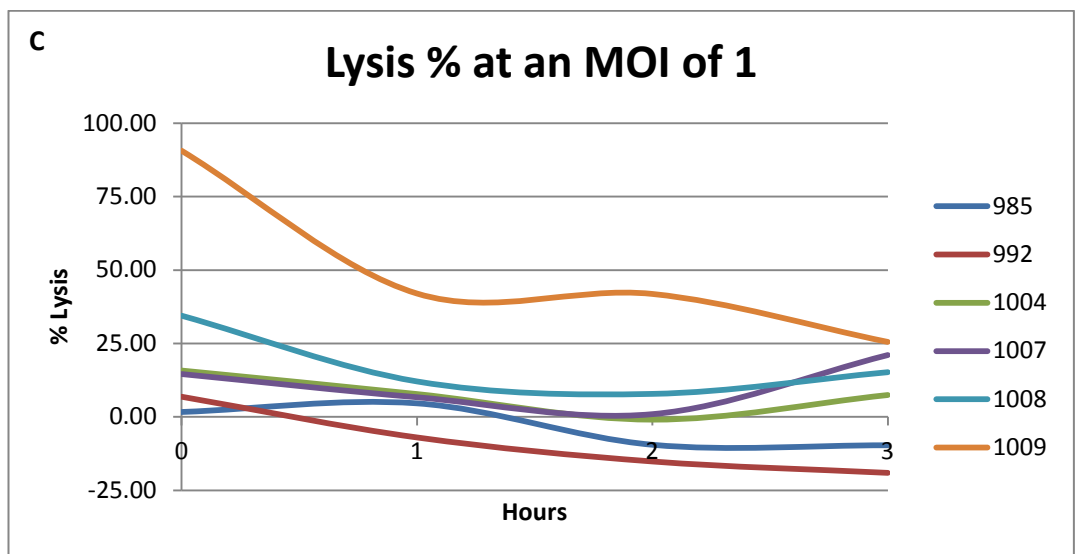
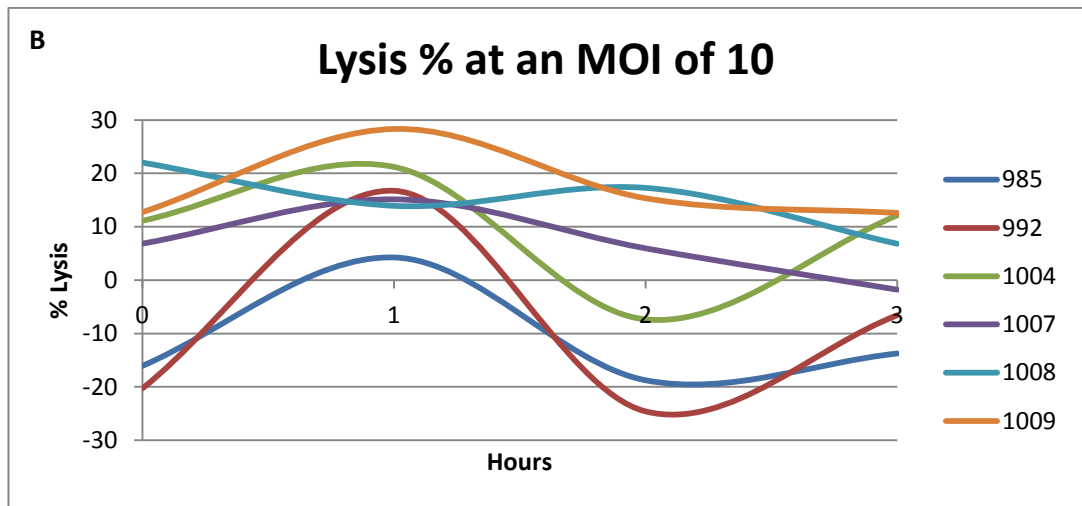
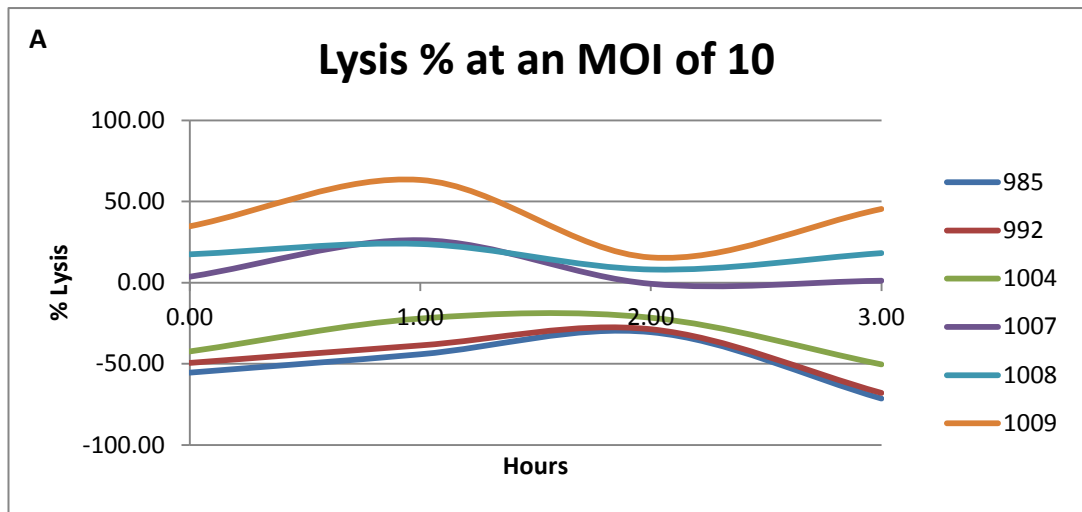


Figure 9: The percent of macrophage lysis over 3 hours at an MOI of 1 and 10. The six *P. aeruginosa* isolates were incubated with J774 macrophages for 3 hours. Every hour 200 μ L of the supernatant was taken, spun down and 100 μ L taken and added to 100 μ L of reagents from a Clontech LDH Cytotoxicity Test. The percent of lysis compared to 100% lysis of macrophages with 1% TX-100 in DMEM was plotted. Graph A and B are at an MOI of 10 and graph C at an MOI of 1. N=1

At an MOI of 10 over three hours for every isolate is hugely variable and show no conclusive results. Graph A shows that 1007, 1008 and 1009 all have mostly positive % lysis and 985, 992 and 1004 all have negative lysis percentages. The general trend in graph A for all positive results is an increase over the first hour followed by a decrease at 2 hours and then a slight increase at 3 hours. The negative lysis all show an increase of lysis percent over 2 hours followed by a decrease at 3 hours. Graph B shows 1009, 1008 and 1007 having positive lysis and 985, 992 and 1004 varying between positive and negative lysis. 985, 992 and 1004 show an increase within the first hour followed by a decline in lysis at two hours and then an increase at 3 hours. Isolate 1008 showed the opposite trend to 985, 992 and 1004 with a decrease at 1 hour then increasing at 2 hours followed by a decrease at 3 hours. 1007 showed an increase within the first hour then a slow decrease over the next two hours. 1009 shows a similar trend to 1004 but has the same lysis percent from 2 to 3 hours. At an MOI of 1 (2 μ g/mL) there is generally no change over the 3 hours for all of the isolate except 1009. All isolates have a positive lysis percent between 0 and 90% at the initial time point and only 985 and 992 ending up after 3 hours having a negative lysis percent. 1009 shows a significant difference between it and all other

isolates lysing 90% of the macrophages at the initial time point followed by a decline to 42% over the next hour. Between 1 and 2 hours 1009 plateaus and then declines to 25% after three hours which is close to the percent of lysis by isolate 1007.

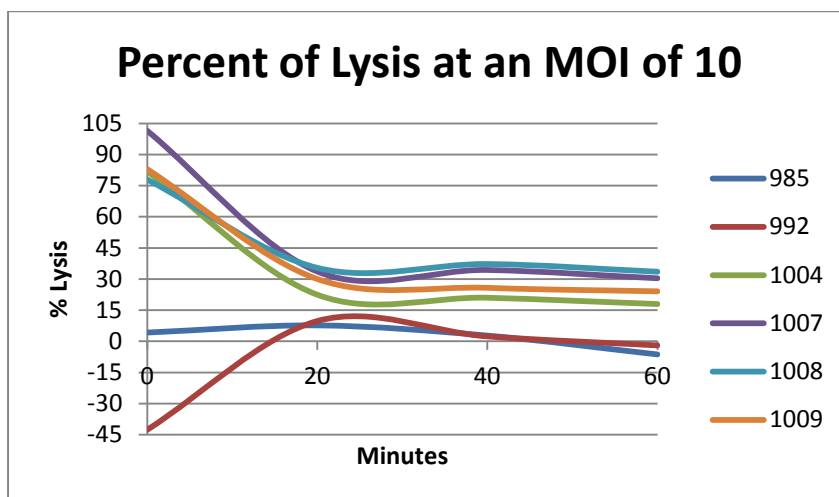
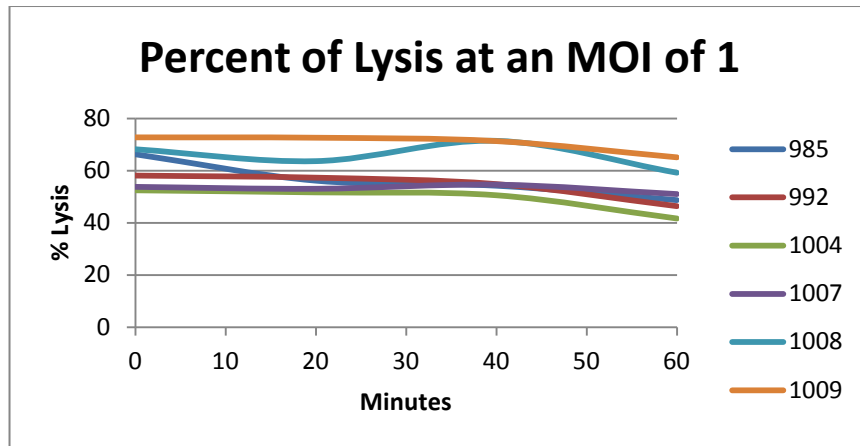


Figure 10: The percent of macrophage lysis over one hour at an MOI of 1 and 10.

The six *P. aeruginosa* isolates were incubated with J774 macrophages for 1 hour.

Every 20 minutes 200 μ L of the supernatant was take, spun down and 100 μ L taken

and added to 100 μ L of reagents from a Clontech LDH Cytotoxicity Test. The percent of lysis compare to 100% lysis of macrophages with 1% TX-100 in DMEM was plotted.

Graph A is at an MOI of 1 and B at an MOI of 1. N=1

Over the period of an hour at an MOI of 1 there is no significant change in the lysis percent. All isolates start between 52 and 73% and finish between 41 and 65% with an average drop of only 10%. The largest percent drop for all isolates is between 40 and 60 minutes with the exception of 985 which had its largest drop between 0 and 20 minutes. At an MOI of 10 there is a dramatic change to all isolates over an hour. Isolates 1004, 1007, 1008 and 1009 all have positive percent of macrophage lysis where as 985 and 992 vary between positive and negative lysis percentages. All the positive lysis percentages show the same pattern with a massive drop within the first 20 minutes followed a levelling off over the next 40 minutes. On average there is a 55% decrease in all isolates with a positive lysis percent. The four positive percent isolates start between 77 and 101% and all finish between 17 and 33%. The trend for 992 has an increase of 52% within the 20 minutes followed a minimal decline over the next 40 minutes. Isolate 985 only varies 10% over the course of an hour.

Morphology

985



992



1004



1007



1008



1009



Figure 11: Morphology of the six *P. aeruginosa* isolates. Each isolate was incubated at 37°C overnight on LB agar. Isolate 1004 which is resistant to meropenem was much smaller, round and capsular than all the other sensitive isolates. Images were taken with a Nikon Coolpix digital camera.

All of the meropenem sensitive isolates except 985 have identical morphologies. They are large, flat and appear to spread rapidly indicated by central darker area with a pale ring surrounding it. Isolate 985 has an intermediate morphology between the resistant isolate 1004 and the sensitive isolates. Each colony is smaller and less spread out than the sensitive isolates but not as small and round as the resistant isolate. The resistant isolate 1004 has small, capsular colonies that do not swarm out from the centre and have a more viscous texture. All isolates produce a bluish green colour once allowed to grow for around 24 hours.

Discussion

MIC

Six clinical *P. aeruginosa* isolates were obtained from the Queen Elizabeth hospital in Birmingham. These isolates were taken from water and from one patient undergoing antibiotic treatment. Isolates 992 and 1004 were taken from water and 985, 1007, 1008 and 1009 were taken at different times throughout a two week antibiotic treatment. The reason *P. aeruginosa* was tested against imipenem and meropenem for their MIC was that they showed variability in their MIC when tested at the Queen Elizabeth hospital. To test if there was any difference in population dynamics a resistant and susceptible isolate has to be found. Unfortunately all six isolates were determined to be resistant to imipenem so differences between resistance and susceptible isolates could not be compared. Meropenem showed that 1004 was resistant ($> 8 \mu\text{g/mL}$) whereas all other isolates were susceptible ($2 \mu\text{g/mL}$) so throughout this study 1004 was used as the resistant isolate. It was interesting to see that all the isolates tested sensitive to imipenem at the (QE) but were resistant when test at the beginning of this study. Isolate 1007 was shown to be resistant to imipenem and insensitive to meropenem at the QE but was sensitive to meropenem when tested during this study. One reason that could account for this difference in sensitivity is that at the QE the *P. aeruginosa* isolates were tested using the disc diffusion method whereas during this study the MIC was determined by liquid broth method.

Growth Curves

To understand the rate at which the six different isolates grow, growth curves were produced using Lysogeny Broth (LB) and Dulbecco's Modified Eagle's Medium (DMEM). Optical density (OD) readings at 600nm can show the rate at which *P. aeruginosa* is proliferating as the number as the number of bacteria increase so will the OD readings. There was no difference between the growth rates of the six isolates of *P. aeruginosa*. This shows that even with meropenem resistance (1004) *P. aeruginosa* was not able to proliferate faster than any of the other isolates. Having antibiotic resistance does not benefit the bacterium in terms of growth rate compared to the other isolates which were susceptible to meropenem. If a bacterium was able to proliferate quicker whilst infecting its host it would be far more likely to survive and spread. The proliferation rate has to be controlled as if it was too quick then the bacterium may destroy the host before spreading. It is controlled depending on how much nutrients are available in the environment.

Compared to LB the growth rate of *P. aeruginosa* in DMEM was much slower and did not result in a dramatic increase in OD. *P. aeruginosa* was grown in DMEM to show the extent of proliferation as this media was used in LDH release assay and attachment assay over a time period. For that reason it was useful to know how *P. aeruginosa* responded to growth in DMEM. The largest increase in both of the types of media was between 2 and 12 hours showing that the amount of time it takes *P. aeruginosa* to proliferate is the same but the amount of bacteria is vastly different.

Sodium benzoate was used as the only carbon source that was added to minimal M9 media to measure the growth of *P. aeruginosa*. This was to replicate the condition the bacteria may have to grow under when in contact with many wound dressings. It is clear that all six *P. aeruginosa* isolates were able to utilise the glucose in the control far more effectively as after the initial exponential growth there was a continuous increase in OD readings. One interesting finding was that at 0.5% sodium benzoate after the exponential growth phase there was no significant decrease in OD reading and therefore the amount of bacteria stayed constant. Both 0.1 and 0.2% showed a decrease in OD reading after the growth phase and 0.5% was expected to show a decrease as well.

Killing Curves

Killing curves were used to show the effect each of the antibiotics, imipenem and meropenem, had on the six *P. aeruginosa* isolates. All of the isolates were classed as resistant to imipenem but only one (1004) was resistant to meropenem. All other isolates were classed as sensitive to meropenem as the MIC was 2 µg/mL. This was then taken as the MIC for both meropenem and imipenem when testing the antibiotics on *P. aeruginosa*. The imipenem killing curves show that every isolate was able to proliferate equally well as when no imipenem was present. This shows that all isolates have high levels of resistance to imipenem as even at 20 times the MIC (40 µg/mL) the rate of proliferation did not change. As all isolates were classed as resistant to imipenem this result is not surprising and supports the claim that the isolates are

highly resistant to imipenem. Only one isolate showed resistance to meropenem and again the killing curves reflect this. All of the susceptible isolates had a decrease in OD reading over the 20 hours at 1 MIC or more which shows that the *P. aeruginosa* was dying. Interestingly there was little difference between and MIC of 1 and 10 indicating that using a greater concentration of antibiotic does not kill these isolates faster. The resistant isolate was able to maintain level OD reading at all different MIC proving this isolate is able to survive at concentrations of up to 20 µg/mL. There is no increase in the OD at any MIC, except MIC of 1, which indicates that unlike imipenem the resistant isolate is not able to proliferate above it the MIC but only able to maintain level growth. This shows that above the MIC for susceptible isolate the meropenem has more of a bacterial static effect on the resistant isolate. To see if the difference stages of the *P. aeruginosa* growth curve influenced the growth in Meropenem an susceptible (1008) and resistant (1004) isolate were incubated for 0, 2, 3 or 4 hours before adding meropenem at two different MIC. The two isolates showed very similar profiles and both 1 MIC and 10 MIC with an initial increase in OD followed by a slow decline. The only slight difference was at 1 MIC with 1004 where it was able to maintain a higher OD for longer before starting to decline. As for the different time points at which meropenem was added it made no difference, it merely moved the general profile of the curve along the time scale. An interesting follow up to this study would be to take a sample of an sensitive and resistant isolate after incubation with meropenem and then incubated it again with different concentrations of meropenem. This would show if the isolate is able to produce more effective

antibiotic resistance than is already has or if there is a maximum level of resistance it can obtain.

FimH and *P. aeruginosa* Fluorescence

The FimH anti-adhesion molecule that was tested during this study was 4-methylumbelliferyl- α -D-monopyranoside. This molecule has fluorescence properties which were used to see if the molecule was visible at different concentrations. Unfortunately because *P. aeruginosa* has such a high fluorescent intensity at an OD of 0.3 there would be overlap between *P. aeruginosa* and the FimH molecule if the OD of *P. aeruginosa* was increased. From 1nM to 1mM of FimH there is no significant difference between the fluorescent intensity. This means that at an excitation of 355 nm and emission at 460 nm the difference between 1 nM and 1 mM cannot be distinguished. The emission wavelength that was used in the study is much higher than the optimal wave length (375 nm) of this FimH compound. When read at 374nm there was significant difference between 1 mM to 1 μ M but anything lower shows no significant difference. At all concentrations of FimH read at 374nm the fluorescent intensities were significantly lower than at 460nm. *P. aeruginosa* was not measured at 374nm but all concentrations of FimH at 374 nm had lower intensity than at *P. aeruginosa* at 460nm. The measurements taken at 374 nm where done on a different more advanced microplate reader which could account for these differences in fluorescence intensities.

Attachment

These results show that the meropenem resistant isolate was able to attach significantly more to macrophages compared to all the other sensitive isolates. Although this assay was to measure the attachment of *P. aeruginosa* to macrophages it cannot be determined that *P. aeruginosa* was being phagocytosed rather than *P. aeruginosa* invading the macrophages. The mechanisms that are used in bacterial invasion compared to attachment of *P. aeruginosa* are very similar and would need further investigation to understand the exact mechanisms. To see if the FimH functions as an anti-adhesion molecule, without using fluorescence to detect it, an attachment assay in the presences of the FimH molecule could be used. Although using the current microplate reader used in this study the difference between concentrations could not be determined using an attachment assay in the presence of FimH but by plating out all unbound *P. aeruginosa* would circumvent this problem. It would also be interesting to see the level of attachment using epithelia cells. During a *P. aeruginosa* infection the bacterium would come into contact and attach to epithelia cells as part of the initial stages of infection. The main idea behind anti-adhesion therapy is to stop this initial attachment and therefore help prevent the spread of the bacteria. By stopping the attachment of the bacteria to epithelia cells the bacteria would not be able to gain as much nutrients from the host cells as direct contact between *P. aeruginosa* and the host is need to extract optimal nutrient levels. This would mean *P. aeruginosa* could not proliferate as much and the rate at which the infection spreads would be slowed down. This would allow for the body's immune system to have a higher chance of clearing the infection.

LDH

Lactate dehydrogenase (LDH) is an enzyme that is released when macrophages are lysed. To understand if during a *P. aeruginosa* infection the bacteria are able to overcome the hosts natural defence, the immune system, LDH release assay were performed. The test works by reducing NAD⁺ to NADH/H⁺ through the LDH catalyzed conversion of lactate to pyruvate. Diaphorase is a catalyst in the LDH Cytotoxicity Detection Kit which transfers the H/H⁺ from NADH/H⁺ to the tertazolium salt INT, reducing it to a formazan dye which is red in colour. The optimal wavelength for measuring this colourimetric assay is at 500 nm but when initial absorbance readings were taken at this wavelength the values rapidly reached 2 at which point there is no direct correlation between LDH release and the level of absorbance. For this reason all readings were taken at 600 nm as there is minimal interference of the tertazolium salt INT and the formazan dye is still visible.

Two separate experiments were performed at an MOI of 10 over three hours. During both experiment four out of the six isolate produce negative lysis percentages although isolate 1007 had a very minimal negative lysis percentage. This indicates that compare to a negative control significantly less macrophage underwent lysis when infected with isolates 985, 992 and 1004. Graph A in figure 9 shows that this negative lysis was continuous where as graph B shows variation over the three hours. Interestingly between the start and finish of the three hours there is only a maximum of and 18% difference showing that although there was massive variation during one experiment there was little change in the lysis percentage. At an MOI of 1 over three

hours there was also minimal difference in lysis percentage with all isolates except 1009 having <25% difference. One interesting difference between and MOI of 10 and 1 is that there are less negative values at an MOI of 1. This could indicate that at a low MOI the *P. aeruginosa* has less of an effect on macrophages releasing less LDH than macrophages in the negative control.

The level of LDH release was also measure over an hour time period to see how quickly the *P. aeruginosa* have an effect on macrophages. At an MOI of 1 there is a little difference over the one hour period with all isolates having <18% difference in lysis. With an MOI of 10 the macrophage experienced a massive drop within the first 20 minutes of lysis percent for isolates 1004, 1007, 1008, 1009. After 20 minutes there is no variation over the next 40 minutes indicating that as soon as the *P. aeruginosa* is introduced there is a high percent of lysis. This initial high lysis percentage was also seen at an MOI of 1 but it was maintained throughout the hour where as at an MOI of 10 there was a significant drop within the first 20 minutes. The difference between the initial lysis percentages in the long (3 hours) and short (1 hour) infection period shows that optimisation of the protocol is necessary in order to obtain reproducible results. To get a clearer picture of what happens to macrophages a longer time course would be needed.

Conclusion

Anti-adhesion therapy is a potentially a new method of treating infections caused by pathogenic bacteria. Antibiotic treatment can lead to bacteria evolving resistance to such molecules much faster than new ones are discovered. Anti-adhesion therapy has the potential to reduce the evolution of resistance by putting the bacterial pathogen under little or no selective pressure allowing the host's immune system to combat the infection. To assess the population and evolutionary dynamics of bacteria during anti-adhesion therapy six clinical isolates of *Pseudomonas aeruginosa* were obtained from the QE hospital in Birmingham.

The isolates showed varying levels of resistance to imipenem and meropenem when tested at the QE with isolate 1007 being resistant to imipenem and insensitive to meropenem. When tested during this study, all isolates were found to be resistant to imipenem and all except isolate 1004 were sensitive to meropenem. When grown in LB all isolates proliferated at the same rate regardless of their antibiotic susceptibility. As all isolates were resistant to imipenem it was no surprise that they were all able to grow at the same rate when incubated with varying level of imipenem. When the isolates were incubated with different concentrations of meropenem only the resistant isolate (1004) was able to maintain level OD readings over the 20 hour period. All susceptible isolates showed a decrease in OD indicating they were being killed by the antibiotic.

To understand how *Pseudomonas aeruginosa* interacts with the immune system which is a vital part in the elimination of infections the six isolates where

incubated with J774 macrophages. The level of attachment and lysis was measured using an attachment assay and LDH release assay. The attachment measured the amount of bacteria that are able to become attached to the macrophages but does not show if the bacteria are binding to the macrophages or the macrophages are phagocytosing the bacteria. The assay showed that double the amount of meropenem resistant isolate attached compared to all other isolates. The LDH release assay measured the level of macrophage lysis over a 3 hour and 1 hour period. The level of lysis fluctuated over the three hours but there was only a maximum difference of 25% in the level of lysis. This showed that at both an MOI of 1 and 10 there is no change in the amount of lysis and further times should be investigated to gain a more detailed analysis.

Unfortunately the fluorescence FimH anti-adhesion molecule was not able to be measured on the micro plate reader used in this study. The emission wavelength incorporated into the micro plate reader was at 460 nm instead of 375 nm which is the optimal wavelength of the FimH molecule. This meant that any concentrations below 1mM were not able to be distinguished from each other. The fluorescent intensity of *P. aeruginosa* was too intense at this emission wavelength and even at a low OD of 0.3 the fluorescent intensity was around the same level as the FimH molecule at high concentrations. This meant that the anti-adhesion parameter could not be assessed but experimental data for the other parameters such as growth and killing rate and phagocyte interactions can be used to improve mathematical models.

References

- Almant M, Moreau V, Kovensky J, Bouckaert J, Gouin SG, (2011) Clustering of Escherichia coli type-1 fimbrial adhesins by using multimeric heptyl α -Dmannoside probes with a carbohydrate core. *Chemistry*; 17:10029-38.
- Anderson BN, Ding AM, Nilsson LM, Kusuma K, Tchesnokova V, Vogel V, (2007). Weak rolling adhesion enhances bacterial surface colonization. *J Bacteriol*; 189:1794-802.
- Birnbaum J, Kahan FM, Kropp H, MacDonald JS, (1985). Carbapenems, new class of beta-lactam antibiotics. Discovery and development of imipenem/cilastatin. *Am J Med*; 78(6A):3-21.
- Boeser KD, (2008) Are all carbapenems the same? *PharmD Infectious Disease News*.
- Cambray G, Guerout AM, and Mazel D. (2010). Integrons. *Annu. Rev. Genet*; 44: 141–166.
- Chemani C, Imberty A, de Bentzmann S, Pierre M, Wimmerová M, Guery BP, Faure K. (2009). Role of LecA and LecB lectins in Pseudomonas aeruginosa-induced lung injury and effect of carbohydrate ligands. *Infect Immun*; 77:2065-75.
- Drissi M, Ahmed Z B, Dehecq B, Bakour R, Plesiat P and Hocquet D. (2008). Antibiotic susceptibility and mechanisms of β -lactam resistance among clinical strains of *Pseudomonas aeruginosa*: first report in Algeria. *Med. Mal. Infect*; 38: 187–191.

El Gamal M I, and Oh CH. (2010). Current Status of carbapenem anti-biotics. *Curr. Top. Med. Chem*; 10: 1882–1897.

Gupta V. (2008). Metallo β -lactamases in *Pseudomonas aeruginosa* and *Acinetobacter* species. *Expert Opin. Investig. Drugs*; 17: 131–143.

Han Z, Pinkner JS, Ford B, Chorell E, Crowley JM, Cusumano CK, (2012). Lead optimization studies on FimH antagonists: discovery of potent and orally bioavailable ortho-substituted biphenyl mannosides. *J Med Chem*; 55: 3945-59.

Hartmann M, Papavlassopoulos H, Chandrasekaran V, Grabosch C, Beiroth F, Lindhorst TK, (2012). Inhibition of bacterial adhesion to live human cells: activity and cytotoxicity of synthetic mannosides. *FEBS Lett*; 586:1459-65.

Hubbard LL, Wilke CA, White ES, Moore BB. (2011). PTEN limits alveolar macrophage function against *Pseudomonas aeruginosa* after bone marrow transplantation. *Am J Respir Cell Mol Biol*; 45:1050-8

Jiang X, Abgottspon D, Kleeb S, Rabbani S, Scharenberg M, Wittwer M, (2012). Antiadhesion therapy for urinary tract infections--a balanced PK/PD profile proved to be key for success. *J Med Chem*; 55:4700-13.

Jones RN. (1998). Important and emerging β -lactamase-mediated resistances in hospital-based pathogens: the Amp C enzymes. *Diagn. Microbiol. Infect. Dis*; 31: 461–466.

Jones RN, Stilwell M G, Rhomberg PR, and Sader HS. (2009). Antipseudomonal activity of piperacillin/tazobactam: more than a decade of experience from the SENTRY Antimicrobial Surveillance Program (1997–2007). *Diagn. Microbiol. Infect. Dis*; 65: 331–334.

Krachler AM, Orth K. (2013). Targeting the bacteria-host interface Strategies in anti-adhesion therapy. *Virulence*; 4: 284–294

Klein T, Abgottspon D, Wittwer M, Rabbani S, Herold J, Jiang X, (2010). FimH antagonists for the oral treatment of urinary tract infections: from design and synthesis to in vitro and in vivo evaluation. *J Med Chem*; 53:8627-41.

Livermore DM. (1992). Interplay of impermeability and chromosomal β -lactamase activity in imipenem-resistant *Pseudomonas aeruginosa*. *Antimicrob. Agents Chemother*; 36: 2046–2048.

Loveday H.P. et al. (2014). Association between healthcare water systems and *Pseudomonas aeruginosa* infections: a rapid systematic review. *The Journal of hospital infection*; 86:7–15.

Lovewell RR, Patankar YR and Berwin BL. (2014). Mechanisms of Phagocytosis and Host Clearance of *Pseudomonas aeruginosa*. *American journal of physiology. Lung cellular and molecular physiology*.

Morita Y, Tomida J and Kawamura Y. (2014). Responses of *Pseudomonas aeruginosa* to antimicrobials. *Frontiers in microbiology*; 4: 4422.

Okamoto, K., Gotoh, N., and Nishino, T. (2002). Alterations of susceptibility of *Pseudomonas aeruginosa* by over-production of multidrug efflux systems, MexAB-OprM, MexCD-OprJ, and MexXY/OprM to carbapenems: substrate specificities of the efflux systems. *J. Infect. Chemother*; 8: 371–373.

Pai H, Kim J, Kim J, Lee JH, Choe KW and Gotoh N. (2001). Carbapenem resistance mechanisms in *Pseudomonas aeruginosa* clinical isolates. *Antimicrob. Agents Chemother*; 45: 480–484.

Papp-Wallace KM, Endimiani A, Taracila MA, Bonomo RA. (2011). Carbapenems: Past, Present, and Future. *Antimicrob Agents Chemother*; 55 :4943-60

Pinkner JS, Remaut H, Buelens F, Miller E, Aberg V, Pemberton N, (2006). Rationally designed small compounds inhibit pilus biogenesis in uropathogenic bacteria. *Proc Natl Acad Sci USA*; 103:17897-902

Poole, K. (2004). "Efflux pumps," in *Pseudomonas, Vol. 1. Genomics, life style and molecular architecture*; 635–674.

Poole, K. (2007). Efflux pumps as antimicrobial resistance mechanisms. *Ann. Med;* 39: 162–176.

Poole, K. (2011). *Pseudomonas aeruginosa*: resistance to the max. *Frontiers in microbiology*; 2:65.

Queenan AM and Bush K. (2007). Carbapenemases: the versatile β -lactamases. *Clin. Microbiol. Rev*; 20: 440–458.

Radin NS, (2006). Preventing the binding of pathogens to the host by controlling sphingolipid metabolism. *Microbes Infect*; 8:938-45;

Salabi AE, Toleman MA, Weeks J, Bruderer T, Frei R and Walsh TR. (2010). First report of the metallo- β -lactamase SPM-1 in Europe. *Antimicrob. Agents Chemother*; 54:582.

Scharenberg M, Schwardt O, Rabbani S, Ernst B, (2012). Target Selectivity of FimH Antagonists. *J Med Chem*; 55:9810-6;

Schurek KN, Breidenstein EBM and Hancock REW. (2012). *Pseudomonas aeruginosa*: a persistent pathogen in cystic fibrosis and hospital-associated infections in *Antibiotic Discovery and Development*; 1 :679–715.

Svensson A, Larsson A, Emtenäs H, Hedenström M, Fex T, Hultgren SJ, (2001). Design and evaluation of pilicides: potential novel antibacterial agents directed against uropathogenic *Escherichia coli*. *Chembiochem*; 2:915-8;

Svensson M, Frendeus B, Butters T, Platt F, Dwek R, Svanborg C. (2003) Glycolipid depletion in antimicrobial therapy. *Mol Microbiol*; 47:453-61

Tomas M, Doumith M, Warner M, Turton JF, Beceiro A, Bou G, Livermore DM, and Woodford N. (2010). Efflux pumps, OprD porin, AmpC β -lactamase, and multiresistance in *Pseudomonas aeruginosa* isolates from cystic fibrosis patients. *Antimicrob. Agents Chemother*; 54:2219–2224.

Trias J, and Nikaido H. (1990). Outer membrane protein D2 catalyzes facilitated diffusion of carbapenems and penems through the outer membrane of *Pseudomonas aeruginosa*. *Antimicrob. Agents Chemother*; 34: 52–57.

Vettoretti L, Floret N, Hocquet D, Dehecq B, Plesiat P, Talon D and Bertrand X. (2009). Emergence of extensive-drug-resistant *Pseudomonas aeruginosa* in a French university hospital. *Eur. J. Clin. Microbiol. Infect. Dis*; 28: 1217–1222.

Villegas MV, Lolans K, Correa A, Kattan JN, Lopez JA and Quinn JP. (2007). First identification of *Pseudomonas aeruginosa* isolates producing a KPC-type carbapenem-hydrolyzing β -lactamase. *Antimicrob. Agents Chemother*; 51: 1553–1555.

Walsh TR. (2010). Emerging carbapenemases: a global perspective. *Int. J. Antimicrob. Agents*; 36: 8–14.

Walsh TR, Toleman MA, Poirel L and Nordmann P. (2005). Metallo- β -lactamases: the quiet before the storm? *Clin. Microbiol. Rev*; 18: 306–325.

- Wolter DJ, Kurpiel PM, Woodford N, Palepou MF, Goering RV and Hanson ND (2009). Phenotypic and enzymatic comparative analysis of the novel KPC variant KPC-5 and its evolutionary variants, KPC-2 and KPC-4. *Antimicrob. Agents Chemother*; 53: 557–562.
- Yuehuei H, Dickinson RB, Doyle RJ. (2000). Molecular Basis of Bacterial Adhesion. In: Yuehuei H. An, Friedman RJ, eds. *Handbook of Bacterial Adhesion Principles, Methods, and Applications*: Springer; 29-41.
- Zhao WH, and Hu ZQ. (2010). B-lactamases identified in clinical isolates of *Pseudomonas aeruginosa*. *Crit. Rev. Microbiol*; 36: 245–258.
- Zilberberg MD, Chen J, Mody SH, Ramsey AM and Shorr AF. (2010). Imipenem resistance of *Pseudomonas* in pneumonia: a systematic literature review. *BMC Pulm. Med*; 10: 45

Molecular and Cellular MRes Project 2

**The purification and crystallization of five *Bdellovibrio* proteins used
during attack phase**

Abstract

Bdellovibrio bacteriovorus are small highly motile predatory bacteria capable of invading Gram negative bacteria. Once inside the host *Bdellovibrio* use the nucleic acids, proteins and other macromolecules to grow and then divides depending how much nutrients are available. It then exits the host and returns to hunting down its next prey. During this attack phase when *Bdellovibrio* comes into contact with its prey certain proteins are up regulated. Some of these proteins are located at the invading nose of *Bdellovibrio* and five of these proteins; Bd 2093, 1482, 3099, 3100 and RomR are examined in this study. The aim of this project was to purify and concentrate these five proteins in order produced crystals for x-ray diffraction. Bd 1482, 3099, 3100 and RomR were produced in this study but only RomR was soluble. All the other were insoluble proteins but Bd 3099 was able to be refolded in both Tris and CHES buffer and purified to 20 and 40 mg/mL respectively. Bd 3099 was also purified to around 7 mg/mL using an off column purification protocol. Bd 1482 and 3100 were refold in a sodium acetate (NaAc) but was not purified. RomR was purified using affinity chromatography to around 20 mg/mL to create a crystal of a high enough standard for x-ray diffraction which diffracted at around 9 angstroms.

Introduction

Aims and Objectives

The overall aim of this study was to crystallise *Bdellovibrio* proteins that are used during predation and gain structural knowledge through x-ray crystallography. In order to create protein crystals, the protein has to be at a high concentration, at least 10mg/ml and at least 99% pure. This means cloning the correct gene, transforming it into an *E. coli* expression strain and then expressing the protein. The protein then has to be purified, concentrated and crystallised. This study examines five different *Bdellovibrio* proteins: Bd 1482, 2093, 3099, 3100 and RomR and how well they are able to be purified and crystallised. Each of these proteins are thought to be involved in the predatory actions of *Bdellovibrio*, either sensing prey or attaching to them, so gaining structural information could prove to be very valuable. *Bdellovibrio* has the potential to be a “living antibiotic”, but only if we can control it and the structures of these proteins may be able to shed light on this problem. These proteins may also have homologous proteins in other pathogenic organisms and understanding the way these proteins function may help the fight against these organisms and even reduce antibiotic resistance.

Bdellovibrio Lifecycle

Bdellovibrio bacteriovorus are small highly motile δ -proteobacteria capable of killing other Gram negative bacteria. They accomplish this by preying on Gram negative bacteria, invading them and replicating within their periplasm. Since its discovery in 1962, *Bdellovibrio* has gone through physiological and biochemical studies in the 1960 and 70's, then recombinant DNA studies in the 1990's which has directed the work towards molecular studies in the 21st century (Sockett, 2009). The recombinant DNA and protein studies will help us understand the precise mechanisms which control the different parts of the complex predatory lifecycle of *Bdellovibrio*. The way in which *Bdellovibrio* has a unique ability to invade and destroy Gram negative bacteria can be used to mankind's advantage once these mechanisms are fully explored. It is well known that antibiotic resistance is on the rise and new ways of treating resistant bacteria are needed. *Bdellovibrio* could be used a new form of antibiotic termed "living antibiotic" as it is able to kill pathogenic Gram negative bacteria such as *Pseudomonas*, *E. coli* and *Salmonella* (Dwidar, 2012). Water treatment and crop protection are two other areas in which *Bdellovibrio* may one day be utilised to replace current strategies.

The typical life cycle of *Bdellovibrio* is through a host-dependent (HD) manner (figure 1). However there is a small percentage of around 1 in 10^7 that are able to survive in a host-independent (HI) fashion. *Bdellovibrio* are polar rod shaped bacteria around 0.2-0.5 μm wide and 0.5-2.5 μm in length and are capable of swimming up to 160 $\mu\text{m sec}^{-1}$ (Hobely, 2012; Lambert, 2006). The propulsion system on these highly

motile bacteria is a single sheathed flagellum at the tail end which used to move liquid medium. Movement on solid surfaces is through the use of gliding motility machinery such as adventurous gliding proteins (Lambert, 2011). Investigations into the exact proteins involved are still ongoing but it is thought that cyclic-di-GMP is involved in the regulations of gliding motility. It has been suggested *Bdellovibrio* can sense prey through chemotaxis in prey rich areas, potentially even biofilms. What is known is that *Bdellovibrio* will only prey on Gram negative bacteria and are able to distinguish them from inert objects and Gram positive bacteria. The vast majority of *Bdellovibrio* grow within the periplasm which is only found in Gram negative bacteria. This first stage is known as the attack phase where the *Bdellovibrio* are highly motile ready to find their next target.

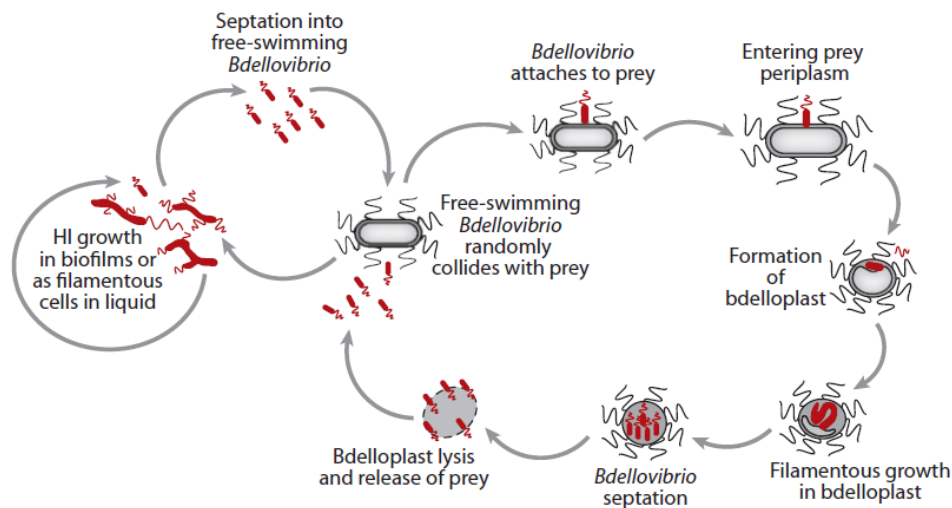


Figure 1: The host dependent (HD) and host independent (HI) life cycles of *Bdellovibrio* (Sockett, 2009).

Once a potential prey has been sensed, *Bdellovibrio* is able to attach itself using type IV pilli (Sockett, 2009). This initial recognition and attachment phase last between 5-10 minutes (figure 2). Once tightly bound *Bdellovibrio* will proceed to create a small pore around 200nm across using hydrolytic enzyme that solubilise and alter the peptidoglycan found in the outer membrane (Lambert, 2006). The exact amount and precise function of some of these enzymes are unknown but recent research suggests that upon attachment many genes are upregulated and localised at the nose of *Bdellovibrio*. Some of these proteins will be used in the direct attachment of *Bdellovibrio* to its prey and others for signalling in predatory pathways. *Bdellovibrio* is able to squeeze itself through the pore into the periplasmic space between the inner and outer membrane of its prey, creating its own niche (Lerner, 2012). The large flagellum is now cleaved off and the pore in which the *Bdellovibrio* entered is sealed up using altered lipopolysaccharide (LPS) (Sockett, 2009).

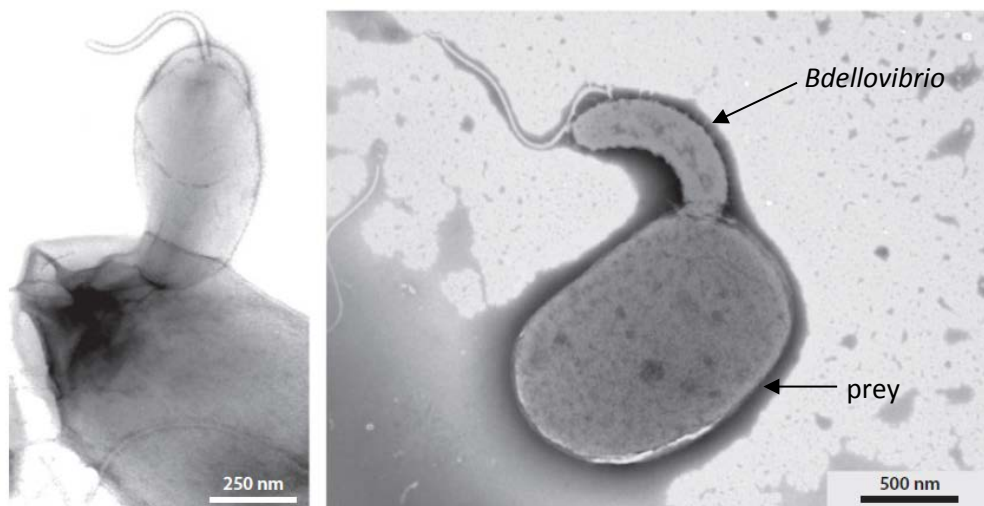


Figure 2: *Bdellovibrio* attaching to its prey (Sockett, 2009). Arrow showing the attachment of the nose of *Bdellovibrio* to its prey.

After about 25 minutes a bdelloplast is formed by rounding of the host cell membrane using proteins to create a pseudo-exoskeleton and by altering the host's peptidoglycan. This makes sure all the nutrients and macromolecules stay within the host and the host does not burst before full replication has occurred. Another advantage of this bdelloplast is the protection it gives *Bdellovibrio*, as other predators will not invade the host once the bdelloplast is formed. The *Bdellovibrio* can now start to enzymatically digest the hosts DNA, proteins and other macromolecules using them as nutrients to grow. *Bdellovibrio* first grows as a long filamentous progeny replicating its DNA as many times as possible before the nutrients within the host are exhausted (Sockett, 2009; Lambert, 2006). The single large filamentous progeny will then separate into smaller progeny according to how many times the DNA has been replicated which can be either an odd or even amount (Shilo, 1969). This growth and development stage takes around an hour and is capped off by synthesising new flagellar for the new progeny.



Figure 3: The progeny of a *Bdellovibrio* that has replicated with its host (Sockett, 2009).

Once mature the progeny will lyse the host membrane and return to attack phase hunting down its next victim. It has been shown that although the vast majority of *Bdellovibrio* are host-dependent around 1 in 10^7 are able to survive independently of hosts (figure 4). The host-independent life cycle depicted in figure 2 shows that *Bdellovibrio* can replicate outside of the host by forming biofilms or filamentous cells (Sockett, 2009). They are also able to enter attack phase when prey is sensed splitting off into free-swimming *Bdellovibrio* searching for its next host.

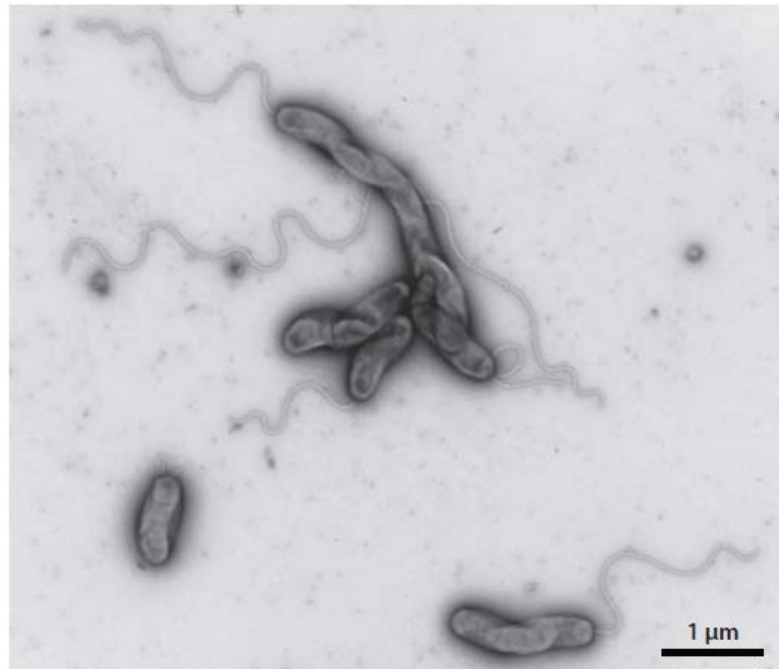


Figure 4: Host independent living of *Bdellovibrio* in a biofilm formation (Sockett, 2009).

Bdellovibrio Proteins

During predation *Bdellovibrio* upregulate certain proteins towards its polar nose and it is thought that because of the timing and location of these proteins they are involved in the invasion process either directly or by acting as signalling proteins. This study looks at some of these proteins in more detail with the ultimate goal of producing crystal structures. Five proteins were examined during this study of which little is known about their structure or function. The most well characterised protein is RomR (Bd 2176). Two proteins (Bd 1482 and Bd 3100) contain PilZ domains and are involved in cyclic-di-GMP (c-di-GMP) signalling. Bd 3099 which is homologous to Bd 1483 is a MIDAS protein and is believed to be involved in metal binding. The least well characterised is Bd 2093 is assumed to be implicated in the adhesion process.

Both Bd 1482 and 3100 contain GYF and PilZ domains with Bd 1482 only having one GYF and Bd 3100 possessing two GYF domains. PilZ domain proteins acts as effector proteins that can bind c-di-GMP, a secondary messenger involved in bacterial life style choices such as biofilm formation, motility and virulence. Studies have shown that by knocking out proteins that are involved in synthesising c-di-GMP *Bdellovibrio* phenotype completely changes. As PilZ domain proteins are effector proteins for c-di-GMP it indicates that PilZ domains are implicated in the virulence of *Bdellovibrio* most likely through the action of c-di-GMP and therefore good candidates for structural studies. GYF domains are known to bind proline rich sequences but not much is known about their function in *Bdellovibrio* (Kofler, 2005).

C-di-GMP in *Bdellovibrio*

Cyclic-di-GMP is a secondary messenger known to have an effect on bacterial lifestyle choices. In proteobacteria which *Bdellovibrio* are included in c-di-GMP controls the switch between single motile cell and biofilm formation (Ryan). In *Bdellovibrio* this could translate to be the difference between host-dependent and host-independent stains. The synthesis of c-di-GMP is through diguanylyl cyclases contain GGDEF domains which in *Bdellovibrio* have been implicated in phenotypical changes. A study conducted by Hobley et al. (2012) deleted various GGDEF contain genes to find a variety of different phenotypical outcomes. Two opposite phenotypes were produce when deleting Dgc B (Bd 0742) and Dgc C (Bd 1434), which made an obligatory axenic mutant and an obligatory predatory mutant respectively. The deletion of Dgc A (Bd 0367) created a strange intermediate version, where gliding motility was eliminated, could still invade prey but not escape from within them. It is unclear if the deletion of Dgc A effected flagellar synthesis but what Hobley et al noted is that “at the 5’ end of one of 4 operons of gliding motility genes of *B. bacteriovorus*, there is a gene, Bd1482, encoding a PilZ domain protein, which may be a candidate for receiving signals from DgcA to effect gliding...”

This gives evidence that altering the c-di-GMP synthesis in *Bdellovibrio* the lifestyle of this bacterium is distorted. This could of course also happen if the expression or structure of phosphodiester (PDE) enzymes which are responsible for the degradation of c-di-GMP are modified. PDE enzymes contain EAL or HD-GYP domains and the HD100 *Bdellovibrio* strain incorporates 1 EAL and 6 HD-GYP domains. Within the HD100 strain of *Bdellovibrio* there are 5 enzymes containing

GGDEF domain of which three are stated above. These two enzymes, diguanylyl cyclases and phosphodiesterases are capable of synthesising and degrading c-di-GMP respectively, but it is the PilZ domain that is capable of binding c-di-GMP using it to convey a message. This message in *Bdellovibrio* can travel down either a predatory or axenic route with PilZ acting as an effector protein (Hobley, 2012; Amikam, 2006).

PilZ domain

It was thought that other than cellulose synthase there was no known proteins that binds c-di-GMP. The PilZ domain was first discovered in 1989 by Amikam and Benziman when labelled c-di-GMP was found to be mostly bound to the β -subunit of cellulose synthase BcsB in *Gluconacetobacter xylinus*. This data suggested that BcsB was the c-di-GMP bind protein but subsequent studies showed that the actual protein was a 200 kD membrane-bound protein complex. It was suggested by Saxena and Brown that this could be the dimer of the α -subunit or a second form of cellulose synthase. The PilZ domain is now known to be the c-di-GMP binding region of cellulose synthase. Since then the PilZ domain has been identified in a variety of bacterial species including *Bdellovibrio* (Amikam, 2006).

In many bacterial species of bacteria c-di-GMP is known to be involved in virulence pathways so it is no surprise that the PilZ domain is also found within these bacteria. In *P.aeruginosa* PilZ is encoded by the PA2960 gene which when mutated can produce normal amounts of pilin, but is unable to construct functional pili. In *Geobacter sulfurreducens* GSU3262 was found to have a PilZ domain with a REC domain accompany it which may imply a regulatory role. More than 600 sequences

were found when a PSI-BLAST search was done on the C-terminal fragment of GSU3262 over a variety of bacteria (Amikam, 2006). Interestingly the eukaryotic cellulose synthase found in slime mould *Dictyostelium discoideum* and marine urochordate *Ciona savignyi* contained no PilZ domain or GGGDEF domains and probably do not produce c-di-GMP. In *Bdellovibrio* the gliding and flagellar motility are affected by c-di-GMP signalling pathways and as it is known PilZ can bind c-di-GMP which would indicate that Bd 1482 and 3100 are implicated in motility.

RomR

RomR is a protein that has been found in two types of δ -proteobacteria, *Bdellovibrio bacteriovorus* and *Myxococcus xanthus* but has a different function in each of them. RomR in *M. xanthus* (RomR_{MX}) is known to be involved in gliding motility whereas in *B. bacteriovorus* (RomR_{BD}) it has been linked to predatory invasion (Milner, 2014). The work that was done on *M. xanthus* has helped further the understanding of *B. bacteriovorus* and its complex predatory and invasive lifestyle. There are many similarities between these two species but with minor differences and it is these minor differences that has enabled the characterisation of specific proteins and pathways. *M. xanthus* has two types of motility known as social (S-motility) and adventurous or gliding motility (A-motility). Just like *B. bacteriovorus*, *M. xanthus* uses type IV pili and can only be regulated at the polar end but the difference is that *M. xanthus* can switch which polar end that is (Kaiser, 2012; Milner, 2014). The type IV pili found in *M. xanthus* are used in the motility of the bacterium where as in

B. bacteriovorus they are used in the attachment to prey. It is the control of this polar switch in *M. xanthus* that has led to a clearer understanding of what RomR does in *B. bacteriovorus*.

B. bacteriovorus and *M. xanthus* are both bidirectional when using gliding motility which is very useful as this type of motility is much slower than using a flagellar system with *B. bacteriovorus* moving at $16 \mu\text{m hr}^{-1}$ and *M. Xanthus* travelling at $24\text{-}36 \mu\text{m hr}^{-1}$. The system that controls the polarisation and reversal of direction in *M. Xanthus* is known to be controlled by a Ras-like GTPase, MglA (Keilberg, 2012; Milner, 2014). MglA is need for the activation of both A and S motility and is controlled by a GTPase activating protein (GAP) MglB. When MglA is removed from *M. Xanthus* it is both A and S non-motile and has been shown, along with its interacting partner RomR, to control pole switching and therefore the bidirectional movement. A Frz chemosensory system sends signals to RomR which can then interact and regulate MglA in *M. Xanthus* but although RomR is conserved in *B. bacteriovorus* the Frz chemosensory is not (Keilberg). *B. bacteriovorus* does contain MglA in the HD100 genome but there is no MglB homologue, so what is the function of MglA and RomR in *B. bacteriovorus* is the gliding motility of *B. bacteriovorus* is controlled by cyclic-di-GMP.

It was shown by Milner et al (2014) that even though *B. bacteriovorus* does not contain a MglB homologue, MglA_{BD} does still play a role in the gliding behaviour but is not necessarily essential for gliding motility. MglA_{BD} was also proven to be necessary for invading prey and RomR_{BD} plays a key role in the growth of *B. bacteriovorus*. These two proteins were also found to interact with a previously

unknown binding partner known as a tetratricopeptide repeat protein (TRP) which has been linked to be required for predation. TRP and RomR were able to interact in a bacterial two hybrid experiment done by Milner et al (2014) and were also found to be expressed at the nose of *B. bacteriovorus* where it interacts with prey. Another protein that is localised at the invading pole was Bd 3125 which is degenerate GGDEF (GVNEF) known as CdgA. As mentioned before it is this GGDEF domain that is linked to a production of c-di-GMP a known secondary messenger in *B. bacteriovorus*. CdgA can interact with both RomR_{BD} and TRP_{BD} through a bacteria two-hybrid assay. As all of the proteins (CdgA, RomR and TRP) are all located at the invasive pole of *Bdellovibrio* and are shown to interact with each other, they could play a part in the invasion process. This is backed up by the fact when *romR*_{BD} was deleted for both host dependent and host independent strains of *B. bacteriovorus* it was not able to grow showing that RomR is needed for both types of growth.

How are these proteins involved with each other?

As mentioned before not much is known about BD 3099 other than it is thought to be a MIDAS protein capable of binding metal and Bd 2093 is assumed to be involved in the adhesion process of *Bdellovibrio* and has a predicted secondary structure of a β -barrel. This study intends to shed some light on the structure of these proteins and therefore their function. A little more is known about the three other proteins in this study Bd 1482, 3100 and RomR. Both Bd 1482 and 3100 have PilZ domains which can interact with c-di-GMP which is produced by BD 3125 (CdgA) at the invading nose of *Bdellovibrio*. RomR has been shown to interact with CdgA so

RomR could be a potential moderator of c-di-GMP production by CdgA and therefore influence the actions of Bd 1482 and 3100 through the PilZ domain. As all these proteins are thought to be located at the invading nose of *Bdellovibrio* it is believed that they are all involved in the invasion process either directly (Bd 2093) or indirectly through c-di-GMP signalling.

Materials and Methods

Plasmid preparation and PCR

In order to produce purified protein for crystallisation the correct gene has got to be cloned from genomic DNA and inserted into a plasmid. Once the correct gene is inserted into the plasmid it is propagated and then transformed into *E. coli* for production. Below are the steps taken in this polymerase chain reaction (PCR) process for Bd 2093 and Bd 3099. The other genes of interest in this study Bd 3100 and RomR had already gone through the two rounds of PCR and were successfully transformed into our expression strain of *E. coli* BL21.

1st round PCR or primer PCR is performed to identify and clone our gene of interest from *Bdellovibrio* genomic DNA. This was done by ordering both forward and reverse PCR primers that were specific to the gene. Primers were then diluted down to working stock concentration with dH₂O. Forward and reverse primers can either be added together in a primer mix or used separately. In the case of Bd 3099 and 2093 a primer mix solution was made up using 10 µl of each primer adding them to 80 µl of dH₂O. The PCR reagents were the same for both Bd 3099 and 2093 are as follows: 4 µl of the primer mix, 72.5 µl dH₂O, 20 µl of 5x Velocity buffer, 1 µl of 100mM dNTPs, 1 µl of 1/20 *Bdellovibrio* gDNA and 1.5 µl Velocity enzyme. The final 100 µl of primer PCR were made into 30 µl aliquots and placed into the PCR machine. Below is a table of the general primer PCR program that was used.

	Temperature (°C)	Time	Repeat
Initial denaturation	98	2 minutes	1
Denaturation	98	30 seconds	25-35
Annealing	50 -64	30 seconds	25-35
Extension	72	15-30 sec/kb	25-35
Final Extension	72	4-10 minutes	1

The annealing temperature used for Bd 3099 was 50°C whereas Bd 2093 used a range of annealing temperatures between 50 and 64°C as the optimal annealing temperature was unknown. The primer sequences for Bd 2093 and 3099 are as follows:

Bd 2093 forward primer:

GTTTAACTTTAAGAAGGAGATATACATATGGCGACTTTCGACGTGCCAGTCTCTG

Bd 2093 reverse primer:

GCTGCACTACCGCGTGGCACAAGCTTCACTGAAATAGTGCCATCTTGACTG

Bd 3099 forward primer:

CCTCGCTGCCAGCCGGCGATGGCCGCACAGAATGTGTCATTGATCTTC

Bd 3099 reverse primer:

CTCAGTGGTGGTGGTGGTCTCGAGGTTTCGCGTCTTTAGGTTTGAAATCC

Once the primer PCR was completed the amplified DNA were purified using a QI Aquick PCR Purification Kit and the manufactures instructions followed. The steps and reagents are as follows: 5x the volume of PB buffer added to 1x PCR products. In this case it was 500 μ l of PB buffer added to 100 μ l PCR products. This was placed into the spin column provided and span at 13,000 rpm for 60 seconds to bind the DNA to the column. The column was washed with 750 μ l of PE buffer by again spinning at 13,000 rpm for 60 seconds. Before eluting off with 30 μ l dH₂O the spin column was spun at 13,000 rpm for 60 seconds to get rid of any leftover PE buffer. The 30 μ l of purified primer PCR products were using in the 2nd round PCR.

2nd round PCR is performed using the 1st round products which is now the gene of interest. This is then inserted into the plasmid of choice. The plasmids used in this study were pET 26 for Bd 3099 and pET 41c for Bd 2093 for 2nd round PCR. Each of these plasmids contained a Kanamycin resistance gene, an IPTG promoter gene and a HIS tag. The process and reagents for 2nd round are as follow: 4 μ l 1st round PCR product, 20 μ l of 5x Velocity buffer, 1 μ l of 100mM dNTPs, 1.5 μ l pET 41c or 0.5 μ l of pET 26b, 1.5 μ l Velocity enzyme and made up to 100 μ l with dH₂O. The 2nd PCR program used was the same as stated above with the 100 μ l being separated into 30 μ l aliquots and spread across a range on annealing temperatures. This PCR was done without any restriction enzymes. After 2nd round PCR the products are cleaned up using 1 μ l of DNP1 per 100 μ l of PCR product and left for 1-2 hours at 37^oC, they were then purified using the same purification kit and protocol as stated above.

To analyze the 1st and second round PCR products they were ran on a 1% agarose gel containing 5 µl of SYBR green dye per 50 ml of gel. The gels were loaded with 4 µl 2nd round PCR product mixed with 2 µl loading dye and ran at 100 volts for 30 minutes to 1 hour. Using a gel photo machine the gels were imaged and analysed.

Competent Cells and Transformation

Once the gene of interest was successfully cloned and inserted into the correct plasmid it had to be amplified in DH5α cells and then transformed into BL21 cells. In order for this to work the cells have to be made competent to allow the plasmid into the cells. The protocol and reagents are the same for both types of cells and is as follows: a single colony from an overnight LB agar plate of streaked out cells was picked and used to inoculate 10 ml of LB which was incubated overnight at 37°C. 100ml LB was inoculated with 1ml of overnight culture and shaken at 37°C until an OD₆₀₀ of 0.5 is reached. The culture was then cooled on ice before being centrifuged for 5 minutes at 4°C at 4,000 rpm. The cell pellet was resuspended in 30ml of cold TFB 1 buffer and kept on ice for 90 minutes. This was then centrifuged for 5 minutes at 4°C at 4,000 rpm and resuspended in 4 ml of cold TFB 2 buffer. These were then aliquoted out, flash frozen in liquid nitrogen and frozen at -80°C.

Transformation of the plasmid into DH5α for plasmid amplification was done by adding 15 µl of 2nd round PCR to 100-120 µl of competent DH5α cells and left on ice for 30 minutes- 2 hours. They were then heat-shocked at 42°C for 60-90 seconds and placed back on ice for 60 seconds. 800 µl of LB was added to the cells and placed

in 37°C for 90 minutes then plated out on LB agar containing kanamycin and incubated overnight at 37°C.

Colony PCR was then done on a selection of DH5α colonies to determine if the colony contains the plasmid. Each colony is has a total reaction volume of 30 µl made up of half the total volume of Bio Mix Red, 2 µl of each primer (forward and reverse) at working concentrations and was made up with dH₂O. The PCR products are then run on a 1% agarose gel as above and the ones that contained the plasmid were then incubated overnight in 10 ml of LB at 37°C and subjected to a Mini Prep.

Once the colony had been incubated overnight 4 ml were centrifuged at 13,000 rpm for 3 minutes at room temperature. The pellet was resuspended in 250 µl of P1 buffer mixed then 250 µl P2 buffer was added and mixed. Finally 350 µl N3 buffer was added and mixed. This was centrifuged at 13,000 rpm for 10 minutes at room temperature and the supernatant was applied to the spin column provide in the Mini Prep Kit and spun through. The column was then washed with 500 µl of PB buffer followed by 750 µl of PE buffer. The plasmid was the eluted off with 50 µl of dH₂O and sent for sequencing. If the sequence was correct then the plasmid was transformed into the expression strain of *E. coli* BL21 using the same protocol as the DH5α cells.

Once the plasmid had successfully been transformed into BL21 cell a 10ml overnight culture was produced. This was then be aliquoted out and mixed 50/50 with 60% glycerol, flash frozen and stored at -80°C.

Protein Expression and Purification

To gain a high enough concentration and purity of the protein of interest, in this case Bd 1482, 3099, 3100 and RomR, the protein must be over-expressed and then purified. The protocol for this was as follows: 15 ml overnight cultures of BL21 *E. coli* in LB containing kanamycin (15 µl of 100mg/ml) were grown and then 5 ml was used to inoculate 500 ml of 2xLB containing kanamycin. This was then grown in a shaker at 37°C until a 0.5 OD₆₀₀ is reached at which point it was induced with either 50 µM (Bd 3099) and 500 µM (Bd 1482 and RomR) IPTG and incubated at 20°C for 24 hours. The cultures were then centrifuged at 6000 rpm for 6 mins with Fiberlight (JLA 10.5) rotor. The cell pellet was then resuspended in 30mL of Buffer A (20mM Imidazole, 300mM NaCl, 0.05% Tween 20 (pH 7)) and tumbled for 30-40mins at RT. This was then sonicated 6 x 20 sec ON and 2 mins OFF while on ice and then centrifuged at 20,000 rpm for 1 hour at 4°C.

If the protein was contained in the soluble supernatant according to an SDS PAGE gel, it was loaded onto a 1mL nickel affinity column and purified on an AKTA purification system. The column was first primed with 50 mM NiSO₄ and equilibrated with a buffer A. Once the supernatant was loaded onto the column the column was washed with buffer A and then attached to the AKTA. Buffer A was passed over the column until a base line was established. The protein was eluted by increasing the amount of buffer B (500 mM Imidazole, 300 mM NaCl and 0.05% Tween 20) at 10% increments. Once the correct amount of buffer B was reached and all the protein was eluted off the fractions were pooled together into a dialysis bag with a molecular

weight cut off of 30 kD or 10 kD and dialysed overnight in 20mM Hepes, 200mM NaCl (2L pH 7). The protein concentration was then measured using Bradford reagent and concentrated using a 30 kD molecular cut off spin concentrator spun at 4000rpm at 4°C until the concentration reaches 10 mg/ml or higher. This was then flash frozen in liquid nitrogen in 50 µL aliquots and stored at -80°C for crystallization.

If the protein was contained in the insoluble pellet of the centrifuged culture then it was tumbled in 30 ml of 20mM Hepes, 200mM NaCl, 2% w/v Triton X (pH 7.5) for 2 hours at RT. After which it was centrifuged at 16,000 rpm (20,000 g) for 25 mins. The pellet was then tumbled overnight in a low imidazole GuHCl Buffer (20mM Tris-HCl, 0.5M NaCl, 5mM Imidazole, 6M GuHCl and 1mM beta-mercaptoethanol). This was then centrifuged at 16,000 rpm (20,000 g) for 25 mins and the supernatant was kept. If the supernatant was still cloudy and containing contaminants it was centrifuged in an ultra-centrifuge at 50,000 rpm for 30 minutes. The supernatant was then loaded on a nickel affinity purification column which had been equilibrated with low imidazole GuHCl buffer. The column was then washed with the low imidazole GuHCl buffer (at least 3x bed volume) before elution with high (500mM) imidazole GuHCl buffer (at least 3x bed volume) and the elution fractions were collected. The protein concentration was measured using Bradford reagent and if needed was dilute to around 5 mg/ml in 0mM imidazole, 6M urea. The protein was then examined in a buffer screen to determine which buffer was optimal for refolding. The buffer screen was set up in 2 ml cuvettes and measured at 340nm. The buffer screen is comprised of 4 different buffers at 50mM with 6 different additives over a pH range as shown below.

Buffer Screen Table:

	EDTA 1mM	B-ME 10mM	NaCl 200mM	KCl 100mM	NDSB 100mM	20% Glucose
NaAc pH 4						
MES pH 5.5						
Tris pH 7						
CHES pH 8.5						

Layout of the buffer screen comprising of four different buffers over a pH range and the six different additives added to each of the buffers.

50µl of the protein diluted protein (around 5 mg/mL) was added to 950µl of the buffers. The one with the lowest OD was then scaled up and the eluted protein was dilute 1/20 into the chosen buffer. This was then loaded onto either a nickel or ion exchange column depending of the buffer used in the previous step. Once eluted with either buffer B for the nickel column or a high salt buffer for the ion exchange the purified protein was dialysed overnight in 20mM Hepes or Tris 200mM NaCl (2L at pH 7). The protein concentration was measure using Bradford reagent and then concentrated using a spin concentrator with a 30 or 10 kDa MWCO at 4,000 rpm at 4°C until a concentration of 10mg/ml of higher is reached.

Crystallization:

RomR was the only protein that was I able to be purify to a high enough concentration and purity that would enable crystallization. Three crystal screens were used to get a variety of different conditions. The three crystal screens were PACT, JCSG+ and Proplex, all from Molecular Dimensions. In each of the screens RomR was used at a concentration of around 20 mg/ml. The screens were performed in 96 sitting drop trays with each of the tray containing all condition from that individual screen. The reservoir for all the different conditions was 120 μ l and the drop size was 1.8 μ l. To seal the sitting drop trays Crystal Clear tape was used and the trays were stored at 18°C. The trays were checked regularly until crystals were formed. Once crystals were form they were extracted then placed into the same conditions and a cryoprotectant was added based on the condition used. These were then sent to the Diamond Light Scource Synchrotron to be diffracted and gain a diffraction pattern.

Results

PCR and Sequencing

PCR was performed on Bd 2093 and Bd 3099 with Bd 3100 and RomR, prior to this study, successfully cloned and transformed into BL21. Primary, secondary and colony PCR was carried out on Bd 2093 and 3099. Bd 1482 had already been transformed in DH5 α cells so only colony PCR was completed.

Primary and Secondary PCR

Bd 2093 and 3099 both underwent the primary and secondary PCR protocols as stated in the materials and methods section. The annealing temperature for primary PCR was at 50°C for Bd 3099 and Bd 2093 was done over a range of temperatures to confirm the optimum temperature. Figure 1 shows the analysis of the agarose gels of Bd 3099 (A) and Bd 2093 (B). These results show that a fragment of *Bdellovibrio* DNA was extracted and amplified. It is unknown at this point whether this fragment is the correct gene. Secondary PCR was performed to insert the DNA fragment into our chosen plasmid which was pET 26b for Bd 3099 and pET 41c for Bd 2093. The results for Bd 2093 in figure 2 shows that over the range of annealing temperatures the pET 41c plasmid was amplified but does not confirm if it contains our gene of interest. No data is available for the second round of PCR on Bd 3099.

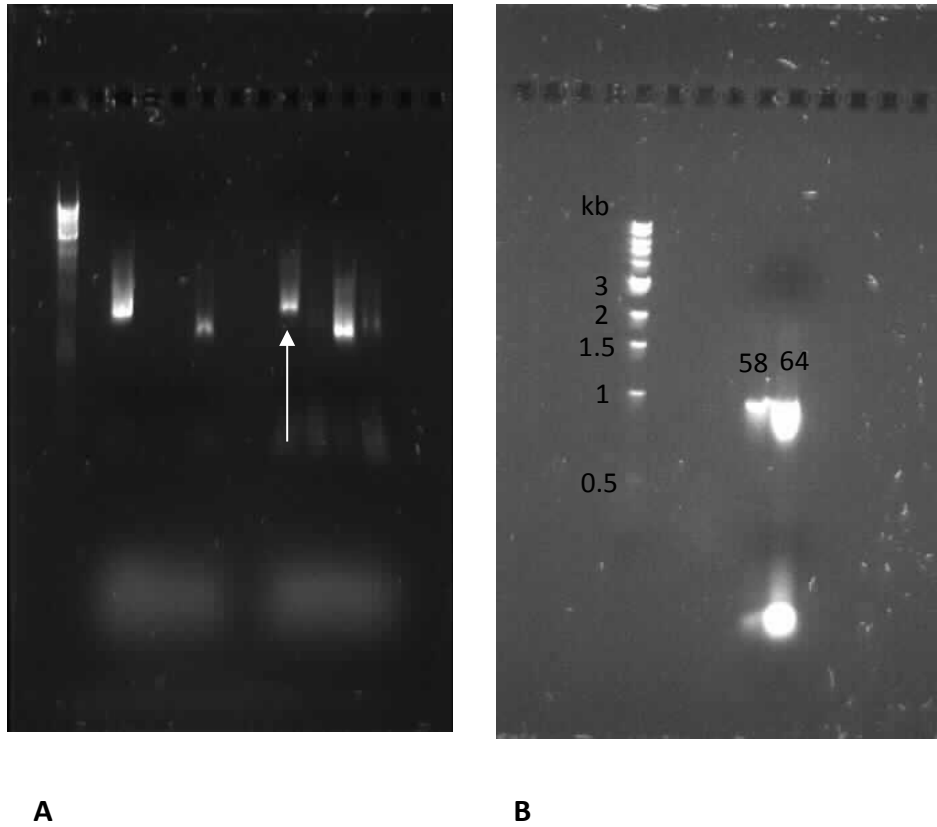


Figure 1: First round PCR products of Bd 3099 (A) and Bd 2093 (B). The arrow in A shows the Bd 3099 DNA fragment. B shows the DNA fragment of Bd 2093 at 58 and 64°C. Both gels were 1% agarose in TBE and contained SYBR DNA dye.

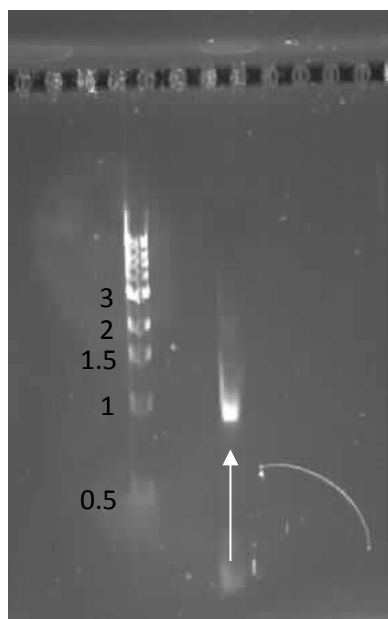
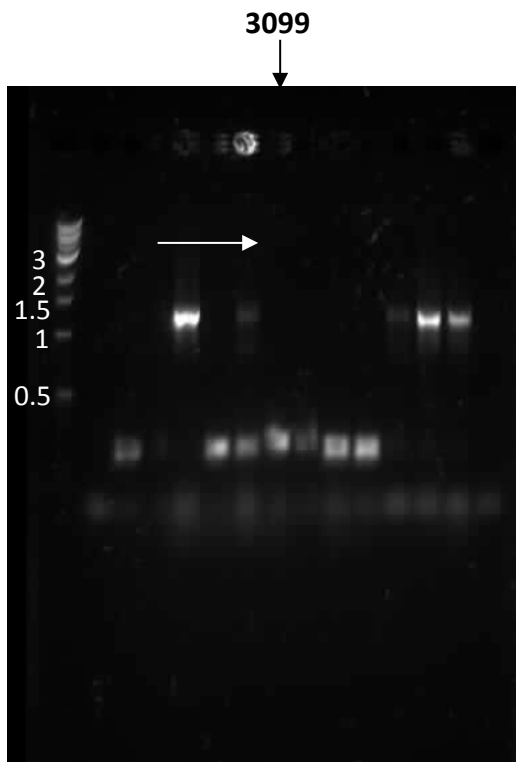


Figure 2: Second round Bd 2093 product. The arrows shows the position of the pET 41c plasmid but still unconfirmed if it contains the Bd 2093 gene. Sample was run on a 1% agarose gel in TBE and contained SYBR DNA dye.

Colony PCR and Sequencing

To confirm if the plasmids were transformed into DH5 α cell colonies PCR and sequencing were carried out. Figure 3 shows the results for the colony PCR of Bd 3099 (A) and Bd 2093 (B and C). It is clear that the Bd 3099 plasmid was not successfully transfected into the DH5 α cells and Bd 2093 showed a complete lack of any transformation in all three of the colonies (figure 3 B) when colony PCR was performed. After a Mini Prep was executed to produce more plasmid it was confirmed by the bands in figure 3C that the Bd 2093 plasmid was present in all three colonies. Colony PCR was also performed a second time on five more Bd 3099 DH5 α colonies and two of these colonies contained plasmids, data not shown. The two Bd 3099 and three Bd 2093 colonies were then sent off sequencing at the University of Birmingham. The sequencing data showed that Bd 3099 was successfully incorporated into the pET 26b plasmid and was successfully transformed into the BL21 expression strain. Bd 2093 had unfortunately not been integrated in the pET 41c plasmid. Due to time constraints Bd 2093 was not taken any further. Colony PCR and sequencing was also performed on Bd 1482, data not shown, which verified the correct gene was incorporated in the plasmid and was then successfully transformed into BL21 cells.

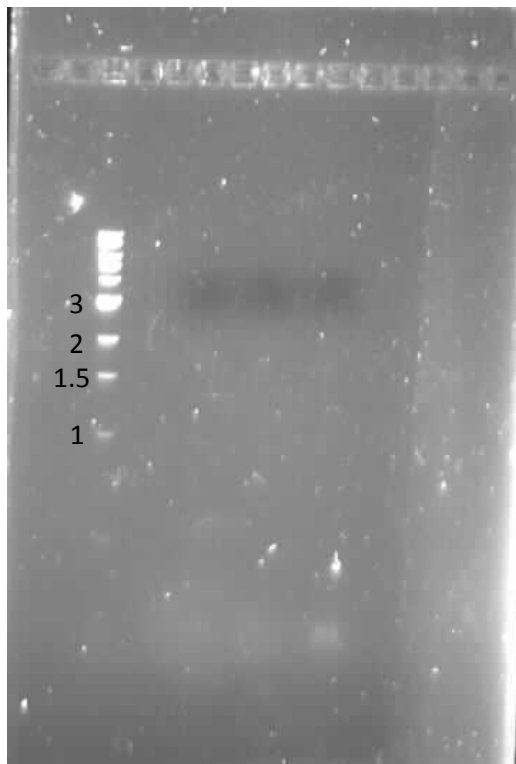


A

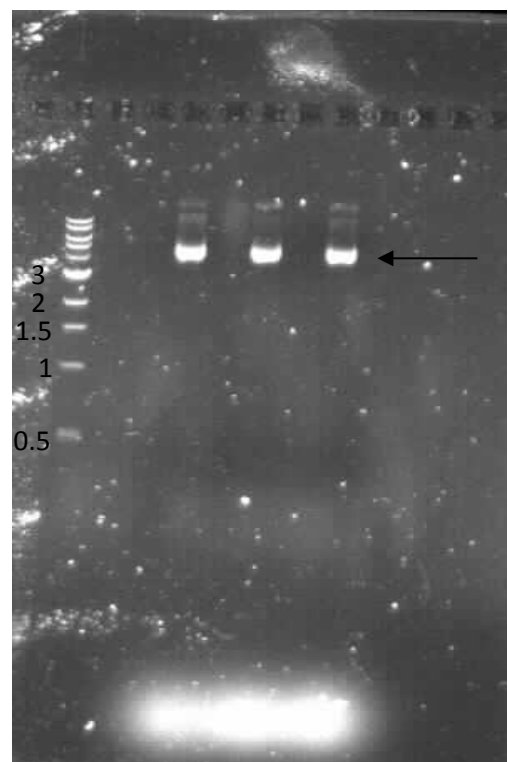
Figure 3: Colony PCR of Bd 3099 and 2093.

Gel A shows Bd 3099 colony PCR but the colony did not contain the plasmid (arrow).

Gel B shows the three Bd 2093 colonies after PCR but no plasmid was present. After a Mini Prep the three Bd 2093 colonies revealed they contain the plasmid as shown in gel C. Samples were run on a 1% agarose gel in TBE and contained SYBR green dye.



B



C

Trial Expressions of Bd 1482, Bd 3099 and Bd 3100

Trial expression was performed to find out in which fraction of the cell lysate the proteins were expressed in, soluble or insoluble. Bd 1842, Bd 3099 and Bd 3100 were examined in this way as RomR had already been shown to be expressed in the soluble supernatant. Bd 3100 had previously been shown only to be expressed in the whole cell sample and not in the supernatant. To confirm this Bd 3100 was expressed with varying concentrations of IPTG and at both 20°C and 37°C. Figure 4 shows SDS PAGE gels that verify Bd 3100 is only present in the whole cell sample and not in the supernatant at various IPTG concentrations and at the different temperatures. Bd 3100 was only expressed in the whole cell fraction in every condition confirming what had previously been shown meaning Bd 3100 is most likely to be insoluble.

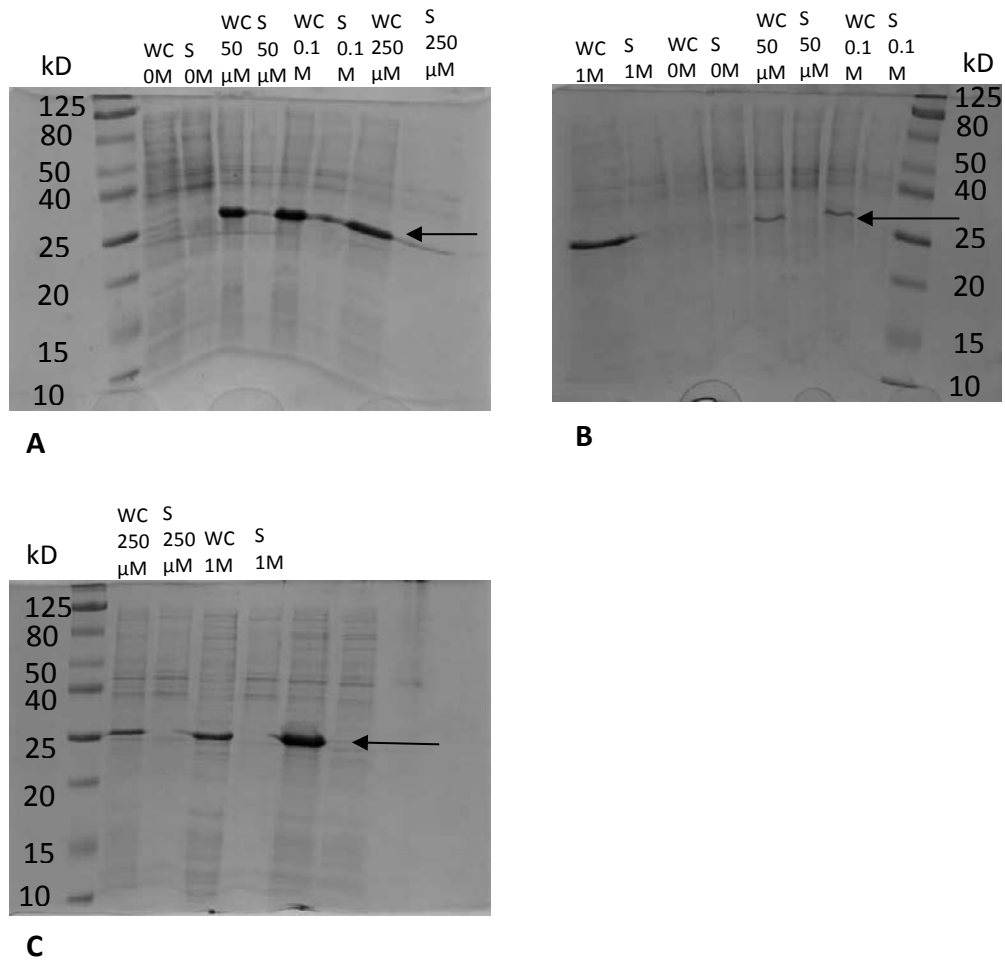


Figure 4: Whole cell (WC) and supernatant (S) samples of Bd 3100 (31 kD). Bd 3100 was expressed at 20°C and 37°C with varying concentrations from 0 to 1 M of IPTG. Gel A shows the 37°C expression along with the first two lanes in gel B, with the other lanes showing 20°C samples. Gel C shows the rest of the 20°C samples. Bd 3100 was only found in the whole cell sample and not the supernatant in every expression condition.

Bd 1482 was only expressed at 20°C with varying amounts of both LB and IPTG concentration (figure 5). Samples of the whole cell and supernatant were taken at 5 hours and 20 hours. In both cases no Bd 1482 was expressed in the supernatant (figure 5) at either of the different concentrations of LB and IPTG. The whole cell samples showed that after 5 hours there was a difference in the levels of expression with 2xLB + 10µM IPTG having the least expression and 2xLB + 500µM IPTG having the largest expression. At 20 hours there is no visible difference between any of the concentrations of LB and IPTG as shown in figure 5. For this reason 2xLB + 500µM IPTG was chosen to be the expression condition for Bd 1482 with the idea that higher concentrations of IPTG would stimulate more expression even though the protein is expected to be insoluble.

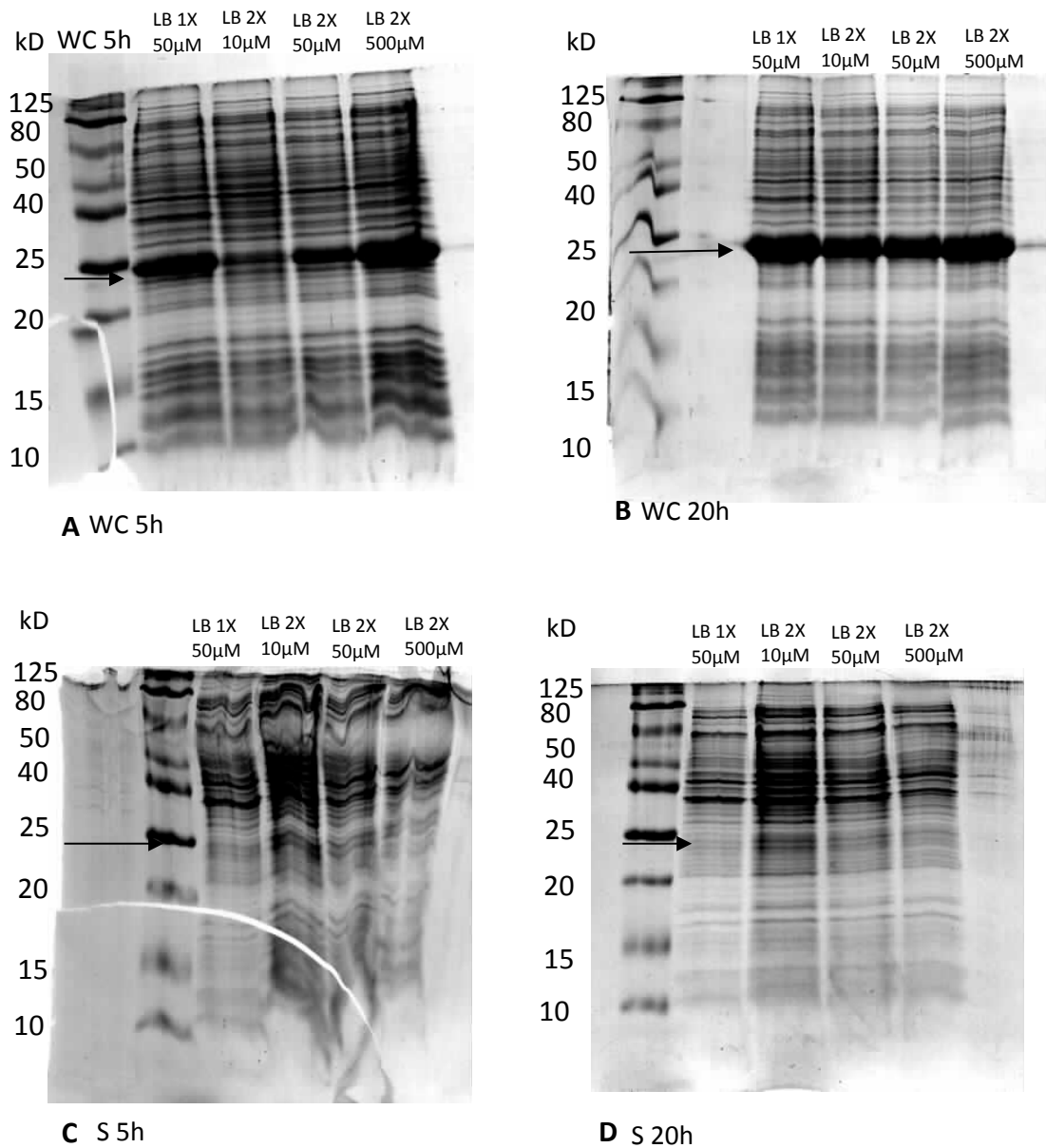


Figure 5: SDS gels showing the trail expression of Bd 1482 (23kD) at 20°C. Gel A and B are the whole cell (WC) samples taken at 5 and 20 hours respectively. These show the expression of Bd 1482 at around 23 kD. Gel C and D are the supernatant (S) samples at 5 and 20 hours respectively. The arrow indicates where Bd 1482 should be

shown if it were present. The LB strength and IPTG concentrations are stated above each lane.

The same expression test was implemented on Bd 3099 only this time the whole cell and supernatant sample were taken at 3 hours and 20 hours. After 3 hours the only visibly large amount of expression was in both the whole cell and supernatant of 1xLB + 50µM IPTG. After 20 hours the expression levels dramatically changed with large amounts being produced in all conditions except 2xLB + 500µM IPTG where expression levels were not visible in the supernatant fraction. Figure 6 shows there is more expression in the whole cell sample after 20 hours compared to the supernatant but there is still visible over expression of Bd 3099 in the supernatant except at 2xLB + 500µM IPTG. From this result it was concluded that Bd 3099 was expressed in the soluble supernatant and the 2xLB + 50µM IPTG would be used for expression.

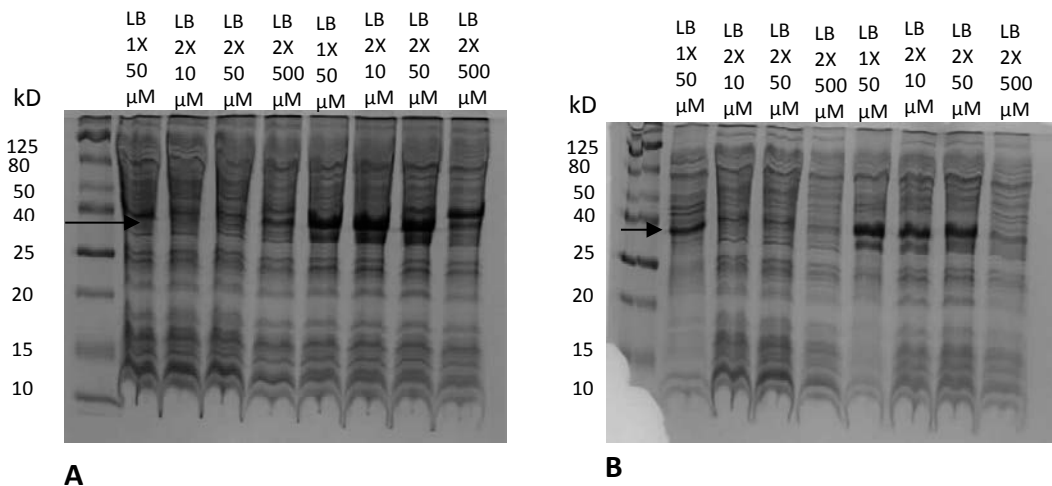


Figure 6: Trail expression of Bd 3099 (35kD) at 20°C. Gel A shows the whole cell samples taken at 3 hours (first four lanes) and at 20 hours (last four lanes). Gel B shows the supernatant samples in the same layout. The arrow shows the position of

Bd 3099 at around 35kD. The LB strength and IPTG concentrations are stated above each lane.

Purification of Soluble and Insoluble Proteins

Soluble RomR

RomR was tagged at the N and C terminus, RomR N and RomR C respectively, with a HIS tag which was used for purification on a nickel affinity column. Most RomR purification experiments were performed on an ATAK using a low Imidazole (20 mM) as buffer A and a high Imidazole buffer (500 mM) as buffer B (p 82).

A RomR N cell pellet that had previously been cultured by another member of the team was pelleted and stored at -20°C was then lysed and the supernatant was loaded on the nickel column. Buffer B was increased at 10 percent increments to increase the imidazole concentration until all the protein was eluted off as shown in figure 7 A. Samples of the whole cell, supernatant, insoluble and flow through fraction was taken along with purified fractions believed to contain RomR N were ran on an SDS gel (figure 7 B) to confirm the whereabouts of the protein. The SDS gel (figure 7 B) shows that large amounts of RomR N were contained in the whole cell, supernatant, flow through fractions with minimal amounts in the insoluble fraction. The elution fractions all contain high levels of RomR N with minimal contamination with the exception of 100% buffer B fraction.

RomR N was also expressed at 20°C with an induction concentration of 500µM IPTG. This led to similar results with most of the elution fractions containing RomR

with few contaminating proteins (figure 7 C). In both case the elution fractions were pooled together in a dialysis bag with a molecular cut off of 30 kDa and dialysed overnight in 2L of dialysis buffer. The dialysed fractions were then spun down to around 20 mg/ml using a 10 kDa MWCO spin column.

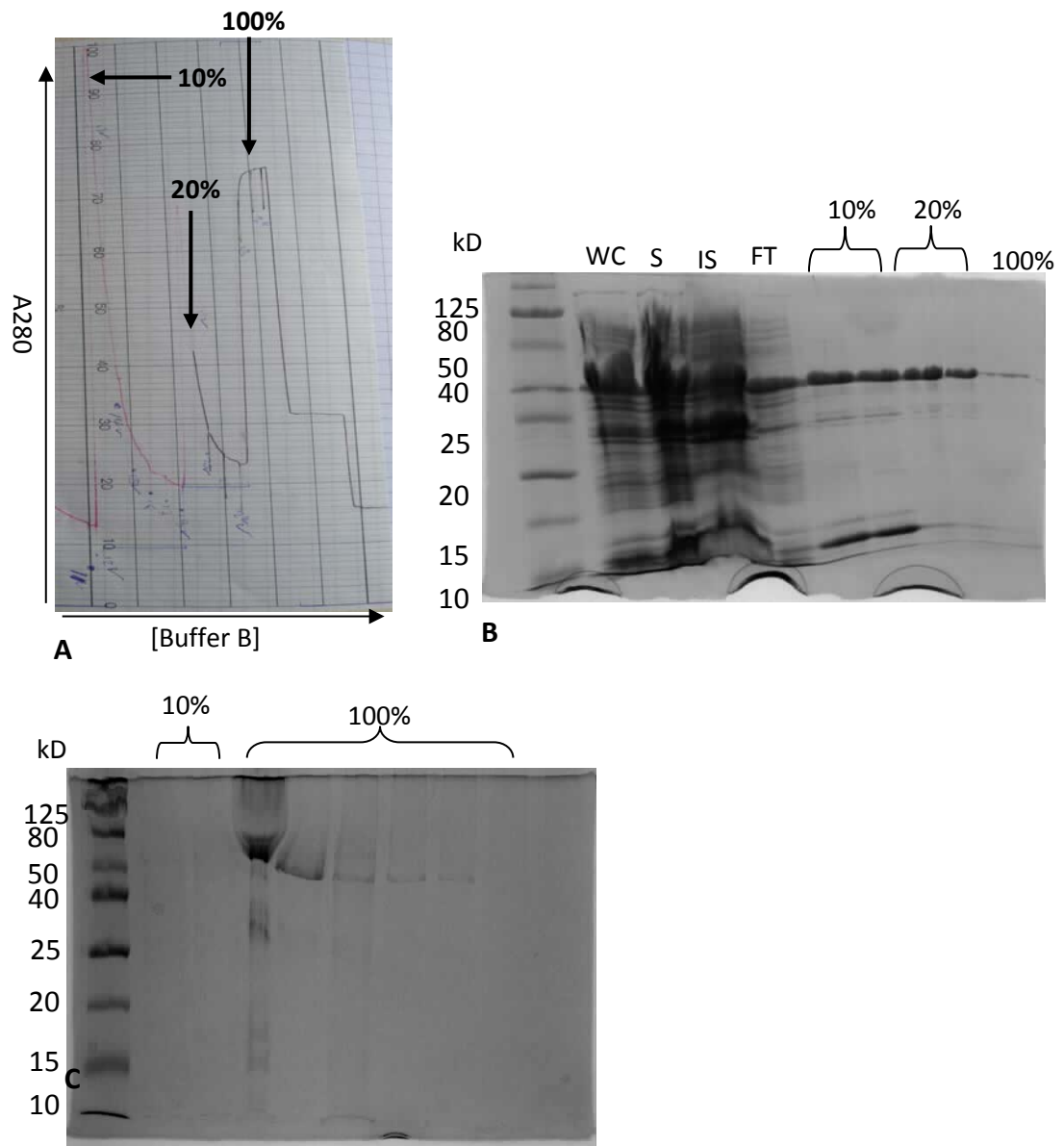


Figure 7: Purification of RomR N. (A) shows the elution profile of the RomR cell pellet with the arrows indication the peaks where samples were taken and the percentage

of buffer B. These samples along with whole cell (WC), supernatant (S), insoluble (IS) and flow through (FT) are shown in gel B with RomR N at 50kD. Gel C shows the elution fractions at 10 and 100 % buffer B (p 82) of another RomR N purification.

RomR C was also expressed and purified under the same conditions and the different fractions are shown in figure 8. Figure 8 A shows the cell fractions along with the flow through and wash step during purification. This revealed that an excessive amount of RomR C was contained in the flow through and a sizeable amount was washed off during the wash step. The elution profile showed not significant peaks but sample were taken and shown in figure 8 B. These elution fractions have extremely minimal amounts of purified RomR C with most of them containing the same amount of contaminating proteins as RomR C itself. The imidazole in flow through was diluted to around 7mM before it was loaded back onto the column and washed with a very low imidazole (5mM) buffer A. The same buffer B (p 82) was used to elute off RomR C and the elution profile had no significant peaks. Some elution fractions were taken and analysed on and SDS gel (figure 8 C). This illustrated that most of RomR C did not bind to the nickel column and again fractional amounts were eluted off. These factions were not pooled together and dialysed as they did not contain high enough concentrations of RomR C.

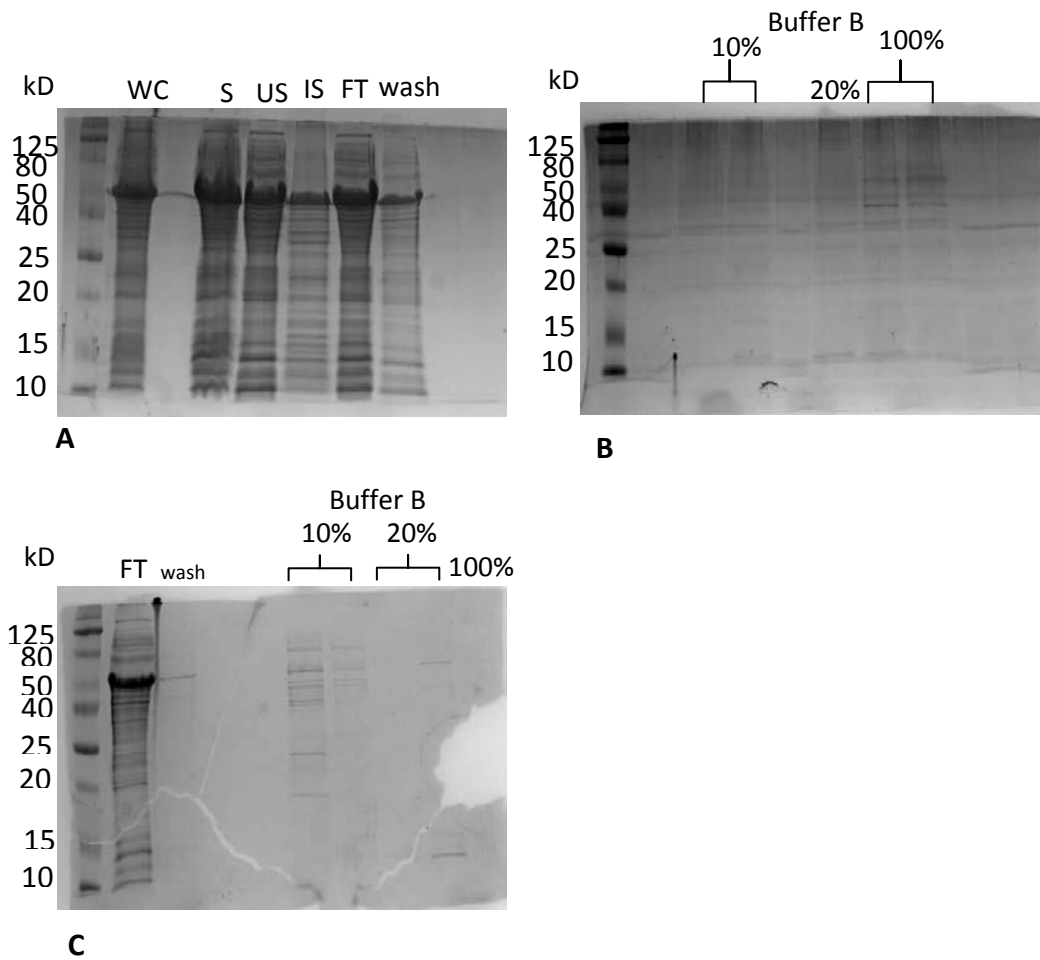


Figure 8: Purification of RomR C. Gel A shows the cell samples of whole cell (WC), supernatant (S), ultra centrifuged supernatant (US), insoluble (IS), flow through (FT) and the wash step. Gel B show the elution fractions taken at 10, 20 and 100% buffer B. Gel C shows the flow through samples including the elution fractions taken at 10, 20 and 100%.

Insoluble Bd 3099 and 1482

Bd 3099

The SDS PAGEs in figure 6 revealed that Bd 3099 was contained within the supernatant and was most likely soluble. When tried in large scale expression and purification it was exposed that most of the protein was contained within the insoluble fraction. The supernatant was purified using the same methods as RomR N and the elution fraction are also shown in figure 9 A . The SDS gel is not very clear but does depict that minimal amounts of Bd 3099 are present in both the supernatant and flow through when compare to the whole cell and insoluble fractions. The purification profile showed no significant peaks and the three elution fractions taken at 20, 50 and 100% buffer B indicated that only minimal amount of Bd 3099 was eluted off at 20% buffer B. A second trial of this was performed with very comparable results. Figures 9 B and C show the cell fraction and the elution fractions respectively. Again large amount of Bd 3099 are in the whole cell and insoluble fraction with minimal amount contained in the supernatant and flow through. The elutions profile was very similar to the first attempt. Elution fractions were taken at 0, 10, 20 and 100% buffer B but this time no Bd 3099 was displayed in any of the elution fractions. There was only minimal amount of contaminating protein seen in the 20 and 100% buffer B fractions.

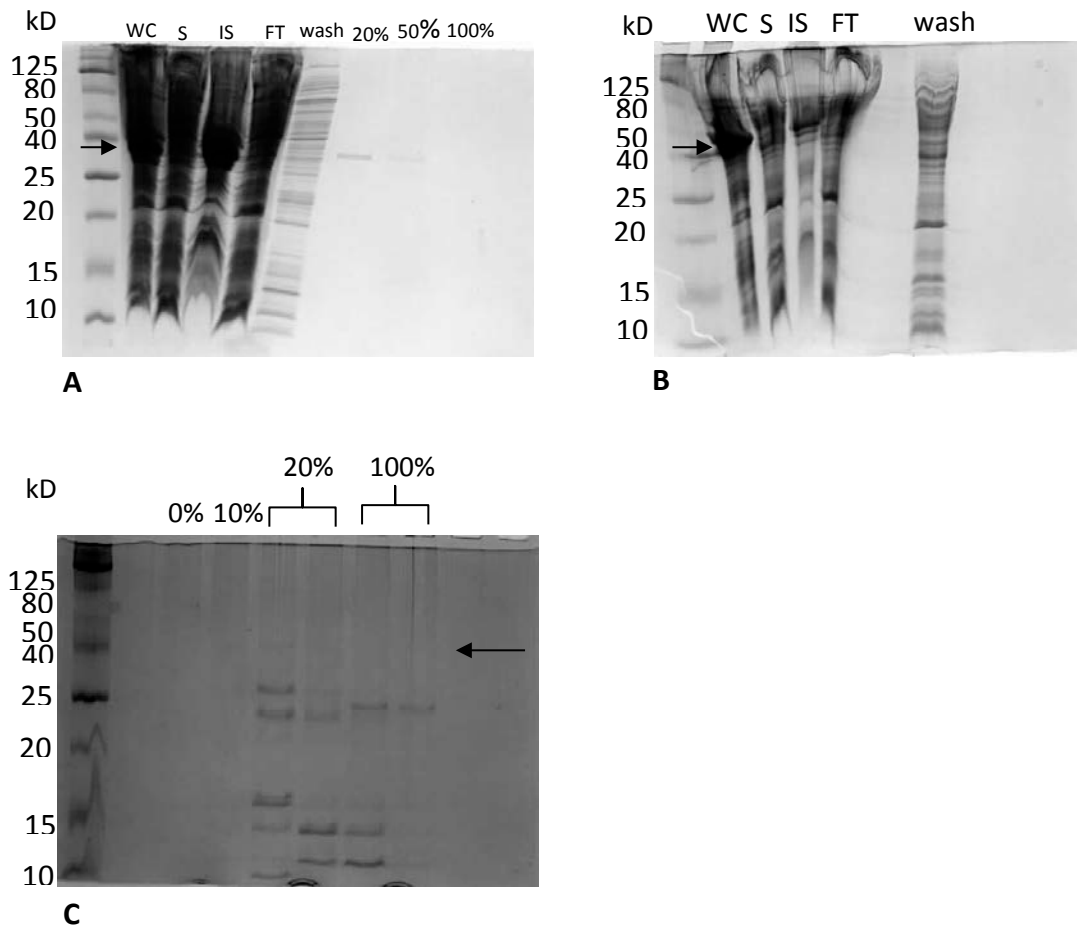
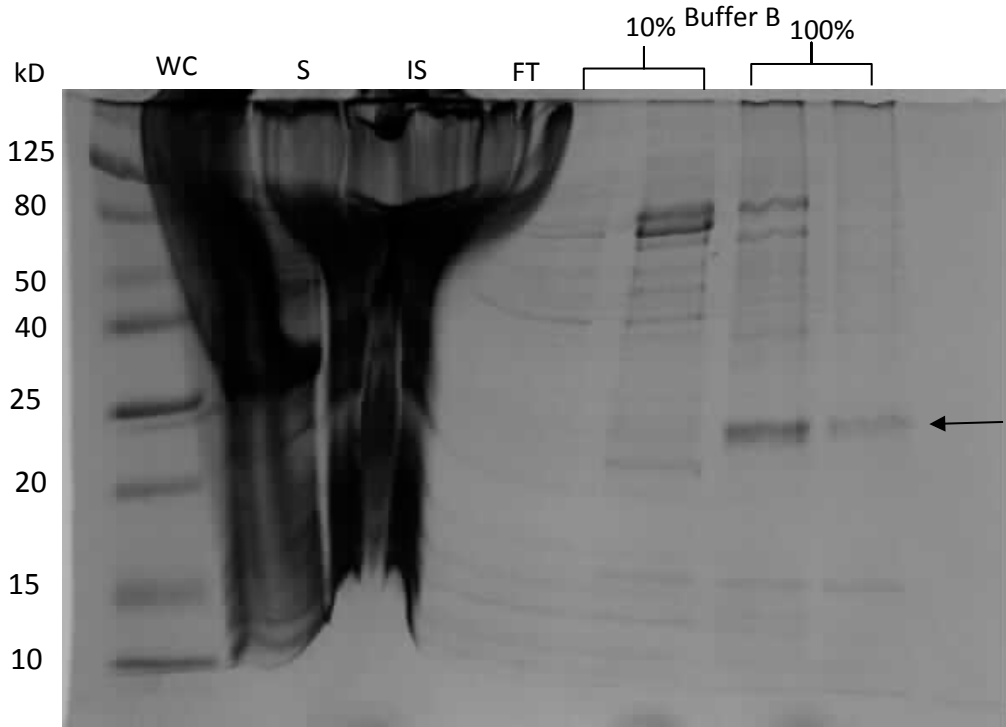


Figure 9: Elution profile of Bd 3099 from nickel column. Gel A shows the cell fractions: whole cell (WC), supernatant (S), insoluble (IS) and flow through (FT) along with three elution fractions at 20, 50 and 100% buffer B. Gel B displays the cell samples from the second attempt at Bd 3099 purification and gel C shows the elution fractions that were taken at 0, 10, 20 and 100% buffer B which contain no Bd 3099. The arrow shows where Bd 3099 is present.

Bd 1482

Bd 1482 was expected to be insoluble as during the trial expression only the whole cell samples contain the over expressed protein. The supernatant of the large scale was still purified to confirm the insolubility. Figure 10 A does not clearly prove that the protein is in the insoluble fraction as the three cell fraction and the flow through have all merged together. The purification profile in figure 10 B shows no peaks above the base line of buffer B, but elution fraction at both peaks were still taken and analysed. The elution fractions that were taken at 10 and 100% buffer B showed only negligible amounts of Bd 1482 along with other contaminating proteins. This indicated that Bd 1482 was insoluble and the insoluble fraction was re-solubilised in a 6M guanidine hydrochloride buffer. This was then refolded on column using a 6M urea buffer which was slowly diluted down to 0M on the nickel column. Bd 1482 was then eluted off using a gradient of 20mM imidazole to 500mM imidazole but no peaks were shown on the elution profile. As there were no significant peaks showing that elution had occurred no fractions were taken to be analysed.



A

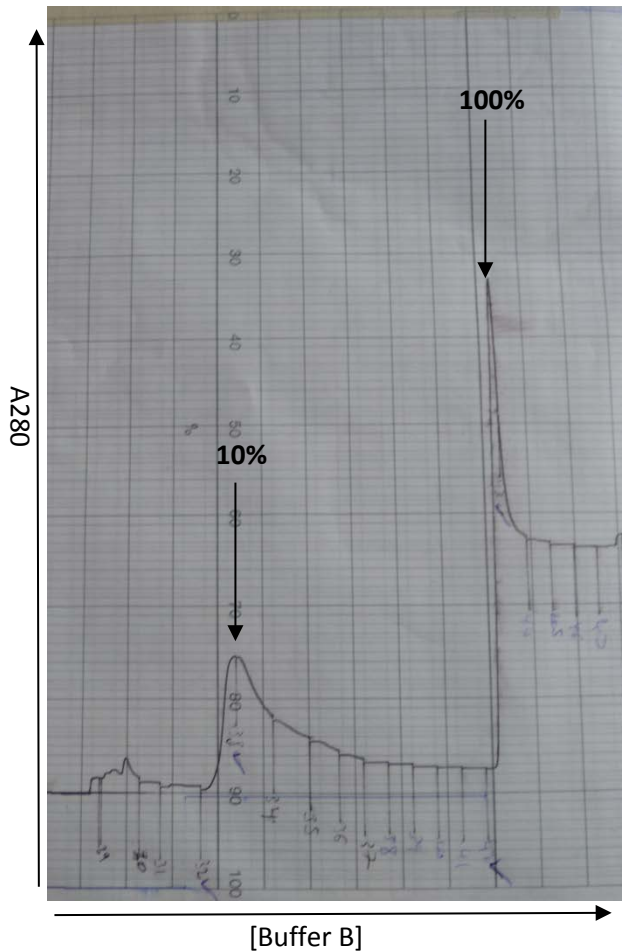


Figure 10: Purification of Bd 1482 (23 kD). Gel A depicts the cell samples whole cell (WC), supernatant (S), insoluble (IS) and flow through (FT) along with the elution fractions taken at both the peaks in purification profile indicated by the arrows in B and the percentage of buffer B (p 82).

Refolding Insoluble Bd 3099, 1482 and Bd 3100

If the proteins were contained within the insoluble fraction of the cell lysate they were purified using a series of refolding buffers and purification steps. Bd 3099 and Bd 1482 were shown to be insoluble during this study and Bd 3100 had already been shown to be insoluble was also proved in this study. These three proteins all underwent the refolding with varying success.

Bd 3099

Bd 3099 was the most successful, in terms of concentration and purity of the protein. After elution from a nickel drip column using the GuHCl buffer it was diluted down to around 6mg/ml and was tested against a buffer screen. The results are presented in figure 11 where six different additives were used in four different buffers over a range of pH creating a smorgasbord of different refolding conditions. This clearly shows that only 6 out of the 24 buffers had very low absorbance levels and allowed refolding to take place. Three out of the six screening results were using a CHES buffer, two were using a Tris buffer and one was using a Sodium Acetate (NaAc) buffer. The most successful additive in aiding the refolding process was EDTA followed by 20% Glucose. The buffer screen also contained a variety of pH with the higher pH values (pH 7 and 8.5) performing better overall.

	EDTA 1mM	B-ME 10mM	NaCl 200mM	KCl 100mM	NDSB 100mM	20% Glucose
NaAc pH 4	0.007	0.010	0.089	0.023	0.019	0.028
MES pH 5.5	0.901	1.046	1.27	1.115	0.604	0.714
Tris pH 7	0.027	0.987	0.459	1.026	0.866	0.130
CHES pH 8.5	0.046	1.13	0.120	0.549	0.449	0.115

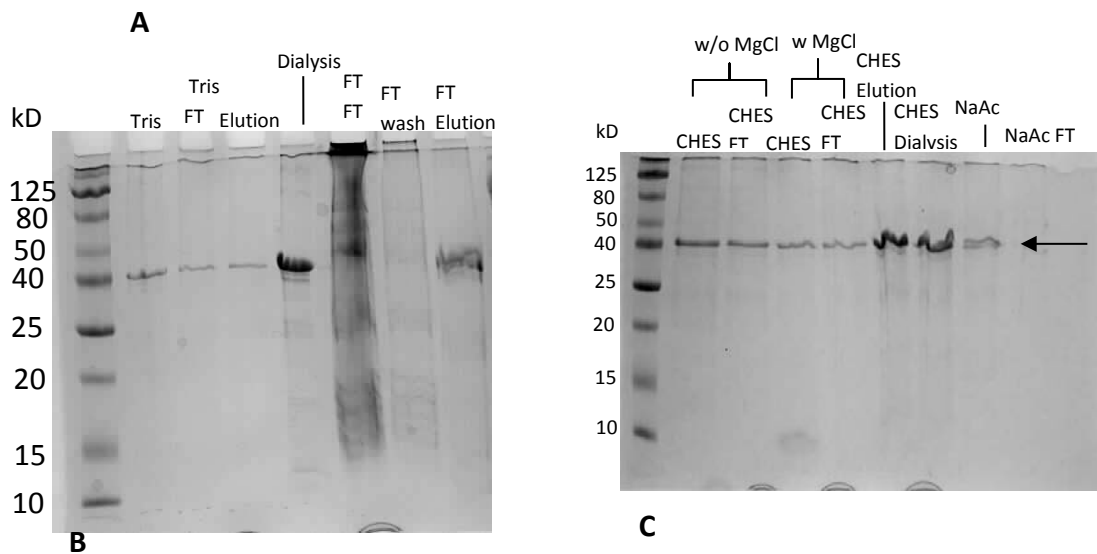


Figure 11: Refolding of Bd 3099. Table A shows the OD₃₄₀ reading of the buffer screen. Gel B shows the elution of Bd 3099 in the Tris buffer along with the elution of the Tris flow through (FT elution). FT FT is the flow through of the Tris flow through (Tris FT) once it had been loaded back onto the nickel column with FT wash and FT elution being the wash and elution of the Tris FT. Gel C shows Bd 3099 in CHES with and without MgCl added and their subsequent flow through along with Bd 3099 in NaAc buffer and it flow through. It also shows the attempted dialysis of CHES buffer to Tris buffer (CHES dialysis). Both the Tris and CHES buffers were loads onto and eluted off a nickel column whereas the NaAc buffer was done on an ion exchange column.

Three buffers were chosen and used on a large scale where 10 mL of the eluted protein was added to 200 mL of the chosen buffer. The three chosen buffers for Bd 3099 were 50mM NaAc with 1mM EDTA at pH 4.2, 50mM Tris containing 1mM EDTA and 20% Glucose at pH 7.2 and a 50mM CHES buffer plus 200mM NaCl and 1mM EDTA. Before loading onto a nickel column 50mM magnesium chloride was added to the Tris and CHES buffers. As NaAc cannot be used on a nickel column the protein contained within this buffer was loaded onto an ion exchange column. The SDS gels in figures 11 show the elution of Bd 3099 from the three buffers. Bd 3099 in Tris and CHES buffers were eluted using 10 ml of the standard buffer B which was pushed over the column using a syringe. Figure 11 B shows the purification of Bd 3099 in Tris buffer before and after elution. The elution fraction contains similar amounts as the flow through with the dialysis fraction containing a larger amount of protein indicated by the larger darker band. The flow through was passed back over the column once it had been cleaned and more protein was eluted off as shown in the FT elution lane.

Figure 11 C shows the elution of Bd 3099 in CHES and NaAc buffer. The SDS gel shows that similar small amounts are contained in both the CHES buffer (with and without adding MgCl) and their respective flow through. The elution and dialysis lanes contain the highest amounts of protein with similar amounts in both. The NaAc lane appears to only contain a small amount of protein and NaAc FT lanes lacks any protein. The elution profile of the ion exchange shows no significant peak and therefore no elution fractions were taken from the ion exchange procedure.

Once the elution fractions from the Tris and CHES purification had been dialysed into a 20mM Tris with 200mM NaCl buffer they were spun concentrated as previously described. Bd 3099 that was refolded using the Tris buffer was concentrated to 20mg/ml whereas Bd 3099 refolded in CHES buffer was concentrated to 40mg/ml. Both of these samples were run through a size exclusion column as shown in the elution profile in figure 12. There are four peaks on the elution profile the first and third representing the two voids as the column is cleaned. The second and fourth peaks are the Tris and CHES samples respectively. This result indicates that both of the samples had no significant amounts of contaminating proteins as there were no other peaks.

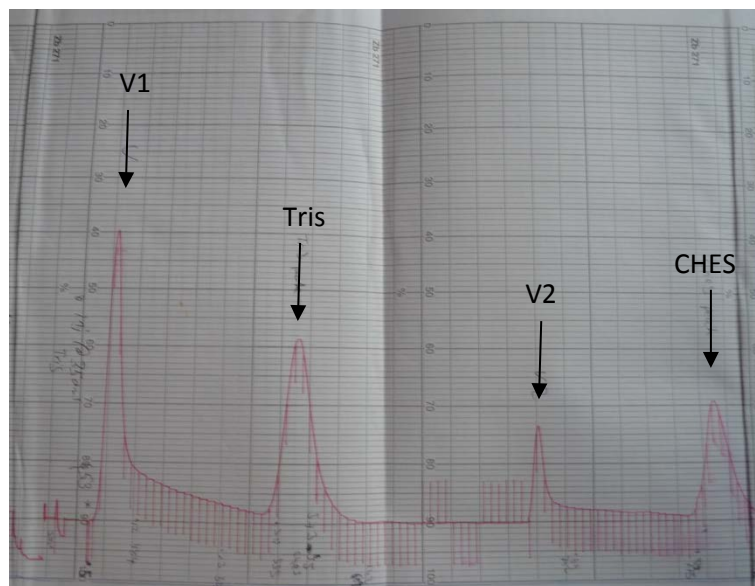


Figure 12: Size exclusion profile of Bd 3099 in Tris and CHES buffers. The first and third peaks are the voids (V1 and V2) of the column with the second and fourth peaks showing Bd 3099 in Tris and CHES buffers respectively.

There were some problems with the nickel drip column during the refolding purification of Bd 3099. To combat these issues Bd 3099 was refolded and purified without using a nickel affinity drop column. Once the insoluble fraction had been through a detergent wash using Triton and then re solubilised in a low imidazole GuHCl buffer as described before it was then dialysed straight into a 50mM Tris buffer containing 1mM EDTA. At this point the concentration was not known so $\frac{1}{2}$ and $\frac{1}{8}$ dilutions of Bd 3099 in GuHCl were made and these were dialysed into the Tris buffer. Large amounts of the $\frac{1}{8}$ dilution precipitated and all of the $\frac{1}{2}$ dilution was a thick with precipitate. The dialysed samples were centrifuged to remove the precipitate and were then run on an SDS gel as shown in figure 13 A. The different dilutions appear to contain similar amounts of Bd 3099 in both supernatant and pellet. The two different dilutions were then pooled together with a concentration of 1.5mg/ml. Once loaded onto a nickel column it was eluted off using the standard buffer B (p 82) and then dialysed into the 20mM Tris buffer with 200mM NaCl as shown in figure 13 B. Bd 3099 was then spin concentrated to around 7mg/ml.

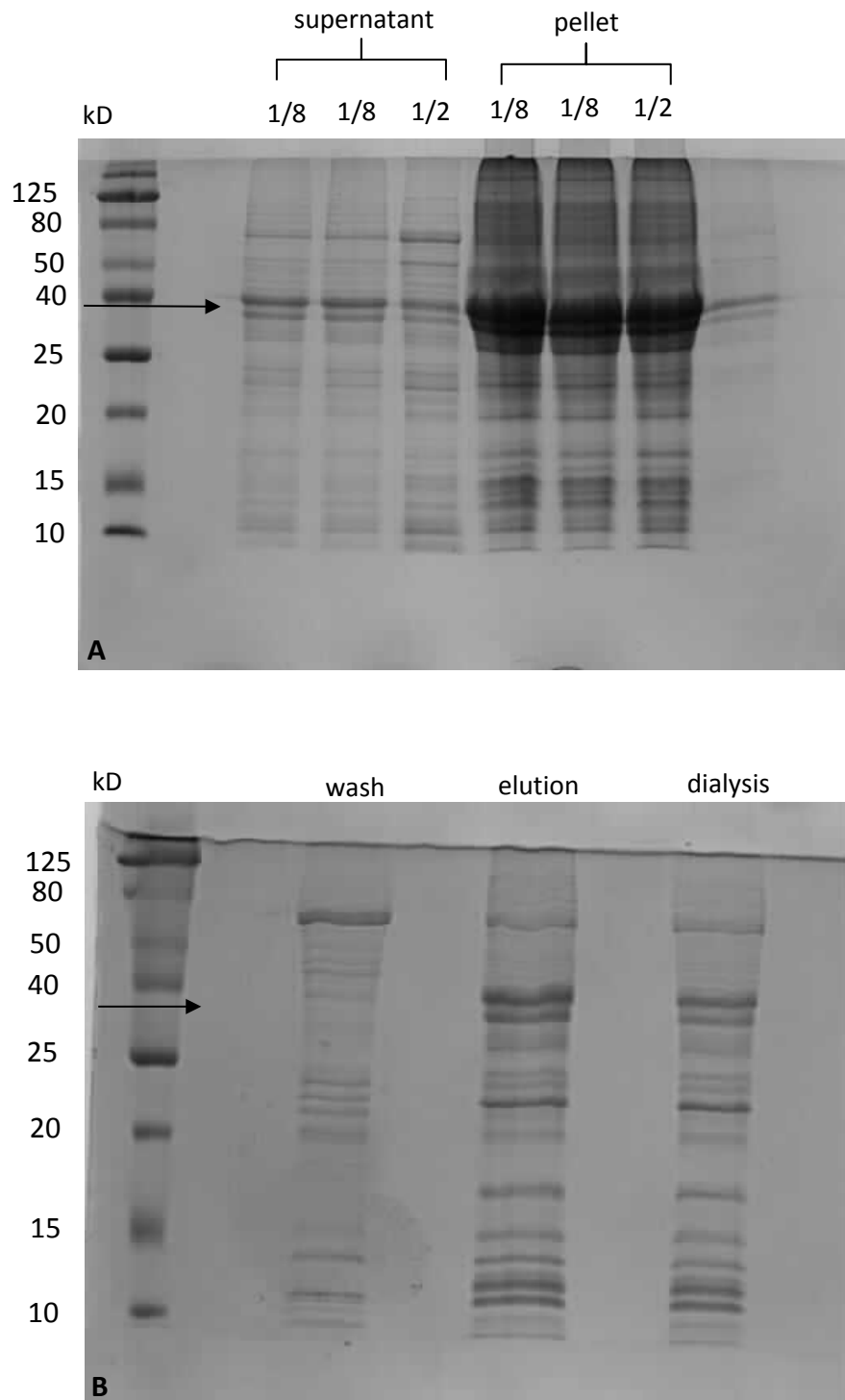


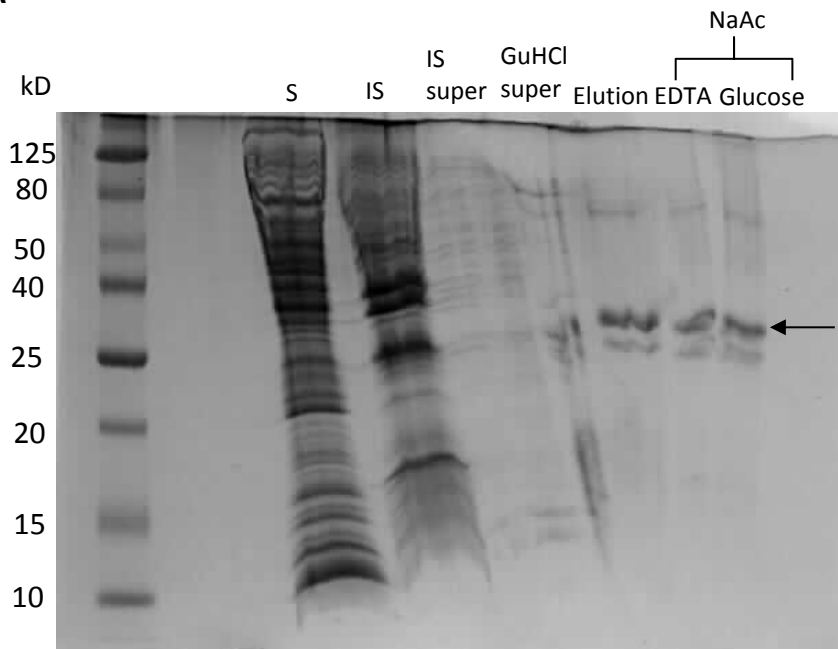
Figure 13: Refold and purifying Bd 3099 (35 kD) without a nickel drop column. Gel A shows the supernatant and pellet of the centrifuged Bd 3099 that precipitated after dialysis. Gel B shows the wash, elution and dialysis after the $\frac{1}{2}$ and $\frac{1}{8}$ supernatant fractions were pooled together.

Bd 1482 and 3100

Bd 1482 and 3100 were also refolded in a same way to Bd 3099 but with much less success. Bd 1482 was eluted off a nickel drip column in a high imidazole GuHCl and then tested on the same buffer screen as Bd 3099. The results shown in figure 14 A illustrate the NaAc buffer at pH 4.2 contain the least precipitate. NaAc containing EDTA had the lowest OD value and NaAc with NDSB or 20% Glucose were the second and third lowest. Two NaAc buffers were chosen for refolding purification once containing 1mM EDTA and the other 20% Glucose and were examined on the SDS gel in figure 14 B. This proves that 1482 was eluted off the drip column and was contained within both of the NaAc buffers. The NaAc with 20% glucose was attempted to be purified on an ion exchange column but no protein was eluted off the column. The pH of the NaAc with 1mM EDTA buffer was attempted to be changed to a higher pH with 1M Tris pH 7.5. Unfortunately this did not work as Bd 1482 precipitated out of solution at pH 6.5.

	EDTA 1mM	B-ME 10mM	NaCl 200mM	KCl 100mM	NDSB 100mM	20% Glucose
NaAc pH 4	0.007	0.058	0.125	0.124	0.037	0.041
MES pH 5.5	0.411	0.710	0.812	0.801	0.637	0.607
Tris pH 7	0.882	0.720	0.954	0.995	0.901	0.800
CHES pH 8.5	0.801	0.917	0.798	0.844	0.895	0.765

A



B

Figure 14: Refolding of Bd 1482 (23 kD). Table A shows the OD₃₄₀ readings of the buffer screen on Bd 1482. The gel in B shows the supernatant (S) and insoluble pellet (IS) of the cell lysate, the supernatant of the insoluble pellet after a Triton wash (IS super), the supernatant after Bd 1482 had been resolubilised in GuHCl and centrifuged (GuHCl super), the elution off the drip column and finally Bd 1482 in the two chosen NaAc buffers. The arrows show where Bd 1482 appears at 23 kD.

After Bd 3100 had gone through the same purification as Bd 3099 and Bd 1482 it was tested against the same buffer screen. Figure 15 B shows that not all protein was bound to the column as some was contained in the flow through but small amounts was eluted off using a high imidazole GuHCl buffer. The GuHCl elution was test against the buffer screen which revealed the buffer with the least precipitate was also NaAc but this time with the addition of 200mM NaCl (figure 15 A). All the other NaAc buffers also contained minimal amounts of precipitate so only the NaAc with NaCl was used on a larger scale. Because the ion exchange on Bd 1482 in a NaAc buffer produced no purified protein Bd 3100 was tested to see if it could be transferred into a buffer suitable for affinity chromatography using a nickel column. The buffers chosen for this were Tris, MES, CHES and HEPES over a pH range. The buffers that contained minimal precipitate were Tris at pH 7 and 8, HEPES pH 8.6 and CHES pH 9.8. These buffers were not tested to verify if they allow for Bd 3100 to be purified on a nickel affinity column.

	EDTA 1mM	B-ME 10mM	NaCl 200mM	NDSB 100mM	20% Glucose
NaAc pH 4	0.029	0.018	0.012	0.017	0.019
MES pH 5.5	0.439	0.594	0.502	0.530	0.475
Tris pH 7	0.440	0.544	0.487	0.493	0.533
CHES pH 8.5	0.410	0.0468	0.505	0.442	0.466
HEPES	0.239	0.308	0.305	0.284	0.350

A

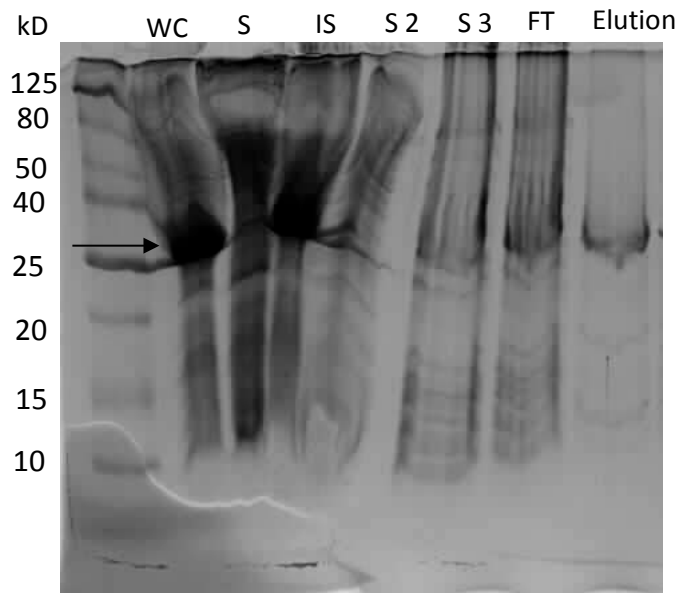
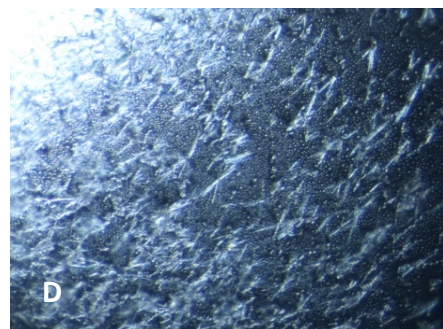
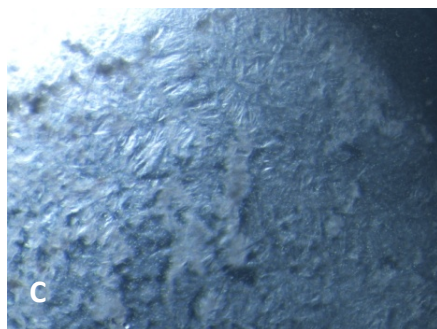
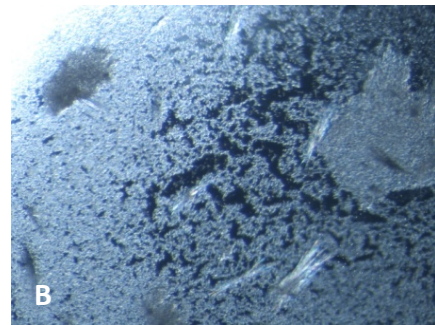
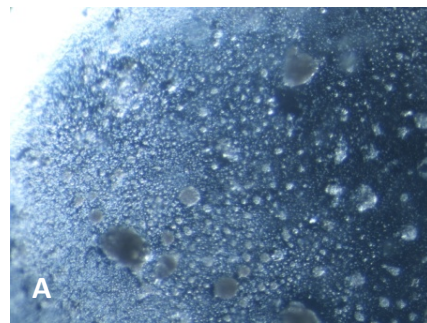
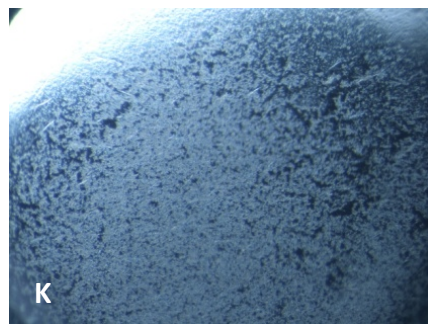
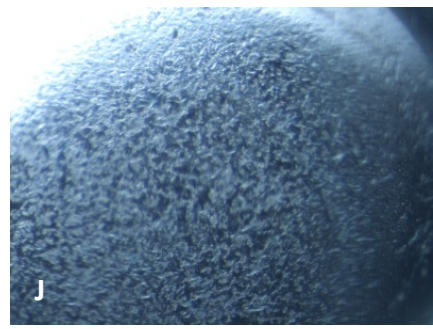
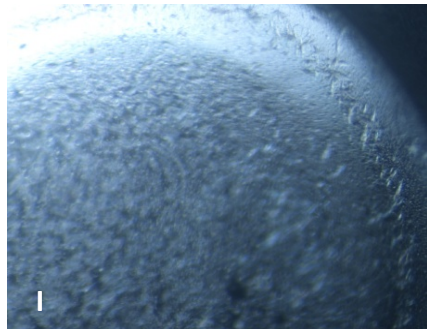
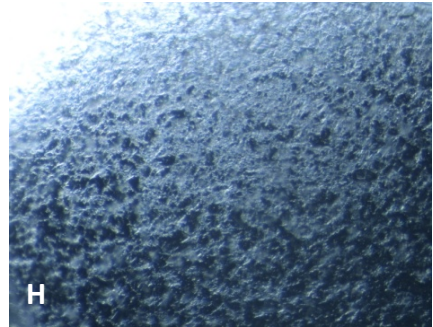
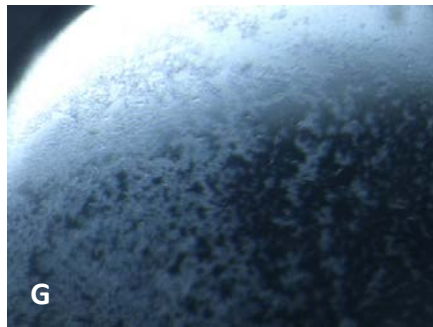
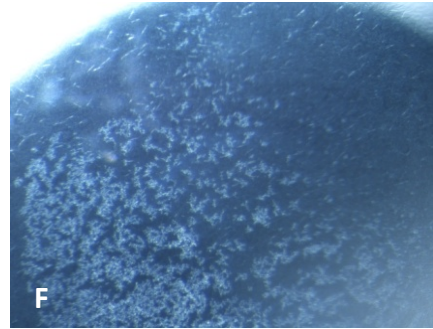
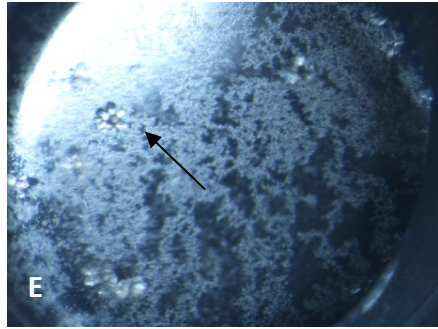


Figure 15: Refolding of Bd 3100 (31 kD). Table A gives the results of the buffer screen which was measured at 340nm. Gel B shows the cell samples whole cell (WC), supernatant (S) and insoluble (IS) along with the supernatants of the Triton wash (S2) and resolubilising in GuHCl (S3). The elution of Bd 3100 off the drip column is shown in the last lane. The arrow indicates the location of Bd 3100 at around 30 kD.

Crystallization of RomR

The only protein that was able to be purified to a high enough purity and concentration (20mg/mL) was RomR with the His tag at the N-terminus (RomR N). It was subjected to three crystal screens: MIDAS, JCSG+ and Proplex with only the latter two screens producing crystals. The JCSG screen had 10 different conditions that produced crystals and Proplex had six different conditions capable of forming crystals. Out of these 16 different conditions only one created a crystal suitable for diffraction. The condition was in the Proplex screen box 2 condition 26 and contained 0.1 M sodium acetate (pH 5.0) and 2 M ammonium sulphate. The pictures in figure 16 show crystals form some of the 16 different crystallising conditions with E showing Proplex box 2 condition 26.





Picture	Screen	Condition
A	Proplex	0.1 M calcium acetate 0.1 M MES 6.0 15% v/v PEG 400
B	Proplex	0.2 M lithium sulfate 0.1 M MES 6.0 20% w/v PEG 4000
C	Proplex	0.1 M calcium acetate 0.1 M sodium cacodylate 5.5 12% w/v PEG 8000
D	Proplex	0.2 M ammonium sulfate 0.1 M MES 6.5 20% w/v PEG 8000
E	Proplex	0.1 M sodium acetate (pH 5.0) and 2 M ammonium sulphate
F	JCSG	0.2 M magnesium chloride 0.1 M sodium cacodylate 6.5 50 % v/v PEG 200
G	JCSG	0.2 M magnesium chloride 0.1 M Na HEPES 7.5 30 % v/v PEG 400
H	JCSG	0.17 M ammonium sulfate None - 25.5 % w/v PEG 4000/ 15 % v/v Glycerol
I	JCSG	0.1 M CAPS 10.5 40 % v/v MPD
J	JCSG	0.2 M lithium sulfate 0.1 M Bis Tris 5.5 25 % w/v PEG 3350
K	JCSG	0.2 M magnesium chloride 0.1 M Bis Tris 5.5 25 % w/v PEG 3350

Figure 16: RomR N crystals. The 11 pictures (A-K) show the conditions which crystals were formed in. The contents of these conditions and which screen they are in are included in the table above. Not all of these are protein crystals and only the crystals in E were taken for diffraction. The condition in E was 0.1 M sodium acetate (pH 5.0) and 2 M ammonium sulphate. The crystals were created in a 96 sitting drop tray with RomR N at 20mg/mL and a drop size of 1.8 μ L.

Diffraction of RomR Crystal

One crystal that was produced in the Proplex screen (box 2 condition 26) was diffracted at the Diamond Light Source. The result in figure 17 shows the diffraction pattern of the RomR N crystal which was able to diffract at 9.18Å.

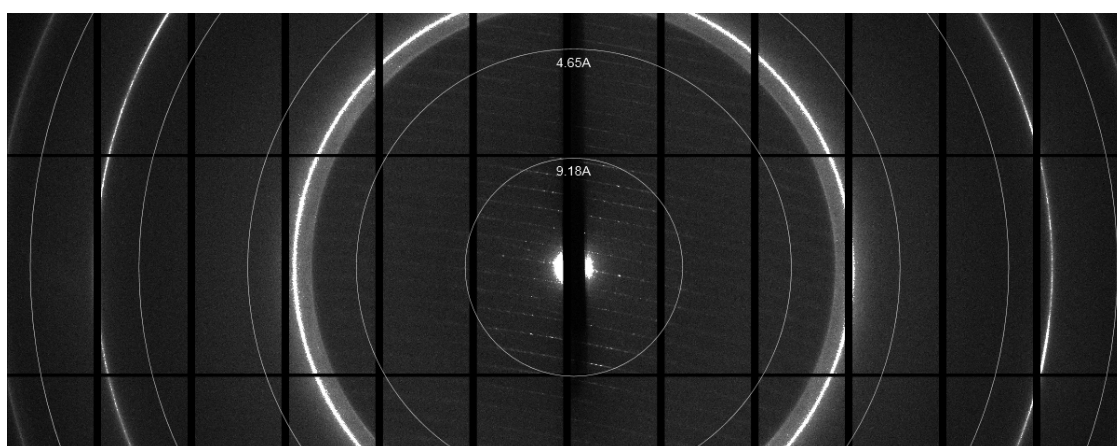
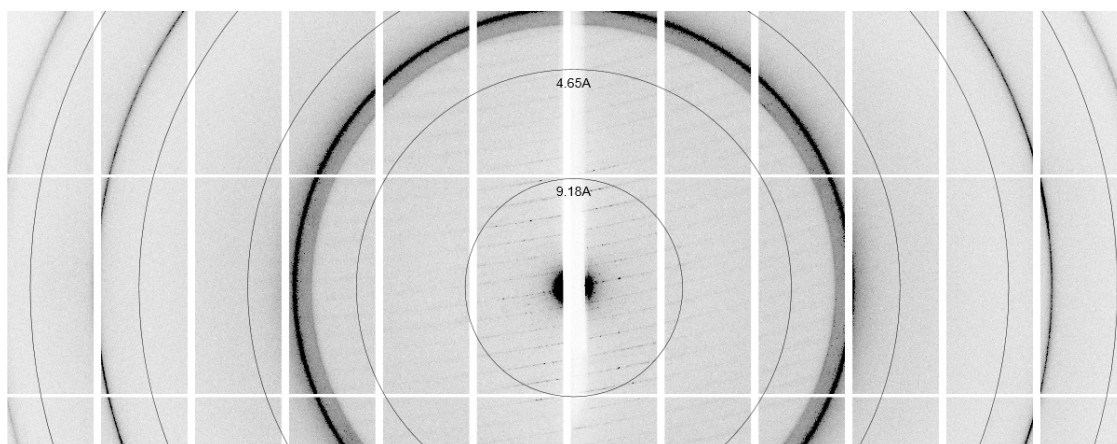


Figure 17: The diffraction pattern of RomR N shown both in the normal form (A) and the inverted form (B). The crystal was grown in 0.1 M sodium acetate (pH 5.0) and 2 M ammonium sulphate and diffracted at the Diamond Light Source. The crystal was able to diffract at 9.18 Å.

Discussion

The only protein in this study that was soluble in the cell lysate was RomR. Consequently RomR was also the only protein that was able to be crystallized. All other proteins Bd 1482, 3099 and 3100 were produced as insoluble proteins and were not able to be purified and crystallized. These proteins went through a vigorous refolding procedure to try and resolubilise them. This was met with limited success and is discussed later. Unfortunately Bd 2093 was not able to be made into a recombinant protein due to PCR complications and time restraints.

RomR

Two versions of RomR had already been produced which contained a His tag at either the N or C terminal. These two types of RomR were created because it was unknown what affect the His tag had on purification of this protein. First a RomR N cell pellet which was previously cultured was tested on its ability to purify. The results showed that the N terminal His tag bound the nickel affinity column with a high enough specificity to allow for high levels of purity and concentration purification. The few contaminating proteins which were present would have been lost during the dialysis procedure resulting in highly pure sample of RomR N ready for crystallization.

The C terminal His tagged RomR was still tested to evaluate whether or not it would produce the similar or higher levels of purification as there was a sizeable amount of RomR N flowed through the nickel affinity column. RomR C was cultured

under the same conditions as RomR N except instead of using Kanamycin as the antibiotic Spectinomycin was used. This should not have an effect on the purification as it only used for sterility and to select for the cells which contain the antibiotic resistant gene in the plasmid and therefore RomR C. Figure 8 shows there were similar amounts of RomR C in the flow through as in the supernatant indicating it did not bind to the nickel affinity column. This was confirmed when RomR C was attempted to be eluted off the column as there was no significant peaks in the elution profile and the SDS gel reinstated this by showing no signs of eluted RomR C. To overcome this problem a lower level of imidazole (5mM) in buffer A was used when loading the flow through back onto the nickel affinity column. Imidazole is used to cleave the proteins off the nickel affinity column by interacting with the His tag. When a too high concentration of imidazole is used in buffer A the proteins will not be able to bind to the column and simply get washed through. Lower the concentration of imidazole should allow for RomR C to bind tighter to the column. This was not the case as shown in figure 8 where it is clear RomR C once again did not bind to the column as was only seen in the flow through.

The results show that RomR with the His tag at the N terminal was able to bind to the nickel affinity column and be purified to a much greater than RomR C. For this reason RomR N was used in the consequence purification and RomR C was not further investigated. Not enough RomR N was produced from the single cell pellet to allow for crystal screens so more was produced under the same condition as this had previously led to a high purity and concentration of the protein. This resulted in RomR

N being purified to a concentration of around 20 mg/ml which is high enough for crystallization.

Out of the three crystal screens done one RomR N only 16 of them produced crystals. Not all of these crystals were protein crystal but were in fact salt crystals, which is very common in crystallography. Some of the conditions were hard to determine if the crystal was salt or protein but one of the conditions in the Proplex screen produced a protein crystal that was large enough for diffraction experiment. The diffraction patten shown in figure 17 proves this crystal can diffract at around 9 Å. To gain a better resolution and more detailed structure of RomR custom crystal screens need to be used. These will allow for a fine tuning of the condition that produced the diffracting crystal and hopefully produce a better structured crystal suitable for diffraction.

PCR and Sequencing

This first step in the PCR process is primary PCR which entails producing PCR primers that will clone our genes of interest. In this study our genes of interest are Bd 2093 and 3099 each having individual primers produced for them. The annealing temperature was known to be 50°C for Bd 3099 from previous experiments done by another member of the team, not shown here. To make sure this previous data was correct a 50°C annealing temperature was used in primary PCR and as shown in figure 1 that annealing temperature was suitable for the selection of Bd 3099. As for Bd

2093 primers were designed for the first time so the optimum annealing temperature was unknown. A range of temperatures from 50 to 64°C were used allowing the optimum temperature to be found. The gel in figure 1 shows increasing brighter bands indicating as the annealing temperature increase the primers can bind tighter to the gene within the *Bdellovibrio* genomic DNA allowing for greater amplification. It was clear after the primary PCR products were purified 64°C was the optimum temperature represented by a much brighter band in figure 1.

At this point it is unclear if the primary PCR products are our genes of interest (Bd 2093 and 3099). The primers used in the primary PCR are highly specific but to clarify if our genes of interest have been extracted correctly they must be inserted into their respective plasmid. No data is available for the second round of PCR for Bd 3099 but 2093 is shown in figure 2. The annealing temperature for the second round PCR for Bd 2093 was also unknown so a range of temperatures were tried. These were then pooled together and purified as shown in figure 2. The plasmids containing our genes of interest were then transformed into DH5α cells which amplified the plasmid. A selection of the colonies produced are taken and examined under colony PCR. Many colonies were produced from the transformation of Bd 3099 but only three were formed for Bd 2093. Different DH5α cells were used when performing the transformation on Bd 3099 and 2093 and it shows the DH5α cells used for Bd 2093 were not as competent. To overcome this problem new chemical competent DH5α cells could have been made or electro-competent DH5α cells used.

The first Bd 3099 colony that was picked for colony PCR did not contain the plasmid (figure 3 A) but two to out of the next five other colonies showed the plasmid was present. The sequence data proved the plasmid contained our gene of interest. One of these colonies was used to amplify the plasmid and after PCR purification of the pET26b plasmid containing the Bd 3099 gene, it was successfully transformed into the E. coli expression strain BL21. All three of the Bd 2093 colonies were also sent for sequencing but the results revealed that although the plasmid was contained within the DH5 α cells the Bd 2093 gene was not incorporated into the pET 41c plasmid. Even though the Bd 2093 gene was cloned from the *Bdellovibrio* genome it was not incorporated into pET 41c plasmid using this range of annealing temperatures. This problem could be overcome by trying a wider range of annealing temperatures, changing the extension time in the PCR programme, using different primers or a different plasmid altogether. Bd 1482 had already gone through the two rounds of PCR but was sent for sequencing as well which showed some DH5 α colonies contained the plasmid and Bd 1482. One colony was picked and transformed into BL21 cells. Due to time constraints the examination of Bd 2093 was not continued and only Bd 1482, 3099, 3100 and RomR were taken further.

Trial Expression

To gain a preliminary understanding of which purification parameters might be needed trial expressions were performed on Bd 1482, 3099 and 3100 all of which are expressed using BL21 cells. This would clarify which section of the cell lysate our

protein was contained in. When the protein is contained within the supernatant of cell lysate it is most likely to be soluble as insoluble protein will aggregate and form an insoluble pellet or inclusion bodies. RomR had already proven to be produced in the supernatant of the cell lysate and optimal conditions for expression were known so no trial expression was carried out.

Pervious experiments had shown that Bd 3100 expresses as an insoluble protein, so to confirm this and to try and solve the problem trial expressions were performed. A whole cell sample and a supernatant sample of Bd 3100 which was expressed at two different temperatures over range of IPTG concentrations was analysed on an SDS gel (figure 4). The whole cell sample confirms the protein is being expressed but is not contained within the supernatant. The trial was performed at 20 and 37°C to investigate if different temperatures would results in a more soluble protein. That was also the idea behind using different concentrations of IPTG. When higher concentrations of IPTG are added to activate the expression of proteins it can result in a massive over production of the protein which could result in protein aggregation and insolubility. This is because large amounts are produced rapidly which is why using lower concentrations of IPTG many help keep the protein soluble. As Bd 3100 was only contained in the whole cell sample at both temperatures and all IPTG concentrations it is likely to be an insoluble protein and will need a more extensive purification procedure.

The trial expression of Bd 1482 was performed in a similar way but this time it was all produced at 20°C. The difference was instead of changing the temperature the

strength of the LB would be changed along with the IPTG concentration. The strength of the LB can affect the growth of the BL21 expression strain and therefore impact the amount of protein produced. Different time points were also taken to see if a change in the LB and IPTG would affect the rate at which Bd 1482 is produced. Figure 5 shows the results of this trail and indicate a change in the LB and IPTG have an effect on protein production but only in the early stages of expression. The whole cell sample at 5 hours proved a lower strength (1x) LB enable the cells to produces more Bd 1482 compared to 2x LB, both having been induced with 50 μ M IPTG. This shows that higher strengths of LB slow the production of this protein early on but after 20 hours there was no difference between of the condition indicating this in not a deciding factor for Bd 1482 production. Unfortunately Bd 1482 was not produced in supernatant of the cell lysate indicating it would also be an insoluble protein. With this in mind the condition chosen for large scale expression was 2x LB inducing with 500 μ M IPTG.

Bd 3099 also underwent the same trail expression as Bd 1482 but this time was produced in the supernatant of the cell lysate along with the whole cell. 3-4 hours after inoculation only minimal amounts of Bd 3099 were produced in whole cell and supernatant of 1x LB with 50 μ M IPTG so it was known that this protein could not be produced quickly. After 20 hours all whole cell and supernatant samples, except 2x LB with 500 μ M IPTG, showed similar production levels. The higher strength LB combined with highest IPTG concentration appeared to significantly reduce the production in the whole cell sample and almost abolishes it in the supernatant. This shows that once again different concentrations of IPTG will affect the production of

these proteins. As Bd 3099 was produced in the supernatant of the cell lysate and is a homologue to 1483, which is soluble, it was expected to also be soluble. Knowing that high concentrations of IPTG would reduce protein production a low (50 μ M) IPTG but high strength (2x) LB was chosen for large scale expression.

Insoluble Protein Purification

Both Bd 1482 and 3100 were only present in the whole cell fractions in the trial expressions making it more than likely these two proteins would be insoluble, especially Bd 3100 as it had already been proven to be insoluble in previous studies. Bd 3099 on the other hand was found in the supernatant during the trial expression demonstrating it was possibly a soluble protein. As it was thought Bd 3099 was soluble it was expressed on a large scale and the supernatant from the cell lysate was purified the same way as RomR_{BD}. During this purification the elution profile showed no significant peaks which could mean the Bd 3099 is not binding to the column like RomR C or that it was never expressed in the supernatant. To examine this sample of all the different cell fractions and certain elution fractions were run on SDS PAGE. Unfortunately the SDS gel in figure 9 is rather unclear due to a too high concentration of sample being added but it does show which fraction Bd 3099 is contained in. This revealed Bd 3099 was actually contained in the insoluble fraction and only minimal amount were contained within the supernatant. Interesting the flow through only contained minimal amounts of Bd 3099 and so did the wash fraction. Both of these results point towards Bd 3099 binding to the column and staying bound during the

wash step. Although this might be true Bd 3099 was not binding to the column in the manner it was intended, by using the His tag. Instead, because of the insolubility of Bd 3099 it was aggregating inside the column forming small insoluble masses that were not able to pass through the column. The reason they were not eluted off during the wash step or any of the elution step was because Bd 3099 was not bound using the His tag. The small insoluble masses the Bd 3099 would have formed would block many of the His tags from binding and as the protein has aggregated together. Only a small amount of Bd 3099 was eluted off showing that some was able to bind. This meant that Bd 3099 was not completely insoluble but could be solubilised and purified using different purification methods. Before this was tried the supernatant of a second Bd 3099 was purified in the same way. Once again it showed similar results as the first experiment with large amounts in the insoluble fraction and none eluted off the column. Upon seeing this result it was clear that a different purification method was needed.

During the trial expression of Bd 1482 only the whole cell sample contained Bd 1482 with the supernatant showing no signs of the protein. This pointed to the prediction that Bd 1482 was an insoluble protein. When sample from the large scale expression were analysed it was still not clear if Bd 1482 was insoluble as all the cells sample lanes merged together. What figure 10 A does show is that the elution fractions which have a distinct lack of Bd 1482. This led to the conclusion that either Bd 1482 was an insoluble protein or was not binding to the column for another reason such as the problems with the column or too high a concentration of imidazole was used in buffer A. The evidence pointed towards Bd 1482 being an

insoluble protein but not completely insoluble as small amounts were eluted off just like Bd 3099. A simple refolding procedure was tested on Bd 1482 which should allow the protein to unfold and then refolded into a more soluble protein. This entailed refolding the insoluble fraction of Bd 1482 in a 6M urea buffer which was then slowly brought down to 0M. What this does is allow the protein to unfold and then slowly refold exposing the His tags allowing the protein to bind to the column. Instead of using a step wise approach to eluting off Bd 1482 a gradient from 20mM to 500mM imidazole was run. Unfortunately the procedure did not work as planned as there were no significant peaks on the elution profile indicating no protein was eluted off. No elution samples were taken to be analysed and it was concluded that for both Bd 1482 and 3099 that different refolding purification steps were needed. This would potentially allow for the proteins to be refolded in the correct way allowing for purification.

Refolding Insoluble Proteins Bd 1482, 3099 and 3100

It was clear from the result of the initial insoluble protein purification that a different approach was needed to purify these proteins. A refolding protocol from Vincentelli was used and modified to accommodate for the properties of these proteins. The refolding procedure briefly it comprises of collecting the insoluble fraction of the cell lysate and performing an extra detergent wash step, solubilisation and purification in a GuHCl buffer, refolding buffer screen test and then a final purification step. The idea behind this strategy is the first detergent wash would

remove any other cellular debris which was left behind from the previous step and help to solubilise the protein. This sample would then be solubilised in a 6M GuHCl buffer. The high concentration of GuHCl allows the protein to become much more soluble and creates an environment suitable for purification because the protein will not be able to form insoluble masses on the column as easily. This is also partly due to the larger 5mL bed volume of the drip column allowing for a greater area for the protein to bind to the column and less likely to interact with each other. Also by using a low concentration of imidazole (5mM) in the GuHCl buffer it would allow for a tighter binding to the column if the protein was struggling to bind due to imidazole concentrations. Once the protein is eluted off using a high imidazole GuHCl buffer it would be tested against a screen of buffers comprising of 4 different buffers and 6 different additives. Not only does the screen of 24 different buffers and their additives give the protein a variety of different conditions for refolding but it also dilutes the protein 20 times. This is a process called rapid dilution which can help the protein refold into its original state as it is not as probable to interact with other proteins. Depending on what the buffer contains a suitable final purification step is used to increase concentration and purity.

The results for the refolding buffer screen on Bd 3099 showed six potential buffer which would allow for it to refold and not precipitate out of solution. From these six buffers three were used for larger scale dilution each contain a different buffer that was successful in the buffer screen. This would allow us to see the effect these different buffers have on the Bd 3099. The Tris and CHES buffer were the most successful with them purifying to around 20 and 40 mg/mL respectively. These two

buffers are compatible with the nickel affinity column unlike the NaAc buffer which had to be used on an ion exchange column but this led to an unsuccessful purification of the Bd 3099. The buffers that were compatible with the nickel affinity column allowed for the refolded 3099 to use its His tag, bind to the column and elute with high concentration of imidazole just like the soluble RomR N. The Tris and CHES Bd 3099 samples were put through a size exclusion column to check for contaminants but it revealed no contaminants. This meant this method could be reproduced to purify insoluble Bd 3099 to a high enough purity and concentration for crystallisation. Although this refolding method does produce refold protein that can be purified and potentially crystallized it is a complicated, long and expensive process and other methods may be easier and less time consuming.

There are of course disadvantages to using this method, first it being very time consuming with multiple overnight steps. Although the GuHCl buffer does a very good job at making Bd 3099 soluble the initial purification of it on the nickel drop column was a very slow process. The drip column was used to give a larger bed volume allowing more space for Bd 3099 but the high concentration of GuHCl made the column run very slowly. The GuHCl can precipitate very quickly which cause the column to clog up and there is no pressure in these columns to help force Bd 3099 through. Once Bd 3099 had been eluted off it was just a matter of find a suitable buffer for it to refold in without precipitating out of solution. The one problem with the buffer screen was it contained buffers with NaAc and EDTA in them. These two compounds cannot be used on a nickel column but if the EDTA containing buffers are supplemented with MgCl they can be used on nickel column. Unfortunately NaAc

buffers have to be used on ion exchange column which was met with no success. Another problem with this method over all was by basing it on the fact that rapid dilution helps the refolding process it creates large volume that have to be loaded onto nickel of ion exchange columns for final purification.

To overcome these problems with the nickel drip column a method was devised that would skip the initial purification on the drip column. As described in the results once Bd 3099 had been solubilised in low imidazole GuHCl (6M) buffer it was dialysed into a Tris buffer containing EDTA as this combination would allow for purification once MgCl was added and was it had the second lowest OD reading on the buffer screen test. Bd 3099 was diluted by $\frac{1}{2}$ and $\frac{1}{8}$ and dialysed overnight with led to both dilution precipitating out of solution but this was expected. The small volume of the dialysis bag and the diluting out of GuHCl forced Bd 3099 to precipitate. This may seem counter intuitive but by centrifuging the precipitated Bd 3099 it left the soluble Bd 3099 in the supernatant which was now in a Tris buffer. The supernatant was a much smaller volume compared to the rapid dilution method and can be loaded directly onto the nickel affinity column and purified saving time and resources. This method was met with moderate success with Bd 3099 being concentrated to around 7 mg/mL.

From the experiments performed on Bd 1482 it was clear this protein was not soluble and the initial refolding with urea was unsuccessful. The same solubilisation and purification involving GuHCl that was used on Bd 3099 was used on Bd 1482. The eluted protein was also subjected to the same buffer screen and the results shows

the only buffers which caused minimal or no precipitation were NaA buffers. Two NaAc buffers were scaled up but this meant they could not be used on the nickel column for the secondary purification. One idea to overcome this problem as the ion exchange did not work for Bd 3099 in NaAc buffer was to slowly change the buffer and pH. The pH of the buffers needed to be at least pH 6.5 before they can be used on the nickel affinity columns in the AKTA. This was done by adding 1M Tris buffer at pH 7.5 to the NaAc buffer with EDTA but did not work as Bd 1482 precipitated out of solution at around pH 6.4. As the pH gets closer to pI of the protein it is more likely to precipitate out of solution. The pI of Bd 1482 is around 6 so it was not surprising it precipitated at pH 6.4. The other buffer that was scaled up was NaAc with glucose and purified on an ion exchange column. No protein was eluted off with the ion exchange so a different purification strategy is needed. One idea to circumvent these problems could be to dialyse the NaAc buffers against a Tris buffer with a high enough pH for nickel column purification.

The same principle of changing the pH of the buffer was used on Bd 3100 as well but with greater range of buffers. The buffer screen showed that once again only NaAc buffers did not precipitate. One NaAc buffer containing NaCl was then tested against an array of different buffers at different pH values by adding 50µl of Bd 3100 to 450µl of the chosen buffer. This would show if Bd 3100 could stay soluble when changing buffers and pH. The results revealed three of the buffers contained only minimal precipitation but were not tested for use in the AKTA. The best candidate for this would probably be a Tris buffer as Bd 3100 was able to stay soluble over a pH range.

Testing against other buffers at different pH values would also be a useful follow up to get a better understanding of how to purify Bd 3100.

Conclusion

The aim of this project was to gain better structural knowledge of five *Bdellovibrio* proteins. All of these proteins are thought to be involved in the attack phase of the *Bdellovibrio* life cycle. Understanding their structure will help gain insight into the function of these proteins and a more detailed understanding of how *Bdellovibrio* functions. This structural information obtained in this study was produced from x-ray crystallography. In order to create protein crystals suitable for x-ray crystallography the protein must be of high purity and concentration. The main goal of this project was to produce these five *Bdellovibrio* proteins to a high enough standard for x-ray crystallography.

The five proteins in this study started at different points along the purification procedure. The genes of two proteins Bd 2093 and 3099 had to be extracted and integrated into expression plasmids before proteins production and purification could be performed. Both Bd 2093 and 3099 were successfully extracted from *Bdellovibrio* genomic DNA but only Bd 3099 was incorporated in its expression plasmid. Bd 1482 was already integrated into its expression plasmid was able to be transformed along with Bd 3099 into BL21 cells ready for protein production. Bd 3100 and RomR had already successfully been produced making it four out of the five proteins were able to be produced during this study.

Four proteins were able to be produced the but only one of them (RomR) was purified and concentrated to a high enough standard for crystallisation. The main reason why the other three proteins (Bd 1482, 3099 and 3100) were not able to be

crystallised was because of their insolubility. It was known before this study that Bd 3100 was an insoluble protein so different culturing techniques were used to try and produce soluble protein. Varying the temperature and IPTG concentration had no effect on protein solubility and so the refolding procedure was attempted on the insoluble protein. This proved difficult as Bd 3100 could only refold in low pH NaAc buffers which are not suitable for purification on a nickel affinity column. Trying to change the buffer through rapid dilution to a different buffer (Tris, CHES, HEPES or MES) with a higher pH also proved mostly ineffective. To get around this problem a larger buffer screen would be useful or instead of rapidly diluting the NaAc buffer it could be done through dialysis and then remove the precipitate as done with Bd 3099.

During the trial expression Bd 1482 was only found in the whole cell fraction indicating it was most likely insoluble. After the supernatant of the cell lysate showed no signs of purified protein when run through the nickel column and initial refolding experiment was performed. The insoluble fraction was re-suspended in 6M urea which was then slowly diluted down to 0M. Eluting Bd 1482 off with a gradient from 20mM imidazole to 500mM was unsuccessful. Bd 1482 was able to be resolubilised and purified in GuHCl but could only be refolded in NaAc buffer. Attempting to change the buffer with a 1M Tris buffer at pH 7.5 was not possible above pH 6.5. Ion exchange was also tried out and was once again unsuccessful but perhaps trying the similar future strategies as Bd 3100 could help to purify this insoluble protein.

The purification of Bd 3099 was the most successful out of the insoluble proteins. When tested on the buffer screen it was able to be refolded in NaAc, Tris and CHES buffers. The Tris and CHES buffers were able to purified to around 20 and 40 mg/mL respectively. They were tested on a size exclusion column to check for impurities and or if dimmers had formed but both came out clean. The NaAc buffer was run through an ion exchange column but no protein was purified. This shows that by solubilising and purifying in GuHCl then refolding in Tris or CHES Bd 3099 can be purified to high enough standard for crystallisation. Purification without the initial purification in GuHCl was also carried out on Bd 3099 as the drip column used for this initial purification proved time consuming and troublesome. After solubilisation with GuHCl Bd 3099 it was diluted to two different concentration ($1/2$ and $1/8$ the original concentration) and then dialysed into a Tris buffer. After the precipitated protein was pelleted the soluble fraction was purified to around 7 mg/ml. Optimising this procedure might help save time and resources in producing soluble Bd 3099 for crystallisation.

The only protein during this study that was able to be crystallised was RomR. RomR had previously been expressed with the His tag at the N and C terminal but it was unknown which one purified better. The N terminal His tag proved to be most effective with RomR N purifying to around 20 mg/ml. This was then used to create protein crystals that were suitable for x-ray diffraction. Only one crystal formed in a condition from the Proplex screen but many other showed signs of crystallisation. By optimising these conditions it would be possible to produce more crystals that could give a better diffraction. The crystal that was produced was only able to diffract at

around 9 Å so greater resolution is needed to gain full structural knowledge of this protein.

The overall goal of this project was to produce purified *Bdellovibrio* proteins that could create crystals for x-ray crystallography. Out of the five proteins examined in this study the only one to crystallise and diffract was RomR N. The other proteins were not as successful but Bd 3099 can now be refolded and purified ready for crystallisation. Unfortunately both Bd 1482 and Bd 3100 were not able to be produced soluble and could only refold in NaAc buffer which are not suitable for affinity chromatography and ion exchange did not work. All in all the overall goal was achieved with varying degrees of success with RomR crystallising, Bd 3099 refolding and Bd 1482 and 3100 needing some optimisation.

Further studies could include the optimisation of the refolding procedure for Bd 1482, 3099 and 3100. But as this is a long and fairly expensive process other ways of producing these proteins as soluble proteins may be more effective and less time consuming. One way to overcome the insolubility problem would be to produce these proteins in the cytoplasm of the BL21 expression strain. As for Bd 2093, which was not successfully cloned into a plasmid, needs more investigation and maybe making different PCR primers. This might allow for the cloning of Bd 2093 and insertion into a plasmid.

References

Amikam D and Galperin MY. (2006). PilZ domain is part of the bacterial c-di-GMP binding protein. *Bioinformatics*; 22: 3-6.

Ash M, Faelber K, Kosslick D. (2010). Conserved β -hairpin recognition by the GYF domains of Smy2 and GIGYF2 in mRNA surveillance and vesicular transport complexes. *Structure*; 18: 944-954.

Capeness MJ, Lambert C, Lovering AL. (2013). Activity of Bdellovibrio Hit Locus Proteins, Bd0108 and Bd0109, Links Type IVa Pilus Extrusion/Retraction Status to Prey-Independent Growth Signalling. *PLoS one*; 8 (11)

Dwidar M and Mitchell RJ. (2012). The dual probiotic and antibiotic nature of Bdellovibrio bacteriovorus. *Biochemistry and Molecular Biology Reports*; 45: 71-78.

Hobley L, Fung RK, Lambert C. (2012). Discrete cyclic di-GMP-dependent control of bacterial predation versus axenic growth in Bdellovibrio bacteriovorus. *PLoS pathogens*; 8 (2): e1002493.

Kaiser D, Robinson M, Kroos L. (2012). Myxobacteria, Polarity, and Multicellular Morphogenesis. *Cold Spring Harb Perspect Biol* 2

Keilberg D, Wuichet K, Drescher F, Sogaard-Andersen L (2012). A Response Regulator Interfaces between the Frz Chemosensory System and the MglA/ MglB GTPase/GAP Module to Regulate Polarity in *Myxococcus xanthus*. *PLoS Genet*; 8

Kofler M and Freund C. (2006). The GYF domain. *FEBS Journal*; 273: 245-256.

Kofler M, Motzny K and Freund C. (2005). GYF domain proteomics reveals interaction sites in known and novel target proteins. *Molecular & cellular proteomic :MCP*; 4: 1797-1811.

Krasteva PV, Giglio KM and Sondermann H. (2012). Sensing the messenger: The diverse ways that bacteria signal through c-di-GMP. *Protein Science*; 21: 929-948.

Lambert C, Morehouse KA, Chang C. (2006). *Bdellovibrio* growth and development during the predatory cycle. *Current opinion in microbiology*; 9: 639-644.

Lambert C, Fenton AK, Hogley L. (2011). Predatory *Bdellovibrio* bacteria use gliding motility to scout for prey on surfaces. *Journal of Bacteriology*; 193: 3139-3141.

Lerner TR, Lovering AL, Bui NK. (2012). Specialized peptidoglycan hydrolases sculpt the intra-bacterial niche of predatory *Bdellovibrio* and increase population fitness. *PLoS pathogens*; 8

Lovering AL, Capeness MJ, Lambert C. (2011). The structure of an unconventional HD-GYP protein from *Bdellovibrio* reveals the roles of conserved residues in this class of cyclic-di-GMP phosphodiesterases. *mBio*; 2

Milner DS, Till R, Cadby I, Lovering AL, Basford SM, et al. (2014) Ras GTPase-Like Protein MglA, a Controller of Bacterial Social-Motility in Myxobacteria, Has Evolved to Control Bacterial Predation by *Bdellovibrio*. *PLoS Genet* 10(4)

Rendulic S, Jagtap P, Rosinus A. (2004). A predator unmasked: life cycle of *Bdellovibrio bacteriovorus* from a genomic perspective. *Science*; 303: 689-692.

Ryan RP, Tolker-Nielsen T and Dow JM. (2012). When the PilZ don't work: effectors for cyclic di-GMP action in bacteria. *Trends in microbiology*; 20: 235-242.

Ryan RP. (2013). Cyclic di-GMP signalling and the regulation of bacterial virulence. *Microbiology*; 159: 1286-1297.

Ryjenkov DA, Simm R, Romling U. (2006). The PilZ domain is a receptor for the second messenger c-di-GMP: the PilZ domain protein YcgR controls motility in enterobacteria. *The Journal of biological chemistry*; 281: 30310-30314.

Saxena IM and Brown RM. (1995). Identification of a second cellulose synthase gene (*acsAII*) in *Acetobacter xylinum*. *J. Bacteriol*; 177: 5276–5283.

Shilo M. (1969). Morphological and physiological aspects of the interaction of *Bdellovibrio* with host bacteria. *Curr. Top. Microbiol. Immunol*; 50:174–204

Sockett RE. (2009). Predatory lifestyle of *Bdellovibrio bacteriovorus*. *Annual Review of Microbiology*; 63: 523-539.

Thomashow MF and Cotter TW. (1992)s Bdellovibrio host dependence: the search for signal molecules and genes that regulate the intraperiplasmic growth cycle. *Journal of Bacteriology*; 174: 5767-5771.

Vincentelli R, Canaan S, Campanacci V. (2004). High-throughput automated refolding screening of inclusion bodies. *Protein Science*; 13: 2782-2792.